T TAURI STARS

by

Alfred Eric Rydgren Jr.

A Dissertation Submitted to the Faculty of the

DEPARTMENT OF ASTRONOMY

In Partial Fulfillment of the Requirements
For the Degree of

DOCTOR OF PHILOSOPHY

In the Graduate College

THE UNIVERSITY OF ARIZONA

1 9 7 5

INFORMATION TO USERS

This material was produced from a microfilm copy of the original document. While the most advanced technological means to photograph and reproduce this document have been used, the quality is heavily dependent upon the quality of the original submitted.

The following explanation of techniques is provided to help you understand markings or patterns which may appear on this reproduction.

1. The sign or "target" for pages apparently lacking from the document photographed is "Missing Page(s)". If it was possible to obtain the missing page(s) or section, they are spliced into the film along with adjacent pages. This may have necessitated cutting thru an image and duplicating adjacent pages to insure you complete continuity.

2. When an image on the film is obliterated with a large round black mark, it is an indication that the photographer suspected that the copy may have moved during exposure and thus cause a blurred image. You will find a good image of the page in the adjacent frame.

3. When a map, drawing or chart, etc., was part of the material being photographed the photographer followed a definite method in "sectioning" the material. It is customary to begin photoing at the upper left hand corner of a large sheet and to continue photoing from left to right in equal sections with a small overlap. If necessary, sectioning is continued again — beginning below the first row and continuing on until complete.

4. The majority of users indicate that the textual content is of greatest value, however, a somewhat higher quality reproduction could be made from "photographs" if essential to the understanding of the dissertation. Silver prints of "photographs" may be ordered at additional charge by writing the Order Department, giving the catalog number, title, author and specific pages you wish reproduced.

5. PLEASE NOTE: Some pages may have indistinct print. Filmed as received.

Xerox University Microfilms
300 North Zeeb Road
Ann Arbor, Michigan 48106

T TAURI STARS

by

Alfred Eric Rydgren Jr.

A Dissertation Submitted to the Faculty of the

DEPARTMENT OF ASTRONOMY

In Partial Fulfillment of the Requirements
For the Degree of

DOCTOR OF PHILOSOPHY

In the Graduate College

THE UNIVERSITY OF ARIZONA

1 9 7 5

THE UNIVERSITY OF ARIZONA

GRADUATE COLLEGE

I hereby recommend that this dissertation prepared under my direction by Alfred Eric Rydgren Jr.

entitled T Tauri Stars

be accepted as fulfilling the dissertation requirement of the degree of Doctor of Philosophy

Stephen E. Strom — 22 July, 1975
Dissertation Director — Date

After inspection of the final copy of the dissertation, the following members of the Final Examination Committee concur in its approval and recommend its acceptance:*

R. E. Williams	21 July 75
Wendy J. Wood	22nd July 1975
Rodger I. Thompson	29 July 1975

*This approval and acceptance is contingent on the candidate's adequate performance and defense of this dissertation at the final oral examination. The inclusion of this sheet bound into the library copy of the dissertation is evidence of satisfactory performance at the final examination.

STATEMENT BY AUTHOR

This dissertation has been submitted in partial fulfillment of requirements for an advanced degree at The University of Arizona and is deposited in the University Library to be made available to borrowers under rules of the Library.

Brief quotations from this dissertation are allowable without specific permission, provided that accurate acknowledgment of source is made. Requests for permission for extended quotation from or reproduction of this manuscript in whole or in part may be granted by the head of the major department or the Dean of the Graduate College when in his judgment the proposed use of the material is in the interests of scholarship. In all other instances, however, permission must be obtained from the author.

SIGNED: Alfred Eric Rydgren Jr.

PREFACE

This project had its inception with Dr. S. E. Strom in 1972. He believed that the T Tauri phenomenon represented a major unsolved problem in pre-main sequence stellar evolution and he further recognized that a renewed observational assault on this timely problem was likely to be fruitful, due to recent advances in astronomical instrumentation. At this point, he invited the author to collaborate with him in this work. The scope of the anticipated observations was so large that a division of labor was required. Thus the infrared observations were obtained by S. E. Strom, K. M. Strom, and F. Vrba, while the author concentrated on the optical photometry and spectroscopy.

S. E. Strom brought to this project his prejudices with regard to the nature of the infrared excess in these objects, as well as the idea of using coeval pairs of T Tauri stars as a test for evolution on a hydrodynamic timescale. Otherwise, the interpretation developed in this dissertation is the work of the author. This includes the important discoveries concerning the T Tauri star spectral energy distributions and the suggested link between the evolutionary state of these stars and their unusual observational properties. As the work progressed, the author's

frequent conversations with S. E. Strom, K. M. Strom, and G. L. Grasdalen served to sharpen the focus on the remaining problems.

A paper describing most of the results of this investigation has been written by A. E. Rydgren, S. E. Strom, and K. M. Strom. This has been accepted for publication in the Astrophysical Journal Supplement Series and should appear in print before mid-1976.

The author wishes to express his gratitude to a number of astronomers for their contributions to this research. First, this project would simply not have been possible without my advisor, Dr. S. E. Strom, whose efforts have been an integral part of this work. Also, his lessons in English prose have undoubtedly had a beneficial effect on the author's writing style. Mrs. K. M. Strom provided invaluable assistance with the infrared observations and reductions and carefully maintained the master data file. Dr. G. L. Grasdalen kindly made available a substantial number of unpublished scanner observations and his incisive comments during many discussions were most helpful. Dr. R. E. Williams devoted many long nights to instructing the author in the fine points of image-tube spectroscopy and displayed a continuing interest in this work as it progressed. Dr. N. J. Woolf contributed several fruitful discussions to this project and his critical reading of an

early draft of this dissertation has resulted in significant improvements. Dr. G. H. Herbig was most kind in replying at length to a letter from the author and in providing important unpublished spectroscopic results. Mr. F. Vrba made some of the infrared observations during the latter part of the investigation and assisted with many of the others.

Finally, the author must thank the Kitt Peak National Observatory for a generous allocation of observing time during the early portion of this project. The resulting scanner observations are incorporated in the analysis, but unfortunately the coudé spectra which were obtained did not prove to be decisive and therefore are not included in this dissertation.

TABLE OF CONTENTS

TABLE OF CONTENTS - Continued

LIST OF ILLUSTRATIONS

LIST OF ILLUSTRATIONS, Continued

LIST OF TABLES

ABSTRACT

Homogeneous spectroscopic and photometric (optical and infrared) observations of 49 T Tauri stars in the Taurus and Rho Oph clouds are presented; these data form the basis for a study of their envelope properties and evolutionary state. This analysis shows that the T Tauri phenomenon is best understood in terms of a model in which a late-type star is surrounded by a hot ($\approx 20{,}000^{\circ}$ K) gaseous envelope. Emission from the envelope accounts for the emission lines, the spectral veiling, and most of the true infrared excess, while temporal changes in the strength of the envelope emission appear to be the principal source of irregular light variations. Some T Tauri stars show silicate emission features at 10 and 20 μ, but emission from circumstellar dust at wavelengths shortward of 10 μ is shown to be insignificant in most cases. The interstellar extinction in the Taurus and Rho Oph clouds is definitely characterized by large values of R.

Proper understanding of the envelope emission processes enables us to correct the observed spectral energy distributions for interstellar extinction and thus obtain reliable bolometric luminosities. These luminosities, together with effective temperatures derived from the

photospheric spectral types, indicate that the T Tauri stars in these two clouds are relatively low mass stars evolving toward the main sequence along quasi-static equilibrium tracks. Masses of less than 3 $M_{\odot}$ and ages generally less than 10^6 years are inferred for these stars from a comparison with theoretical evolutionary tracks. Evidence is presented which indicates that the mass-loss rate and envelope emission strength decrease with time during the T Tauri phase. It is suggested that the T Tauri phenomenon corresponds to a phase of rapid angular momentum loss in convective protostars.

CHAPTER 1

INTRODUCTION

The T Tauri stars were first recognized by Joy (1945, 1949) as a distinct class of emission-line variable stars associated with dark cloud complexes. In the pioneering paper, Joy (1945) isolated a group of 11 known irregular variable stars which showed certain common spectroscopic properties: apparent spectral type F5 to G5, with emission lines resembling the solar chromosphere, and spectroscopic luminosity criteria indicating that the stars are more like dwarfs than giants. He chose the name "T Tauri variables" after one of the brightest and most representative members of the group. Joy followed up his initial work with a more extensive study of T Tauri stars in several fields in Taurus and Orion (Joy 1949). He used the presence of Hα emission on objective prism plates to identify candidate T Tauri stars and then obtained slit spectra of the stars. More than 30 additional T Tauri stars were thus found. These stars showed the same basic emission features as the original 11 stars, but the spectral types ranged from dGe to dM2.5e. Joy's remarkable discovery was further tested by Struve and Rudkjøbing (1949). They obtained slit spectra of 26 faint stars seen in projection

against the large dark cloud Barnard 42 in Ophiuchus. Six of these stars were found to have emission-line spectra similar to those of the T Tauri variables observed by Joy. Thus the T Tauri stars were firmly established as a class of stellar objects associated with dark cloud complexes.

Properties of T Tauri Stars

T Tauri stars exhibit a number of unusual observational properties:

1. Variability: All T Tauri stars appear to be irregularly variable in brightness at optical wavelengths, with observed amplitudes typically several magnitudes (Herbig and Rao 1972). The timescale for significant variations can be as short as hours (Wenzel 1966; Gahm et al. 1974). Variability has also been reported in the infrared (IR) (Mendoza 1968; Cohen 1973a).

2. Emission lines: The spectra of T Tauri stars show a number of prominent emission lines, usually superimposed on a late-type (spectral type G, K, or M) photospheric spectrum. The strongest observed emission lines are the Balmer lines of hydrogen and the Ca II H and K lines. Emission lines of Fe I λλ 4063, 4132 are also characteristic of T Tauri stars. Joy (1945) noted the anomalous strength of these lines and Herbig (1945) showed that they are due to fluorescence involving the combined Hε and Ca II H emission feature. Forbidden emission lines,

especially [S II] λλ 4068, 4076 and [O I] λλ 6300, 6363, are usually but not always observed in T Tauri spectra. In addition, some T Tauri stars also show emission lines of Fe II, Ti II, He I, and other species.

3. Blue-displaced absorption components: Many T Tauri stars exhibit blue-displaced absorption components in the strongest emission lines, indicating a mass outflow from the star with a velocity in the range 100 to 300 km sec^{-1}. From an analysis of the line profiles in bright T Tauri stars, Kuhi (1964, 1966) has derived mass-loss rates on the order of 10^{-7} to 10^{-9} $M_{\odot}$ yr^{-1}. These values are about 10^{6} times greater than the present rate of mass loss from the sun. Red-displaced absorption components have been observed in some T Tauri stars (Walker 1972), suggesting that mass infall can also occur.

4. Broad absorption lines: High dispersion spectra of the brightest T Tauri stars reveal that the photospheric absorption lines are exceptionally broad and shallow (Herbig 1957). This has been interpreted in terms of projected rotational velocities in the range 20 to 65 km sec^{-1}, which are substantially larger than those of the other late-type stars.

5. Li I absorption: The Li I λ 6707 absorption line is unusually strong in T Tauri stars. The lithium abundances derived for several bright T Tauri stars by

Bonsack and Greenstein (1960) and Bonsack (1961) are similar to the value characteristic of the early solar system, and are a factor of about 10^2 greater than in the present sun.

6. Veiling: The ultraviolet (UV) and blue spectral regions of T Tauri stars are "veiled" by what Joy (1949) believed to be an overlying continuous emission. In the most extreme cases, the veiling is so strong that no convincing evidence of a photospheric absorption spectrum can be seen.

7. Infrared excess: Mendoza (1966, 1968) observed the spectral energy distributions of a number of T Tauri stars by means of broadband visual and IR photometry. After correcting for interstellar extinction, he found that these stars showed substantial excess radiation longward of about 1 μ, compared with that expected from a late-type photosphere. To explain this phenomenon, he proposed a model in which an optically thick circumstellar (CS) dust shell absorbs visual radiation from the star and reemits it in the infrared as cool black body radiation.

In the fundamental review paper on T Tauri stars, Herbig (1962) emphasizes that the T Tauri class is defined by a set of spectroscopic characteristics and not by the photometric behavior or other property. Herbig and Rao (1972) attempt to distinguish between legitimate T Tauri stars (type "t") and a class of stars which they refer to as

type "m." These "m" stars are K or M stars of low to moderate luminosity associated with dark cloud complexes and with the Balmer lines, the Ca II H and K lines, and often He I lines all in emission. There is little doubt that these type "m" stars represent a less-extreme manifestation of the T Tauri phenomenon, and we therefore refer to stars of Herbig and Rao types "t" and "m" collectively as "T Tauri" stars.

Pre-Main Sequence Evolution

The proximity of the known T Tauri stars to dark interstellar clouds suggested to Joy and others that there was some causal relationship between the dark cloud material and the unusual properties of the T Tauri stars. This led to the hypothesis that T Tauri stars are normal stars accreting dark cloud material and that this infalling material generates the observed line emission. However, by the middle 1950's, it became clear that the T Tauri stars are recently-formed pre-main sequence (PMS) stars, still located near the dark interstellar clouds in which they were born. This was first suggested by Ambartsumian (1947).

The PMS nature of the T Tauri stars was clearly demonstrated by Walker's (1956) UBV photometry of members of the young cluster NGC 2264. A number of T Tauri stars are present in the band of late-type stars located above the zero-age main sequence (ZAMS) in the color-magnitude diagram

of this cluster. The identification of T Tauri stars as PMS stars is also supported by the association of some T Tauri stars with acknowledged very young objects (Strom, Strom, and Grasdalen 1975) such as Herbig Ae-Be stars, Herbig-Haro objects, and OB-associations, and by the high space density of T Tauri stars near some dark clouds (Herbig 1962). The high lithium abundances found in T Tauri stars are consistent with the picture that stars form with a high initial lithium abundance, and that this is then depleted over time due to convective mixing of surface material into the hotter interior of the star.

The evolution of isolated, non-rotating PMS stars is believed to be described by the standard Hayashi track, Henyey track calculations (Hayashi, Hoshi, and Sugimoto 1962; Iben 1965; Ezer and Cameron 1967a, 1967b). These evolutionary models predict that a PMS star contracts to form a luminous, fully-convective star, which evolves almost vertically downward along its Hayashi track in the H-R diagram. As the radiative core forms and grows, the evolution slows and the star turns and follows its equilibrium radiative track (ERT) to the ZAMS. The Hayashi track and the ERT together comprise the quasi-static equilibrium track (QSET) in the H-R diagram. For the least-massive stars, there is no substantial radiative core, and the evolution proceeds vertically downward in the H-R diagram to the ZAMS.

The predicted isochrones in the H-R diagram are roughly parallel to the ZAMS, with the isochrone corresponding to the youngest age being the farthest up in the diagram. The distribution of the late-type stars above the ZAMS in the color-magnitude diagrams of young clusters seems understandable in terms of this quasi-static equilibrium PMS evolution (Iben and Talbot 1966).

These conventional models have been replaced in part by the hydrodynamic models of Larson (1969, 1972), which numerically follow the collapse of the protostar all the way from interstellar cloud densities. He shows that the inner part of the cloud collapses more rapidly, forming a protostellar core which then accretes the remainder of the cloud. For $M < 1.5\ M_{\odot}$, the evolution of the core in the H-R diagram is dominated by the energy from the infalling matter, but this is hidden from view by the optically thick CS shell of remnant gas and dust. The path of the core in the H-R diagram during this accretion phase is a complex looping track, the details of which are probably model-dependent. The CS shell becomes optically thin near the bottom of the Hayashi track, and the star then settles onto the QSET appropriate for its mass and evolves to the ZAMS in the usual way.

Recent Work

Much of the recent work on T Tauri stars has been done within the framework of a basic conceptual model. The principal elements of this model are the following:

1. T Tauri stars are PMS stars of no more than several solar masses, evolving along some form of equilibrium track toward the ZAMS.

2. The observed emission lines originate either in a very strong chromosphere (thickness small compared with the stellar radius) or from an extended gaseous envelope (dimensions on the order of several stellar radii) surrounding the star.

3. T Tauri stars are surrounded by optically thick CS dust shells; radiation from this dust accounts for the observed IR excesses.

The class prototype, T Tau, has been investigated in some detail. Low et al. (1970) included T Tau in their 0.36 to 22 μ photometric study of unusual IR stars. The observed spectral energy distribution clearly shows a double-peaked structure which is interpreted as photospheric emission shortward of 2 μ and black body emission from CS dust longward of about 2 μ. Cohen (1973a) has observed anticorrelated visual and IR variations in T Tau, suggesting that the observed variability arises from optical depth changes in the CS dust shell. Schwartz (1974, 1975) has

studied spectroscopically the complex nebulosity near T Tau. He finds that the star has a gaseous CS envelope of radius about 0.1 au, which is surrounded by a CS dust shell. Fainter nebulosity extends about 1500 au south of the star and to a distance of about 400 au in other directions. All of these observations lend support to the hypothesis that the prototype T Tauri star is surrounded by an optically thick CS dust shell.

Recent work on other members of the class has strengthened the belief that all T Tauri stars are characterized by CS dust shells. IR spectral energy distributions of many T Tauri stars have been observed by Cohen (1973a, 1974). He finds most of them to be remarkably flat, which is difficult to interpret either as black body dust emission or free-free emission from a heated gas. He suggests a simple model (Cohen 1973b) for explaining the observations, based on a two-component CS dust shell with scattering and a non-gray dust opacity. Moreover he argues that the observed absence of silicate features at 10 and 20 μ in T Tauri stars is evidence that the CS dust shells are optically thick. Gahm et al. (1974) interpret the brightness variations of the T Tauri star RU Lup in terms of changing optical depth in the CS dust shell. Imhoff and Mendoza (1974) have attempted to determine the relative importance of circumstellar and interstellar extinction in T Tauri

stars. They suspect that both forms of extinction are normally present, and that the extinction law may deviate from the standard interstellar extinction law.

A principal topic of debate regarding T Tauri stars is the nature of the line emission region. The similarity of the typical T Tauri emission-line spectrum to that of the solar chromosphere was noted by Joy (1945). Kuhi (1964) has shown, however, that the observed emission-line profiles are best explained by an expanding envelope of material violently ejected from a hot layer near the stellar surface. Further evidence for expanding envelopes around T Tauri stars is provided by Willson's (1974) careful study of the excitation of the fluorescent Fe I lines by the combined H + Hϵ emission feature. She emphasizes the importance of the velocity field in bringing the spectral lines into coincidence, and shows that the most plausible model involves excitation in an expanding envelope by Hϵ rather than by Ca II H. Schwartz (1974) also presents observational evidence for a gaseous CS envelope around the prototype, T Tau.

Recent efforts to interpret the emission-line spectra of T Tauri stars in terms of a strong chromosphere rather than an expanding envelope may be traced to Herbig (1970). He suggested that a chromospheric temperature inversion reaching deep into the stellar atmosphere could

explain not only the observed emission lines, but also the heretofore unexplained blue spectral veiling. The analysis of extensive spectrum scanner observations of T Tauri stars by Kuhi (1974) reveals excellent correlations between the UV continuum flux, the Ca II K line strength, and the Hα strength. This is interpreted as compelling evidence for the origin of all these features in a strong chromosphere. An attempt to verify this hypothesis in a quantitative way has been made by Dumont et al. (1973). They show that an enhanced static chromosphere can account for the basic strength of the strongest Balmer emission lines, but there appear to be serious difficulties regarding the line profiles and the Balmer decrement. It is suggested that a moving chromosphere model would remove some of these problems.

Several authors (Larson 1972; Cohen 1973b) have sought to identify the T Tauri phenomenon with the phase of the clearing dust shells predicted by Larson's models for protostellar collapse. The presence of optically thick CS dust shells around T Tauri stars and the spectroscopic evidence for mass infall in some T Tauri stars (Walker 1972) are taken as supporting this identification. Kuhi's (1974) finding that the G-type T Tauri stars in the Taurus cloud are more heavily reddened than the M-type T Tauri stars is

cited as further evidence that Larson's models apply to T Tauri stars.

In the work discussed above, it is generally assumed that T Tauri stars are relatively low mass PMS stars. This standard view regarding T Tauri masses is challenged by Grasdalen (1973) in his analysis of the remarkable object V1057 Cyg. Prior to 1969, this star was apparently a normal faint T Tauri star, classified as such by Herbig (1958) from a low-dispersion slit spectrogram. During 1969, V1057 Cyg brightened by more than a factor of 100 and assumed the appearance of a late A or early F star of high luminosity; this outburst is strongly reminiscent of FU Ori. Grasdalen finds that the post-outburst star is an object of about 8 $M_\odot$ near its ERT toward the upper main sequence. He believes that the pre-outburst T Tauri star was really an 8 $M_\odot$ star in a low-luminosity hydrodynamic phase of PMS evolution, and that the rapid rise in luminosity represents the transition from the hydrodynamic to the ERT phase of evolution. There is limited support for this identification in Larson's (1972) models for high-mass protostars. Thus Grasdalen concludes that at least some T Tauri stars are not low-mass stars at all, but rather high-mass stars undergoing pre-ERT evolution.

The enigma of V1057 Cyg points up the serious uncertainties in our understanding of T Tauri stars. Excluding

the well-studied prototype of the class, it has not been convincingly proven that T Tauri stars as a class are surrounded by optically thick CS dust shells. The exact nature of the emission line region is not yet clearly understood. It has not been demonstrated through theoretical calculations that either an extreme chromosphere or an extended gaseous envelope can satisfactorily account in detail for the emission features observed in T Tauri spectra. The source of the blue spectral veiling remains unknown, although several theories have been advanced to explain it qualitatively. It is not yet understood what part of a T Tauri object actually changes to give rise to the observed irregular brightness variations. The place of T Tauri stars in PMS stellar evolution remains uncertain, largely because of difficulties in determining reliable bolometric luminosities. The identification of T Tauri stars with low- to intermediate-mass stars somewhere near the base of their vertical evolutionary tracks seems reasonable, but one cannot immediately rule out Grasdalen's suggestion that at least some T Tauri stars are really high-mass stars in a hydrodynamic phase of PMS evolution. A specific objection to the interpretation of T Tauri stars in terms of Larson's models is that the spectroscopic observations plainly show mass outflow rather than mass infall to be characteristic of the class.

Toward a Unified Model

The present state of understanding regarding the T Tauri stars may be summarized as follows:

1. There is essentially universal agreement that T Tauri stars are PMS objects.

2. The physical processes occurring in T Tauri stars are not yet clearly understood. This includes the line emission and spectral veiling, the IR excess, the irregular variability, and the apparent mass outflow.

3. The masses, ages, and evolutionary state of the T Tauri stars are still uncertain.

4. The reason for the unusual properties of T Tauri stars, in terms of their evolutionary state, remains unknown.

Much of the previous work on T Tauri stars has been directed toward explaining isolated phenomena, rather than toward understanding the full range of T Tauri characteristics. This approach does not provide a unified physical model for a T Tauri star, nor does it address the problem of a relationship between the physical processes and the evolutionary state.

In our view, a proper model for T Tauri stars should provide a natural and plausible explanation of all of the "envelope" phenomena: the relation between the UV and blue veiling, the line emission, the mass outflow, the irregular

variability, and the IR excess. Moreover, there should be a causative relationship between the PMS nature of the T Tauri stars and the unusual properties characteristic of the class. This should enable us to understand the diversity within the T Tauri class, as well as the relation of the T Tauri stars to the many other PMS stars which do not exhibit the remarkable properties of the T Tauri class.

An improved understanding of T Tauri stars must be based on more complete observational material, since only in this way can the basic questions relating to the physical processes and evolutionary state be resolved. These answers are clearly prerequisites to the more fundamental question of why T Tauri stars exist.

In order to find a model which satisfies the considerations outlined above, we have undertaken an extensive survey of T Tauri stars in two nearby T-associations. The program stars are selected to cover a wide range of envelope properties and possible ages. Moderate-dispersion spectra provide a measure of line emission and veiling, and an estimate of photospheric spectral type and effective temperature. Visual and IR photometry determine the observed spectral energy distributions over a wide wavelength baseline. Repeated photometry of some of the program stars provides information regarding the amplitude and wavelength dependence of variations. A synthesis of these

spectroscopic and photometric data leads to a plausible hypothesis which appears to account for the observed envelope phenomena. The resulting understanding of the envelope emission processes enables us to correct the observed spectral energy distributions for interstellar extinction and thus obtain reliable bolometric luminosities. Effective temperatures and luminosities for a large number of T Tauri stars then allow us to determine the likely evolutionary state of these stars, and to estimate the age and mass ranges characteristic of the class. The observed relation between envelope phenomena and age can be understood in the context of a "scenario" which incorporates a considerable body of recent evidence concerning the early phases of stellar evolution. Finally, a simple and plausible explanation for the T Tauri phenomenon is suggested, which follows directly from the PMS nature of these objects.

CHAPTER 2

THE OBSERVATIONS

The T Tauri stars on our observing program were specifically selected to include the following:

1. A sample of T Tauri stars with the same age. Stars in this group provide the observational basis for distinguishing among the various alternatives for the evolutionary state of the T Tauri objects.

2. A sample containing T Tauri stars with different ages. Here one seeks to understand the time-dependent behavior of T Tauri envelopes as well as to verify the evolutionary picture derived from the coeval sample.

3. A sample of T Tauri stars covering the complete range of envelope phenomena. This choice provides leverage for understanding the physical processes occurring in T Tauri envelopes.

Satisfaction of the first consideration presents the greatest difficulty. T Tauri stars have been found in association with stellar objects having ages in the range 10^5 to 10^7 years (Strom, Strom, and Grasdalen 1975). While the ages of associated stars can be used to provide crude age ranges for T Tauri objects, they are highly unsatisfactory either for dating groups of stars or for determining

the formation times for individual stars. Consequently, it is necessary to use apparent binary systems involving T Tauri stars to provide small samples of coeval stars. A number of such pairs were selected in the nearby Taurus and Rho Oph dark clouds, primarily from the list given by Herbig (1962) and from the catalog of Herbig and Rao (1972). It is likely that the majority of these are physically-associated coeval pairs, but this cannot be established with certainty in each individual case.

To satisfy the second consideration, the T Tauri stars located in (a) the Taurus dark cloud complex and (b) the Rho Ophiuchi dark cloud (Barnard 42) were chosen for study. These regions were selected because there is evidence that these T-associations differ in age and because they are the two nearest T-associations readily observable from Kitt Peak.

The "Taurus cloud" is not a single dust cloud, but rather a complex of dust lanes and opaque knots spread over some 100 square degrees in Taurus and Auriga. A distance of 150 pc to the Taurus complex is adopted (Herbig 1960), but it is noted that this is not as well known as it should be. More than 50 verified T Tauri stars (types "t" and "m") in the Taurus cloud are identified in the catalog of Herbig and Rao (1972). New UBV photometry, IR photometry, and image-tube spectra were obtained for 33 of these stars and one

bright T Tauri-like star discovered during the course of this investigation. Four additional stars were observed in the IR, but without visual photometry or spectra. The distribution of the known Taurus cloud T Tauri stars in the plane of the sky shows several apparent concentrations. A compact group of eight T Tauri stars located around a small dark cloud near $l = 179^{\circ}$, $b = -20^{\circ}$ was selected for particular attention. This group lies several degrees from the rest of the Taurus complex and includes several stars with unusually strong emission properties along with a huge Herbig-Haro object. We refer to these eight stars as the "HL-XZ group," because of the central position of the pair of T Tauri stars HL Tau and XZ Tau. In addition to the T Tauri stars, the Taurus complex contains one Herbig Be star (AB Aur) which is located near the ZAMS at spectral type B9 (Strom et al. 1972), and several Herbig-Haro objects (Herbig 1974; Strom, Grasdalen, and Strom 1974). Both Herbig Ae-Be stars and Herbig-Haro objects are regarded as "signposts" of very recent star formation (ages less than a few times 10^5 years) (Strom, Strom, and Grasdalen 1975). The presence of these signposts suggests that some of the T Tauri stars in the Taurus complex may be quite young.

In contrast, the known T Tauri stars in the Rho Oph cloud are confined to an area of only about five square degrees, centered on the large dark cloud Barnard 42. This

cloud is located in the midst of the Upper Scorpius OB association, at a distance of about 170 pc from the sun (Bertiau 1958; Garrison 1967). Fifteen stars were selected for study from the list of Herbig and Rao (1972); these were supplemented by nine stars chosen from the Hα emission survey of Dolidze and Arakelyan (1959). The designations of the stars in the Rho Oph cloud are based on the sequential numbers assigned in the spectroscopic survey of Struve and Rudkjøbing (1949) (prefix "SR") and the Hα emission surveys of Haro (1949) (prefix "Haro 1-") and Dolidze and Arakelyan (1959) (prefix "Do-Ar"). IR photometry in some form was obtained for all 24 stars, with spectra for 22 of them and UBV photometry for 17 of the stars. Fifteen of these stars appear to be definite T Tauri stars. The IR photometry of T Tauri stars by Knacke et al. (1973) shows that the Ophiuchus stars have on the average smaller IR excesses than do those in the Taurus complex; this observation was interpreted as evidence of a greater age for the Ophiuchus T Tauri stars. The absence of both Herbig Ae-Be stars and Herbig-Haro objects in the Rho Oph cloud lends support to this suggestion. However, Grasdalen, Strom, and Strom (1973) and Vrba et al. (1975) have discovered a number of IR sources embedded deep within the cloud, which they interpret as the brighter members of a recently-formed star cluster. It is therefore possible that representatives of the

youngest stellar population may still be located deep inside the large dark cloud.

The T Tauri stars selected to fulfill the first two considerations also generally satisfy the third, since they exhibit a wide range of envelope characteristics. However, to ensure adequate representation of stars with strong "envelope" properties, the four Taurus cloud stars with spectral types of "G:e" in the Herbig-Rao catalog were also included in the observing program. These stars appear to be among the most extreme T Tauri stars.

A summary of the photometric and spectroscopic observations of the program stars is given below.

UBV Photometry

The new UBV photoelectric observations of the T Tauri stars in the Taurus and Rho Oph clouds were made primarily by the author, with the single-channel photometer on the venerable Steward Observatory 91-cm telescope. The Steward Observatory 2.3-m telescope was used by the author on two nights (1973 June 24 and 1973 December 19) with the two-channel photometer; V-R colors were also measured on the first of these nights. In addition, a few BV observations were made by S. E. Strom and K. M. Strom in 1972 with an auxiliary cold box on the IR photometer of the Kitt Peak National Observatory (KPNO) 1.3-m telescope. The observations were reduced in most cases with the photometry

reduction program written by W. S. Fitch. A full solution for the transformation coefficients was made for all Taurus observations. Because of the large air mass, the Ophiuchus observations were reduced with mean slopes and extinction coefficients; four secondary standards were used as a consistency check.

The mean error of a single observation of a bright star is typically $0^m.02$ in V, $0^m.02$ in B-V, and $0^m.03$ in U-V. The observational errors for the fainter stars can be estimated from two non-variable foreground stars observed in Ophiuchus. Do-Ar 53 (SR 17) is an early K dwarf with V = 10.9. Based on four observations, the mean error of a single observation is $0^m.01$ in V, $0^m.02$ in B-V, and $0^m.05$ in U-V. SR 23 is a late K dwarf with V = 13.6. From three observations, the mean error of a single observation is $0^m.04$ in V, $0^m.06$ in B-V, and $0^m.09$ in U-V. The larger uncertainty in the U-V color is the result of the faintness of these normal stars in the U filter; most T Tauri stars have a UV excess due to spectral veiling, which leads to a less-uncertain U-V color. Also, the Taurus photometry should be more accurate than the Ophiuchus photometry, because the Taurus stars were observed at significantly smaller air mass. The accuracy obtained is quite adequate, since the UBV photometry is used to study the large-amplitude variability and the spectral energy distributions.

TABLE 1

UBV Photometry of Stars in the Taurus Cloud

Star	UT Date	V	B-V	U-V
T Tau	1973 Sep 27	$10^m.12$	$1^m.22$	$1^m.99$
	1973 Oct 23	10.04	1.27	1.74
	1973 Oct 23	10.07	1.20	1.76
	1973 Oct 24	10.11	1.19	1.79
	1973 Oct 25	10.10	1.25	1.89
	1973 Nov 5	10.12	1.26	1.93
	1973 Nov 6	10.06	1.23	1.91
	1973 Dec 18	10.07	1.23	1.86
	1973 Dec 19	10.08	1.20	1.81
RY Tau	1973 Sep 27	10.52	1.08	1.51
	1973 Oct 23	10.56	1.00	1.41
	1973 Oct 24	10.50	1.04	1.45
	1973 Oct 25	10.44	1.02	1.41
	1973 Nov 5	10.43	1.05	1.50
	1973 Nov 6	10.42	1.03	1.47
	1973 Dec 18	10.54	1.02	1.46
	1973 Dec 19	10.54	1.00	1.37
SU Aur	1973 Sep 27	9.19	0.90	1.35
	1973 Oct 23	9.15	0.87	1.31
	1973 Oct 24	9.17	0.89	1.40
	1973 Oct 25	9.22	0.92	1.39
	1973 Nov 5	9.39	0.92	1.42
	1973 Nov 6	9.44	0.94	1.44
	1973 Dec 18	9.18	0.91	1.35
	1973 Dec 19	9.24	0.88	1.29
RW Aur	1973 Sep 27	10.74	0.69	0.43
	1973 Oct 23	10.76	0.70	0.28
	1973 Oct 24	10.44	0.64	0.44
	1973 Oct 25	10.39	0.61	0.31
	1973 Nov 5	10.43	0.66	0.49
	1973 Nov 6	10.70	0.71	0.34
	1973 Dec 18	10.27	0.61	0.16
	1973 Dec 19	10.34	0.73	0.75
GG Tau	1973 Sep 27	12.30	1.39	1.55
	1973 Oct 23	12.14	1.41	1.07
	1973 Oct 25	12.23	1.45	1.39
	1973 Nov 5	12.30	1.42	1.30
	1973 Dec 19	12.23	1.37	1.40
HN Tau	1973 Sep 27	13.37	1.04	0.96
	1973 Oct 23	13.68	1.03	0.59
	1973 Oct 25	13.15	0.94	0.49
	1973 Nov 5	14.38	0.89	2.05
	1973 Dec 19	14.16	0.95	0.59
DM Tau	1973 Sep 27	13.93	1.03	0.36
	1973 Oct 23	13.78	0.94	0.37
	1973 Oct 25	13.77	0.86	0.33
	1973 Dec 19	14.20	1.11	0.81

TABLE 1, Continued

Star	UT Date	V	B-V	U-V
LkHα 266	1973 Sep 27	$13^m.61$	$1^m.57$	$1^m.84$
	1973 Oct 23	13.69	1.66	2.08
	1973 Oct 25	13.78	1.73	3.13
	1973 Nov 5	13.67	1.63	2.01
HL Tau	1973 Dec 19	14.48	1.32	1.41
XZ Tau	1973 Dec 19	15.11	1.51	1.83
UX Tau	1973 Sep 27	10.77	1.04	1.62
	1973 Oct 23	11.43	1.18	2.16
	1973 Oct 25	10.83	0.98	1.58
	1973 Nov 5	10.72	1.03	
CW Tau	1973 Oct 24	12.94	1.43	1.62
	1973 Oct 25	12.69	1.35	1.63
	1973 Nov 5	12.96	1.29	1.61
	1973 Dec 19	14.40	1.34	1.45
	1974 Sep 15	13.19	1.37	1.54
	1974 Oct 15	14.15	1.45	1.56
FM Tau	1973 Oct 24	14.12	0.73	0.30
	1973 Oct 25	14.31	0.98	0.58
	1973 Nov 5	13.98	0.78	0.35
	1973 Nov 6	14.06	0.84	0.31
	1973 Dec 19	13.74	0.55	0.06
	1974 Sep 15	14.48	0.75	0.69
	1974 Oct 15	14.75:	1.08:	0.81:
HD 283447	1973 Nov 6	10.74	1.34	2.34
	1973 Dec 18	10.59	1.40	2.47
	1973 Dec 19	10.69	1.33	2.34
	1974 Sep 15	10.95	1.36	2.28
	1974 Oct 15	10.69	1.35	2.31
FN Tau	1973 Dec 19	14.95	1.69	2.53
CX Tau	1973 Oct 24	13.73	1.39	1.57
	1973 Oct 25	13.77	1.41	1.65
	1973 Nov 5	13.64	1.66	2.10
	1973 Nov 6	13.63	1.43	1.64
	1973 Dec 19	13.72	1.47	1.96
	1974 Sep 15	13.75	1.51	1.82
	1974 Oct 15	13.76	1.50	2.32
FP Tau	1973 Oct 24	13.88	1.40	1.52
	1973 Oct 25	13.90	1.53	1.90:
	1973 Nov 5	13.94	1.48	2.09
	1973 Nov 6	13.91	1.52	1.94
	1973 Dec 19	13.93	1.55	2.70
	1974 Sep 15	14.05	1.61	2.61
	1974 Oct 15	14.17	1.54	2.98
DD Tau	1973 Oct 23	14.23	0.99	0.53
	1973 Dec 19	14.68	1.23	0.77

TABLE 1, Continued

Star	UT Date	V	B-V	U-V
CZ Tau	1973 Dec 19	$15^{m}.50$	$1^{m}.57$	$3^{m}.12$
DH Tau	1973 Oct 24	13.48	1.16	0.89
	1973 Nov 6	13.27	1.35	1.44
	1973 Dec 19	13.62	1.01	0.74
DI Tau	1973 Oct 24	12.94	1.60	3.18
	1973 Nov 6	12.89	1.61	2.96
	1973 Dec 19	12.90	1.60	3.01
GI Tau	1973 Oct 24	13.04	1.30	1.37
	1973 Nov 6	13.27	1.41	
	1973 Dec 19	12.98	1.41	1.83
GK Tau	1973 Oct 24	12.37	1.34	2.03
	1973 Nov 6	13.26:	1.60:	2.54:
	1973 Dec 19	12.33	1.32	1.69
UZ Tau	1973 Nov 6	12.98	1.32	1.26
DG Tau	1973 Dec 18	11.84	1.00	0.47
	1973 Dec 19	11.90	0.99	0.61
	1974 Sep 15	12.79	1.00	0.50
	1974 Oct 15	12.66	1.03	0.60
DL Tau	1973 Dec 19	13.06	1.06	0.66
DO Tau	1973 Dec 19	13.68	1.12	0.59
	1974 Oct 15	13.75	1.27	0.73
CI Tau	1973 Dec 18	13.58	1.58	1.90
	1973 Dec 19	13.50	1.46	1.65
	1974 Oct 15	13.58	1.43	1.45
AA Tau	1973 Dec 19	13.36	1.28	1.27
	1974 Oct 15	12.87	1.31	1.43
BP Tau	1973 Dec 18	12.22	1.07	0.74
	1973 Dec 19	12.22	1.11	0.94
	1974 Oct 15	12.23	1.00	0.78
DE Tau	1973 Dec 18	13.07	1.40	0.99
	1973 Dec 19	12.95	1.31	0.93
DF Tau	1973 Dec 18	12.15	1.12	0.99
	1973 Dec 19	12.00	1.12	1.01
	1974 Oct 15	12.19	1.23	1.08
DK Tau	1973 Dec 18	11.75	0.98	0.83
	1973 Dec 19	13.03	1.16	0.93
DN Tau	1973 Dec 19	12.50	1.39	1.94
	1974 Oct 15	12.45	1.38	2.07

TABLE 2

UBVR Photometry of Stars in the Rho Oph Cloud

Star	UT Date	V	B-V	U-V	V-R
Haro 1-1	1973 Jun 24	$13^m.34$	$1^m.25$	$1^m.19$	$1^m.11$
Haro 1-4	1972 Jun 17	13.35	1.26		
	1973 Apr 4	13.36	2.12		
	1973 May 1	13.41	1.80	2.18	
	1973 May 31	13.45:	1.83	2.65	
	1973 Jun 24	13.46	1.98	3.38	1.77
Haro 1-8	1972 Jun 17	14.10	1.56		
	1973 Jun 24	13.84	1.66	2.31	1.53
Do-Ar 22	1973 Apr 4	12.48	1.02	1.54	
	1973 May 1	12.60	0.99	1.44	
	1973 May 31	12.76:	1.10	1.88	
SR 4	1973 Apr 4	12.84	1.55	1.72	
	1973 May 1	12.91	1.59	1.88	
	1973 Jun 1	12.82	1.47	1.42	
	1973 Jun 24	12.77	1.48	1.41	1.50
	1974 May 30	12.81	1.54	1.44	
	1974 Jun 22	12.75	1.55	1.59	
Do-Ar 21	1973 Jun 24	13.92	2.27	3.68	2.29
SR 9	1972 Jun 16	11.43	1.21		
	1973 Apr 4	11.32	1.26	2.04	
	1973 May 1	11.48	1.27	1.83	
	1973 May 31	11.40:	1.28	2.02	
	1973 Jun 24	11.51	1.27	1.73	1.21
	1974 May 30	11.36	1.23	1.77	
	1974 Jun 22	11.23	1.25	1.91	
SR 10	1972 Jun 15	13.97	0.95		
	1972 Jun 16	13.91	0.98		
	1973 Apr 6	13.96	0.87	0.34	
	1973 May 1	14.00	1.02	0.79	
	1973 May 31	14.15:	1.04	0.93	
	1973 Jun 24	14.07	1.04	0.64	1.62

TABLE 2, Continued

Star	UT Date	V	B-V	U-V	V-R
SR 12	1973 Apr 6	$13^m.55$	$1^m.51$	$2^m.54$	
	1973 May 1	13.27	1.55	2.57	
	1973 May 31	13.59:	1.60	2.66	
	1973 Jun 24	13.31	1.64	3.26	$1^m.61$
	1974 Jun 22	13.32	1.66	2.60	
SR 13	1973 Apr 4	12.93	0.81	0.30	
	1973 May 1	12.83	0.89	0.14	
	1973 May 31	13.30:	0.96	0.42	
	1973 Jun 24	13.20	0.92	0.46	1.62
	1974 May 30	13.52	1.16	0.69	
	1974 Jun 22	13.48	1.16	0.86	
Do-Ar 38	1973 Jun 24	14.15	2.08	4.27	2.16
Haro 1-16	1972 Jun 16	12.69	1.32		
	1973 Apr 6	12.65	1.38	2.11	
	1973 May 1	12.59	1.37	1.86	
	1973 Jun 1	12.60	1.36	1.80	
	1974 May 30	12.64:	1.30:	1.44:	
	1974 Jun 22	12.67	1.41	1.89	
Haro 1-14	1972 Jun 16	12.05	1.50		
+ comp.	1973 Jun 1	12.29	1.46	2.68	
Do-Ar 51	1973 Apr 6	13.36	1.61	1.61	
	1973 May 1	13.45	1.79	2.93	
	1973 Jun 1	13.54	1.86	2.86	
Do-Ar 53	1973 Apr 6	10.88	0.97	1.85	
	1973 May 1	10.85	0.98	1.85	
	1973 Jun 1	10.86	1.02	1.96	
	1973 Jun 24	10.87	1.00	1.90	0.70
Do-Ar 58	1973 Apr 6	12.22	1.49	2.50	
	1973 May 1	12.59	1.03	2.45	
	1973 Jun 1	12.11	1.52	2.53	

The UBV observations of the Taurus stars are given in Table 1 and the UBVR observations of the Ophiuchus stars in Table 2.

Infrared Photometry

Infrared observations of the program stars were obtained by S. E. Strom, K. M. Strom, and F. Vrba with the KPNO 1.3-m and 2.1-m telescopes, beginning in June 1972. J (1.25 μ), H (1.6 μ), K (2.2 μ), and L (3.5 μ) observations on the system of Johnson (1964) were made with the Dyck PbS photometer and after February 1974, with the InSb system developed by R. Joyce. In addition, a number of observations in the 2 to 20 μ region were made with a gallium-doped germanium bolometer. The bolometer measurements were made through narrow-band filters centered at 2.2 μ, 3.5 μ, 4.7 μ, 8.4 μ, 10.3 μ, 11.1 μ, and 12.6 μ, as well as through broad-band filters centered at 10 μ and 20 μ. The bolometer observations are on a system whose zeropoint is defined by α Lyr. Only the brightest T Tauri stars were observed at all wavelengths, while some of the faintest stars in the sample were not observed longward of K or L.

It is impractical to give individual errors for each observation. The typical mean error of both the bolometer observations and the JHKL photometry obtained with the PbS system is on the order of $\pm 0^m.1$ to $\pm 0^m.2$. The JHKL photometry obtained with the new InSb system is substantially more

TABLE 3

Infrared Photometry of Stars in the Taurus Cloud

Star	UT Date	K	J-K	H-K	K-L	4.8	8.4	10.1	11.1	12.6	10	20
T Tau	1973 Oct 4	5.76	1.38	0.59	1.42							
	1973 Oct 6	5.74	1.33	0.62	1.39							
	1973 Oct 9	5.73	1.39	0.60	1.24							
	1973 Nov 9	5.64			1.05	2.6	1.1		1.3			
	1973 Dec 11	5.71			1.24	2.9	1.3	0.9	0.7	0.1		-2.0
	1973 Dec 25	5.74			1.24	2.9	1.3	1.1	0.6	0.0		-1.9
	1974 Jan 15	5.65			1.15	2.9	1.3		0.7			
RY Tau	1973 Oct 4	5.26	1.94	1.00	1.34							
	1973 Oct 6	5.29	1.99	0.84	1.41							
	1973 Oct 9	5.36	1.98	0.84	1.20							
	1973 Nov 9	5.38			1.22	3.0	1.4		0.6			
	1973 Nov 15	5.40			0.80	3.0	1.6		0.6			
	1973 Dec 11	5.54			1.17	3.5	1.7	0.9	0.7	1.0		-0.8
	1973 Dec 23	5.51			1.16	3.3	1.5	0.6	0.5	0.8		-0.9
	1974 Jan 15	5.50			1.11	3.3	1.7		1.0			
SU Aur	1973 Oct 4	5.74	1.27	0.55	0.46							
	1973 Oct 7	5.77	1.17	0.47	0.88							
	1973 Oct 8	5.83	1.12	0.46	0.83							
	1973 Nov 9	6.03			0.93	4.2	3.0		2.1			
	1973 Dec 11	5.97			0.79	4.6	3.1	2.2	2.2	2.2		-0.2
	1973 Dec 25	6.01			0.79	4.3	3.0	2.1	2.0	2.1		-0.2
	1974 Jan 15	6.01			0.68	4.4	2.7		2.0			
RW Aur	1973 Oct 4	6.71	1.50	0.76	1.21							
	1973 Nov 9	6.97			1.08	4.8	3.6		3.0			
	1973 Dec 11	6.98			0.85	4.8	3.8		3.1	3.1		0.9
	1973 Dec 13	6.96			0.99	4.8	3.8		3.1	3.1		
	1973 Dec 25	6.95			0.99	4.7	3.5	3.0	2.9	3.0		1.5
	1974 Jan 15	6.85			0.88	4.8	3.9					
GG Tau	1973 Oct 5	7.21	1.40	0.39	0.78							
	1973 Dec 11	7.48			1.06	6.0					4.0	
HN Tau	1973 Oct 5	8.11	2.28	0.97	1.43							
	1973 Dec 14	8.64			1.59		4.6		4.0			

TABLE 3, Continued, IR Photometry in Taurus

Star	UT Date	K	J-K	H-K	K-L	4.8	8.4	10.1	11.1	12.6	10	20
DM Tau	1973 Oct 5	9.26										
	1973 Oct 9	9.37	0.85	0.50								
	1973 Dec 14	10.02			0.84						>5.3	
LkHα 266	1973 Oct 5	8.00	1.02	0.21	0.66							
	1973 Dec 14	7.90			0.51						>5.5	
HL Tau	1973 Oct 5	7.20	2.81	1.46	2.05							
	1973 Nov 9	7.43			1.91	4.1	2.6		2.3			
	1973 Nov 11	7.59			2.05	3.8	2.4		2.0	1.5		
	1973 Dec 11	7.20			1.79	3.9	2.3	2.2	1.7	1.2		-1.0
	1973 Dec 14											-0.7
	1974 Oct 19	7.61	2.95	1.61	1.60							
	1974 Nov 23	7.09	3.06	1.59	1.85							
XZ Tau	1973 Oct 5	8.57	1.43	0.72	2.39							
	1973 Nov 11	8.47			1.75	5.4	3.6		2.6	2.6		
	1973 Dec 11	8.65			1.64	5.4	3.9		3.2	2.8		0.6
	1974 Oct 19	8.12	2.01	1.00	1.82							
	1974 Nov 23	7.95	1.81	0.94	1.67							
UX Tau A	1973 Nov 11	7.45			0.69	6.5	6.3		5.7			
UX Tau B	1973 Nov 11	8.77			0.04							
CW Tau	1973 Oct 8	7.02	2.17	0.94	1.06							
	1973 Nov 12	7.27			1.46	5.2	4.2		4.0	3.5		
	1973 Nov 15	7.44			1.56	5.6	4.8		4.0		4.0	
	1973 Dec 13	7.40			1.24	5.2	4.4		4.0	3.8		
	1974 Sep 23	7.33	2.72	1.26	1.43							
	1974 Oct 20	7.03	2.71	1.15	1.07							
FM Tau	1973 Nov 15	8.73			0.43						6.2	
FN Tau	1973 Oct 8	8.14	1.81	0.61								
CX Tau	1973 Oct 8	8.75	1.12	0.20								
	1974 Sep 23	8.93	0.92	0.32								

TABLE 3, Continued, IR Photometry in Taurus

Star	UT Date	K	J-K	H-K	K-L	4.8	8.4	10.1	11.1	12.6	10	20
FP Tau	1973 Oct 8	8.86	0.78	0.11								
	1974 Sep 23	8.99	0.91	0.26								
DH Tau	1973 Nov 15	8.28			0.64						6.4:	
	1974 Dec 22	9.13	0.99	0.33	1.59							
DI Tau	1973 Nov 11	8.63			0.34							
	1973 Nov 15	8.24									6.9:	
	1974 Dec 22	8.59	1.29	0.39	0.44							
GI Tau	1973 Nov 11	8.39			0.89	6.4					4.4	
	1973 Nov 15	7.63			0.80	5.9					4.2	
	1974 Oct 19	7.62	1.49	0.53	0.83							
GK Tau	1973 Nov 11	7.73			0.84	6.0	4.8		3.7		4.3	
	1973 Nov 15	7.49			0.84	6.0					4.2	
	1974 Oct 19	6.74	1.59	0.66	0.83							
DG Tau	1973 Oct 7	6.29	2.04	0.88	1.57							
	1973 Nov 11	6.93			1.67	3.8	2.4		1.6			
	1973 Dec 11	6.65			1.62	3.6	2.2	1.9	1.4	1.3		-0.5
	1974 Sep 21	6.86	2.11	1.11	1.70							
	1974 Sep 23	6.89	2.10	1.05	1.80							
	1974 Oct 20	6.89	1.90	1.05	1.71							
DL Tau	1973 Oct 8	7.86	1.63	0.59	1.56							
	1973 Nov 12	8.09			0.86						4.7	
	1973 Dec 14	7.96			0.85							
	1974 Sep 23	7.89	1.70	0.75	1.30							
DO Tau	1973 Oct 7	7.34	1.91	1.02	1.52							
	1973 Nov 12	7.47			1.15	5.3					3.6	
	1973 Dec 13	7.43			1.16	5.3	4.0		3.4	3.6		
CI Tau	1973 Oct 8	7.73	1.83	0.61	1.02							
	1973 Dec 13	8.19			0.98		5.0					
AA Tau	1973 Oct 7	7.80	1.91	0.68	1.15							
	1973 Nov 15	7.88			0.94	6.7					4.9	

TABLE 3, Continued, IR Photometry in Taurus

Star	UT Date	K	J-K	H-K	K-L	4.8	8.4	10.1	11.1	12.6	10	20
BP Tau	1973 Oct 9	7.77	1.09	0.19	0.46							
	1973 Nov 15	7.92			0.61	6.8	5.4		4.4			
	1973 Dec 14	8.12								4.7		>1.0
DF Tau	1973 Oct 7	6.66	1.31	0.56	1.18							
	1973 Nov 11	7.02			0.66	5.3	4.8		3.9			
	1973 Dec 11	7.10			0.71		4.3		3.6			
	1973 Dec 14	7.01			0.73		4.4		3.8	3.8		
	1974 Oct 20	6.88	1.65	0.57	0.84							
DK Tau	1973 Oct 7	6.98	1.57	0.53	1.07							
	1973 Dec 13	7.16			1.03	5.3	3.6		2.9	2.9		
DN Tau	1973 Oct 7	7.98	1.14	0.23	0.84							
	1973 Nov 15	8.10			0.68	6.8					5.5	
DQ Tau	1973 Dec 13	8.13			0.91		5.2		4.9			
DR Tau	1973 Nov 12	7.47			1.62	5.0	4.2		3.4	3.1		
DS Tau	1973 Oct 9	8.37	1.45	0.50	0.67							
VY Tau	1973 Oct 9	9.16	0.55	0.06								
	1973 Dec 13	8.94			0.60						5.5	
DE Tau	1974 Sep 23	7.81	1.41	0,53	1.48							
DD Tau	1974 Dec 22	7.89	1.57	0.64	1.10							
CZ Tau	1974 Dec 22	9.26	1.13	0.47	0.93							

TABLE 4

Infrared Photometry of Stars in the Rho Oph Cloud

Star	UT Date	K	J-K	H-K	K-L	10 BB
Haro 1-1	1973 Sep 1	$8^m.75$		$0^m.20$		
	1974 Apr 31	8.98	$1^m.09$	0.08		
Haro 1-4	1972 Jun 17	7.59		1.13	$0^m.35$	
	1973 Apr 13	6.05		0.44	0.26	
	1973 Sep 3	7.25		0.57		
	1974 Jan 31	7.71			0.80	
	1974 Jun 2	7.30	1.56	0.48	0.41	
Haro 1-8	1972 Jun 17	8.78		0.26	0.24	
	1974 Jun 2	8.56	1.45	0.31		
Do-Ar 9	1973 Apr 15	9.96		0.49		
SR 22	1973 Feb 9	9.07		0.48		
	1973 Mar 25	7.91		0.48	0.16	
	1973 Apr 18	8.52		1.19		
	1973 Jun 2	8.71	1.31	0.51		
	1974 Apr 29	8.97	1.58	0.47	1.12	
	1974 Aug 20	8.70	1.50	0.49		
SR 4	1972 Jun 15	7.53			0.90	
	1973 Feb 9	7.39		0.54		
	1973 Mar 24	7.45		0.51		
	1973 Mar 31	7.33		0.49	0.35	
	1973 Apr 17	7.24				
	1973 May 21	6.41			0.21	
	1974 Feb 25	7.62			0.75	$4^m.4$
	1974 Feb 27	7.47	1.63	0.59	0.98	
	1974 Apr 29	7.44	1.65	0.59	0.90	
	1974 Jun 7	7.62			0.93	4.3
	1974 Aug 20	7.52	1.75	0.61		
Do-Ar 21	1973 Mar 26	6.12		0.48	0.20	
	1973 Mar 30	6.15		0.56	0.23	
	1973 Apr 13	6.14		0.65	0.24	
	1973 May 21	7.16				
	1974 Feb 27	6.12	1.89	0.35	0.35	
Do-Ar 24	1973 Mar 30	8.05		0.49	0.23	
	1973 Mar 31	8.05		0.42	0.95	
	1974 Jun 2	7.96	1.53	0.41	0.51	
	1974 Jun 7	8.44				4.2:
Do-Ar 24 E	1973 Mar 30	6.61		0.88	0.97	
	1973 Mar 31	6.57		0.79	1.06	
	1974 Jan 31	6.62			1.10	3.1
	1974 Feb 27	6.53	2.26	0.81	0.98	
	1974 Jun 7	6.69			0.87	3.0

TABLE 4, Continued

Star	UT Date	K	J-K	H-K	K-L	10 BB
SR 9	1972 Jun 16	7.18		0.49	0.46	
	1974 Feb 25	7.24			0.77	3.7
	1974 Feb 27	7.08	1.27	0.33	0.74	
	1974 Apr 29	7.04	1.26	0.46	0.54	
	1974 Jun 7	6.91			0.54	4.2
	1974 Aug 20	6.86	1.35	0.45		
SR 10	1972 Jun 16	8.85		0.24	1.03	
	1974 Apr 29	8.56	1.46	0.40	0.68	
	1974 Aug 20	8.64	1.16	0.51		
SR 12	1973 Sep 2	8.33		0.35		
	1974 Apr 29	8.28	1.04	0.22	0.12	
	1974 Aug 20	8.27	0.98	0.23		
SR 24 N	1974 Feb 25	7.36			1.02	2.9
	1974 Aug 20	7.00	2.49	1.07		
SR 24 S	1974 Feb 25	10.15			1.24	
SR 13	1972 Jun 15	8.11			0.35	
	1973 Feb 9	7.79		0.47		
	1973 Apr 13	7.72		0.51	0.90	
	1973 Sep 4	8.23		0.51	0.81	
	1974 Apr 29	7.86	1.07	0.39	0.21	
	1974 Jun 7	8.03			0.41	5.0
	1974 Aug 20	8.02	1.10	0.29		
SR 20	1973 Apr 13	7.55		0.10	0.90	
	1973 Sep 3	7.32		0.30	0.75	
	1974 Jun 2	6.95	1.64	0.43	0.13	
	1974 Aug 20	7.07	1.74	0.47		
Haro 1-16	1972 Jun 16	7.46		0.47	0.69	
	1974 Jun 2	7.21	1.65	0.61	0.77	
	1974 Jun 7	7.47				4.7
Haro 1-14	1972 Jun 16	7.77		0.48	-0.02	
	1974 Jun 7	7.81			0.18	
Do-Ar 51	1973 Mar 29	7.79		0.42	0.25	
	1974 Apr 31	7.74	1.13	0.27	0.05:	
Do-Ar 52	1973 Mar 29	9.14		0.65		
	1973 Apr 15	8.96		0.74		
	1974 Apr 31	9.15	1.69	0.38	0.47	
Do-Ar 53	1973 Mar 29	8.40		0.00	0.25:	
	1973 Mar 30	8.26		0.50	-0.06:	
	1973 Apr 15	7.94		0.83		
	1974 Apr 31	8.54	0.59	0.14	0.49:	
Do-Ar 58	1973 Apr 15	7.54		0.49	-0.25	

accurate and is characterized by a mean error of generally less than $\pm 0^{m}.1$.

The IR observations of the Taurus cloud stars are given in Table 3 and the IR observations of the Ophiuchus stars appear in Table 4.

Spectroscopic Observations

Spectra of the T Tauri stars in the Taurus and Ophiuchus clouds were obtained by the author with the Cassegrain spectrograph and RCA-33063 two-stage image-tube system at the Steward Observatory 2.3-m telescope. A cross-dispersing device (Carswell et al. 1975) was used to provide a low-dispersion echelle format, with orders 6 to 11 covering the wavelength range 3500 to 7000 Å at a reciprocal dispersion of 40 to 73 Å mm^{-1}, depending upon the order. The spectra were usually widened 0.3 mm and have a resolution of several Å. This system is well suited for this survey work, since it records both the blue and yellow-red portions of the spectrum simultaneously.

Spectra of a representative sample of our T Tauri stars are reproduced in Figures 1 and 2. These stars have been chosen to illustrate the wide range of veiling and line emission seen in T Tauri spectra. In this format, wavelength increases to the right along each order and upward from order to order. Some of the spectral features appear

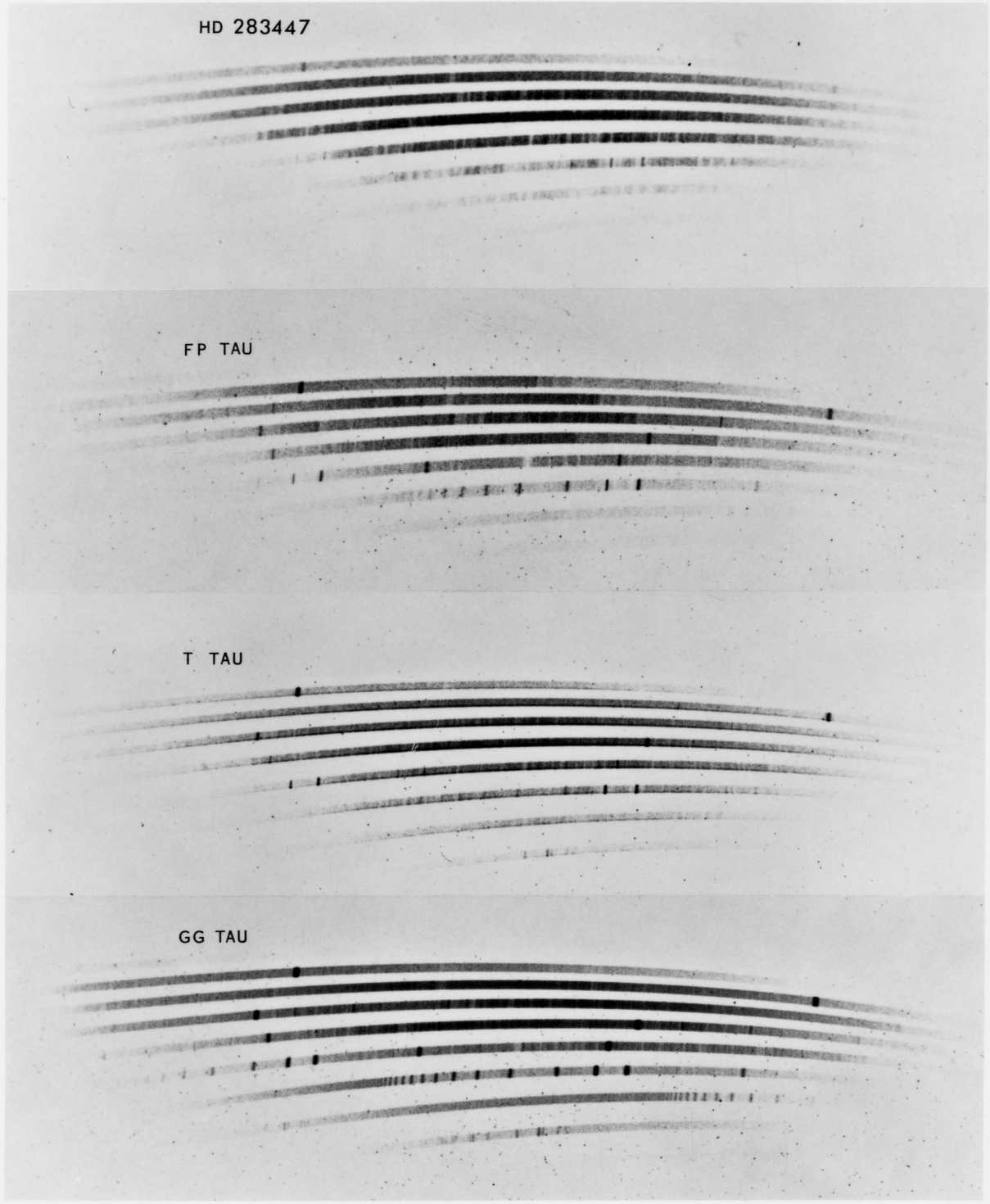

Fig. 1. , Spectra of HD 283447, FP Tau, T Tau, and GG Tau.

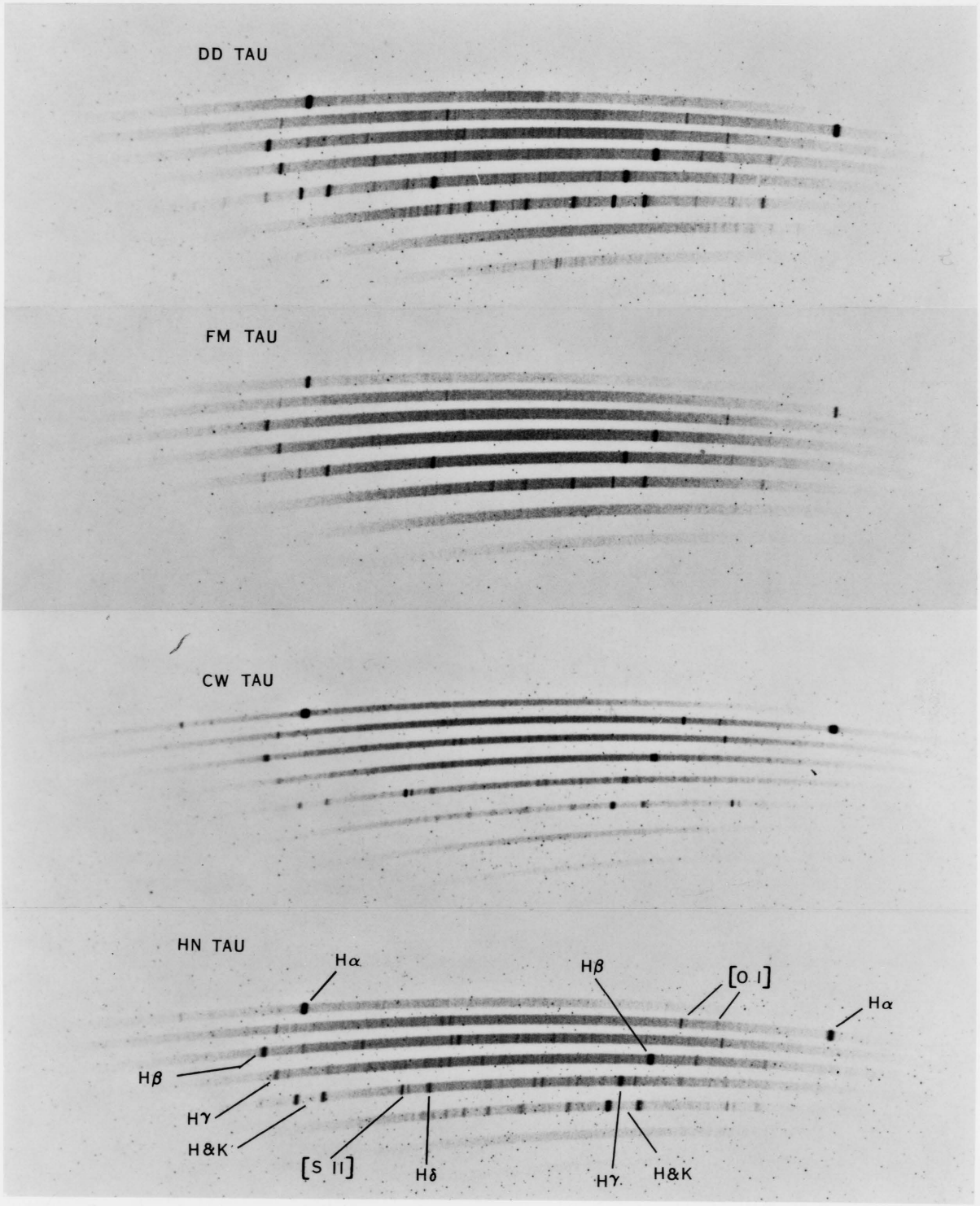

Fig. 2. Spectra of DD Tau, FM Tau, CW Tau, and HN Tau.

on two adjacent orders. The principal emission lines are identified on the last spectrum.

A summary of the photospheric spectral types and more prominent emission lines, as determined from our spectra, is given in Table 5.

Further qualitative descriptions of the spectrograms are given below for stars of particular interest and for objects which did not, at the time of our survey, exhibit T Tauri characteristics.

DM Tau: The Balmer emission lines from the series limit to Hγ and possibly Hβ show strong inverse P Cygni profiles, reminiscent of Walker's (1972) "YY Ori" stars. This profile is not observed at Hα; however, the spectrogram is rather underexposed in the red. Unfortunately, it is not possible to determine the radial velocities of the apparent absorption features from our spectrum. There is a strong suggestion of TiO bands in the yellow and red, implying an early M spectral type. Inverse P Cygni profiles are not seen in any of our spectra of other T Tauri stars in either the Taurus or Rho Oph cloud.

LkHα 266: Herbig and Rao (1972) note that there is another star of similar brightness about 2" away. Our spectrum of the brighter component (LkHα 266 A) shows intense Balmer line emission relative to the continuum. On this night of exceptional seeing, I also obtained a spectrum

TABLE 5

Spectroscopic Properties of T Tauri Stars in the Taurus and Rho Oph Clouds

Star	Sp	Veiling	Balmer Lines	He I	[O I]	[S II]	Fe II
T Tau	~K1	wk	moderate	mod	mod		v wk
RY Tau	~G5	wk	see only Hα and very weak Hβ				
SU Aur	~G2 III	wk	see only very weak Hα				
RW Aur	?	str	strong Hα,Hβ but steep Balmer decrement; Hδ very weak	mod	wk		str
GG Tau	K7	mod	strong emission to series limit; Balmer continuum emission	mod	v wk		wk
HN Tau	?	str	very strong with rather steep decrement	mod	mod	mod	str
DM Tau	M?	str	very strong with absorption on red side				
LkHα 266 A	K7:	mod	very strong emission to series limit; Balmer cont. emission	mod			v wk
HL Tau	~M2	mod	strong	mod	mod	mod	mod
XZ Tau	?	str	strong Hα, moderate Hβ		mod		
UX Tau A	G5	wk	only weak Hα				
CW Tau	?	str	very strong Hα with steep decrement		mod	mod	mod
FM Tau	?	v str	moderate	wk			
HD 283447	K2	wk	Hα clearly in emission				

TABLE 5, Continued

Star	Sp	Veiling	Balmer Lines	He I	[O I]	[S II]	Fe II
FN Tau	M2:	wk	moderate		wk		
CX Tau	M2-	v wk	moderate				
FP Tau	M2+	v wk	weak				
DH Tau	M0	str	strong to series limit	mod			wk
DI Tau	M0	v wk	weak				
GI Tau	K7	mod	moderate				
GK Tau	K5	mod	moderate				
CZ Tau	M2	wk	very weak and sharp				
DD Tau	M1	str	strong to series limit	mod	mod	mod	mod
DG Tau	?	str	strong Hα with steep decrement	mod	mod	mod	str
DL Tau	?	str	strong Hα with fairly steep decrement	mod		mod	str
DO Tau	?	str	strong	mod	mod	mod	wk
CI Tau	?	str	strong				wk
AA Tau	?	str	moderate	mod	v wk		
BP Tau	?	str	strong				
DE Tau	M1	str	strong to series limit Balmer cont. emission				v wk
DF Tau	?	v str	moderate				
DK Tau	K7:	str	moderate				
DN Tau	M0:	mod	weak and sharp				

TABLE 5, Continued

Star	Sp	Veiling	Balmer Lines	He I	[O I]	[S II]	Fe II
Haro 1-1	K7-M0:	str	strong emission to series limit; Hα and Hβ very broad	mod			wk
Haro 1-4	~K7	mod	moderate	wk			
Haro 1-8	K5:	mod	moderate	wk	mod		
SR 4	~K7	mod	moderate				v wk
Do-Ar 24	?	wk	Hα, Hβ moderate				
SR 9	K5	wk	sharp and weak	wk			
SR 10	?	str	strong	mod	v wk		mod
SR 12	~M1	wk	sharp and very weak				
SR 24 NS	?	?	Hα, Hβ strong				
SR 13	~M2	str	moderate	mod	wk		v wk
Haro 1-14	K5-K7:	mod	moderate				
Haro 1-16	K2	wk	weak				
Do-Ar 51	K7-M0	wk	weak				
Do-Ar 52	~M1?	?	moderate				

Abreviations used for veiling and emission line strengths:
v wk = very weak
wk = weak
mod = moderate
str = strong
v str = very strong

of the fainter component (LkHα 266 B). This spectrum shows TiO bands in the yellow and red, and a broad Ca I λ 4226 absorption feature, indicating an early M spectral type. There is sharp weak Balmer line emission at Hα, Hβ, and Hγ, and the Ca II H and K lines are sharply in emission. The very different appearance of the two spectra indicates no substantial contamination of the spectrum of the fainter component. LkHα 266 B appears to be a T Tauri or related star and probably is physically associated with LkHα 266 A.

XZ Tau: The Balmer line emission and the Ca II H and K emission are strong but not exceptional. However, a spectrum taken on 1973 September 20 shows the most intense display of forbidden emission lines seen in any of our T Tauri star spectra. [O I] λ 6300 and [S II] λ 4068 rival the adjacent Balmer lines in strength. The spectrum also shows [O II] λ 3727, [N II] λ 6584, and [S II] λ 6717, 6731, which are not readily seen in our spectra of any other T Tauri stars. The Fe II emission lines normally seen in advanced T Tauri spectra are not present in this spectrum of XZ Tau, but [Fe II] λ 4244 is plainly in emission. TiO bands are definitely present in the yellow and red, indicating a spectral type near M2. A second spectrum of XZ Tau was taken on 1974 November 6. The star appeared somewhat brighter than during the previous year and the spectrum shows noticeably stronger veiling. However, the forbidden

emission lines appear substantially weaker relative to the continuum.

HD 283447: Herbig and Rao (1972) note that this is a K2 star situated between the pair of T Tauri stars CW Tau and FM Tau, but give no indication that it is unusual. Our spectrum confirms the early K spectral type and plainly shows Hα and the Ca II H and K lines in emission (see Figure 1). The UBV photometry shows that HD 283447 is mildly variable and definitely reddened. Since it is seen in projection against an opaque dark cloud, it cannot be a background star. It is suggested that HD 283447 is a member of the Orion population and that it may be physically associated with CW Tau and FM Tau. Herbig (1974) has independently discovered the PMS nature of this star.

Do-Ar 22: The estimated spectral type is A7 V with no evidence of line emission. If it is in the Rho Oph cloud, it is well below the ZAMS. This may be a background star.

Do-Ar 9: The spectral type is approximately K0 with no evidence of line emission. It does not appear to be a T Tauri star.

Do-Ar 21 (Haro 1-6): This star is heavily reddened and our spectrum is too underexposed in the blue for a spectral type to be assigned. Absorption features in the yellow and red suggest that it may be a G or K star. No

line emission is seen and there is no evidence from this spectrum that it is a T Tauri star. Since this object is embedded in the Rho Oph cloud, it could still be a PMS star.

Do-Ar 24: Our spectrum shows solid Hα and Hβ emission superimposed on an absorption spectrum which is probably that of a late K star. This appears to be a T Tauri star.

SR 24 N and S: This is a close pair of faint stars separated by about 6" and with a combined V > 14.0 (visual estimate). Our spectrum of the slightly brighter southern component shows strong Hα and Hβ emission, indicating that it is probably a T Tauri star. A spectrum of the northern component was not obtained.

Do-Ar 38 (SR 20): This star is faint and heavily reddened, so that our spectra are badly underexposed in the blue; the spectral type therefore remains unknown. The spectrum does show extremely broad Hα emission (velocity half-width about 400 km sec^{-1}), which changed from a P Cygni profile in 1973 to emission with a weak self-reversal in 1974. This star probably belongs to the Orion population but its exact nature is uncertain.

Companion of Haro 1-14: This is the brighter star just northwest of Haro 1-14. Herbig and Rao (1972) note that the spectral type is K3. Our spectra confirm the early K spectral type and also show sharp Ca II H and K emission

cores extending above the continuum from the broad H and K absorption features. It is suggested that this may be a PMS star, physically associated with Haro 1-14.

Do-Ar 51, 52, and 53: These three stars form a small group seen against a major dust lane. Do-Ar 53 (SR 17) is the brightest of the three. The spectral type is approximately K3 V with no evidence of spectral veiling or line emission. The visual and IR photometry show that it is an unreddened foreground star, unrelated to the Rho Oph cloud. Do-Ar 51 is definitely a T Tauri star, with a spectral type of about K7 or M0. Do-Ar 52 (Haro 1-7) is the faintest of the three stars. Our spectrum of this star is narrow but shows the Balmer lines and Ca II H and K lines in emission. It appears to be a T Tauri star and is probably physically associated with Do-Ar 51. There is a hint of TiO bands in the red, which suggests that the spectral type of Do-Ar 52 may be near M1.

Do-Ar 58: The spectral type is approximately G8 or K0, with little or no veiling and no line emission on our spectrum. The UBV photometry shows that the star is quite reddened, so it is unlikely to be a foreground dwarf. It does not appear to be a T Tauri star.

CHAPTER 3

THE OPTICAL SPECTRAL REGION

In this chapter, the observed properties of the T Tauri stars in the wavelength range 3500 to 7000 Å are considered in greater detail. First, the spectroscopic characteristics, including the permitted and forbidden emission lines, are summarized. This leads naturally into a discussion of the unexplained veiling of the photospheric absorption spectrum. Finally, the properties of the observed light variations at optical wavelengths are examined. A synthesis of these optical data leads to a working hypothesis for understanding the envelope region surrounding T Tauri stars.

Spectroscopic Characteristics

The principal spectroscopic characteristics of T Tauri stars have been summarized by Herbig (1962). The hydrogen lines and Ca II H and K lines are always seen in emission. Fluorescent Fe I λλ 4063, 4132 emission is also characteristic of the class. When the hydrogen and Ca II lines are strongly in emission, additional emission lines due to [S II], Fe II, and Ti II may be readily seen. The underlying photospheric spectral type lies between late F

and early M. The photospheric spectrum is veiled by what is apparently an emission continuum; in extreme cases the spectrum may show little evidence of a normal absorption-line photosphere. Herbig notes a tendency for the spectral veiling to be strongest in those stars which also show the strongest emission lines. When observable, the photospheric absorption line of Li I λ 6707 is exceptionally strong.

The spectra of the T Tauri stars in our sample show no significant departures from the characteristics outlined by Herbig. The Balmer lines and the Ca II H and K lines are clearly the strongest emission features. The fluorescent Fe I emission lines cannot be identified on all of our spectra, probably because of insufficient resolution. The blue [S II] lines λλ 4068, 4076 are seen in emission in a number of T Tauri stars, but only in XZ Tau are the red [S II] lines λλ 6717, 6731 also plainly observed. As suspected by Herbig (1962), [O I] λλ 6300, 6363 emission is usually seen when the blue [S II] lines are observed. Lines of He I (especially λ 5876) and numerous Fe II lines (λλ 4233, 4582, 4629, 4923, 5018, 5169, etc.) are usually seen in emission in the stars with the strongest hydrogen emission. The Li I λ 6707 absorption line is not resolved on any of our spectra.

The forbidden emission lines seen most readily in T Tauri stars ([O I] and blue [S II]) have higher critical

densities for collisional deexcitation than do most of the common forbidden lines which are observed in H II regions and planetary nebulae. This suggests that the forbidden emission lines in T Tauri stars originate in a region which is denser than a normal gaseous nebula, with the result that the more highly forbidden transitions are effectively quenched. The ratio of [S II] λ 6717 to λ 6731, which is sensitive to electron density, is observed to be in the high density limit in XZ Tau; this supports the suggestion of a relatively dense region for the origin of the T Tauri star forbidden lines. Joy (1945) and Herbig (1961) note that the forbidden line intensities in T Tauri spectra seem more constant with time than the other emission features or the photospheric light; this suggested to Herbig that the forbidden lines come from a larger, more stable region farther from the star.

The observed T Tauri stars can basically be ordered according to the strength of the emission features. The stars with the sparsest emission line spectra (e.g., RY Tau, UX Tau A, and CZ Tau) show only weak emission in the Balmer lines and the Ca II H and K lines, superimposed on an otherwise normal late-type photosphere. At the other extreme are stars such as RW Aur and DG Tau, which show intense spectral veiling, strong hydrogen and Ca II emission lines, and numerous other permitted and forbidden lines in emission.

Our spectra strongly suggest that a continuum of T Tauri types exists between these two extremes (the spectra reproduced in Figures 1 and 2 are basically ordered according to emission strength).

For the purpose of future discussion, it is convenient to isolate a subset of our sample of T Tauri stars; we shall refer to these as the "strong-emission" stars. This group is essentially identical with those stars described by Herbig as showing the most "advanced" T Tauri spectra. The principal characteristics of this subset are (1) veiling so strong that no convincing evidence of a normal photosphere can be seen on our spectra, (2) very strong broad Balmer emission lines, sometimes with a rather steep Balmer decrement, (3) strong Ca II H and K emission, which is noticeably stronger than the adjacent Balmer lines, (4) forbidden emission lines of [O I] and [S II], and (5) numerous Fe II emission lines. These stars show a strong UV continuum, which is usually manifested as a negative observed U-B color. In the Taurus cloud, RW Aur, DG Tau, DO Tau, DL Tau, HN Tau, HL Tau, and CW Tau belong to this subclass of strong-emission stars, while CI Tau and DD Tau appear to be borderline cases. In the Rho Oph cloud, SR 10 is the only star found to show the strong-emission characteristics.

In his original investigation of T Tauri stars, Joy (1945, 1949) classified five Taurus cloud stars with strong

emission (RW Aur, DG Tau, DO Tau, DL Tau, and CI Tau) as spectral type G. Apparently these classifications were based on the extremely blue continuum colors of these stars, since few if any photospheric absorption features can be seen in the blue spectral regions of these stars. There exists up to the present time a general acceptance of these stars as being of spectral type G (e.g., Kuhi 1974), although some reservations have been expressed (Herbig 1952; Gahm 1970). Higher dispersion red spectra of some of these stars obtained recently by Herbig (1974) show late-type photospheric absorption spectra to be present in DO Tau (M1 V), DL Tau (K7 V), and CI Tau (K5 V). It is possible that DG Tau and RW Aur may also be K or M stars. This result is entirely consistent with our spectroscopic survey. In the Taurus cloud, there are no intermediate cases between these supposed G-type stars with strong emission and the legitimate G-type T Tauri stars (SU Aur, RY Tau, and UX Tau A) which are characterized by weak emission. However, there is a continuous sequence from the K- and M-type T Tauri stars with weak emission up to these strong-emission stars.

Spectral Veiling

The veiling of T Tauri spectra was described by Joy (1949) as apparently an overlying continuous emission which fills in the photospheric absorption features in the blue ($\lambda < 5000$ Å) spectral region. Herbig (1962) discusses two

components to the veiling emission - the blue veiling noted by Joy and a strong UV continuum shortward of about 3800 Å. Anderson and Kuhi (1969) and Kuhi (1970) show from spectrum scanner observations that the UV continuum very likely arises from Balmer continuum emission and the crowding of the Balmer emission lines near the series limit; this emission is believed by these authors to originate in an ionized envelope surrounding the star. However, Herbig (1970) has suggested that both the UV continuum and the blue veiling may be explained by a chromospheric temperature inversion reaching deep into the stellar photosphere.

The unusually large wavelength coverage provided by our spectra permits a more general discussion of the veiling phenomenon. Moreover, the wide range of emission properties in our sample of T Tauri stars enables us to explore the relation between the spectral veiling and the other emission features. This leads to the following conclusions:

1. The veiling emission appears to result from a true continuous emission process rather than from the superposition of many weak emission lines. Spectroscopic studies of RW Aur (Gahm 1970) and RU Lup (Gahm et al. 1974) have led to the latter suggestion; however, the spectrograms of stars such as FM Tau (Figure 2) force one to the conclusion that the fundamental veiling process is continuous. This is in accord with the description of the veiling given by Joy.

2. The intrinsic color of the veiling emission is bluer than that of a normal K- or M-type photosphere. This conclusion may be reached by several lines of argument. First, some T Tauri stars (e.g., DD Tau (Figure 2), DE Tau, SR 13), which show strong veiling in the blue, have obvious TiO absorption bands in the yellow and red. Presumably, the photospheric absorption spectrum is overwhelmed by veiling emission in the blue but not in the red spectral region. Second, some T Tauri stars (e.g., DN Tau) have observed B-V colors which are smaller than the B-V color appropriate for their spectral type; this result is particularly striking in view of the likely importance of CS and dark cloud reddening. Third, the spectral energy distributions observed by Kuhi (1974) and by Grasdalen et al. (1975) suggest that the continuum rises progressively above the expected photospheric emission toward shorter wavelengths. Despite the "blueness" of the emission continuum, there is no preferred wavelength which defines the onset of veiling. Rather, the perceptible veiling may in some cases be restricted to the blue, but in others may extend well beyond 5000 Å. These data strongly suggest that the observed spectrum of a T Tauri star is the sum of a late-type photosphere and an emission continuum which is bluer than the photosphere; the contribution of the emission continuum relative to the

photosphere spans a wide range among the members of the T Tauri class.

3. The strength of the UV and blue veiling emission correlates positively with emission line strength. This trend is readily seen in the T Tauri spectra shown in Figures 1 and 2. Quantitative confirmation of the correlation between the UV continuum flux and the Hα flux is provided by the spectrum scanner observations of Kuhi (1974). The correlation between Hα strength and the blue veiling emission is demonstrated in Figure 3. These histograms present the distribution of observed Hα equivalent widths for the T Tauri stars located in the Taurus and Rho Oph clouds. The Hα equivalent widths are mean values computed from the spectrum scanner observations of Kuhi (1974), Grasdalen (1974b), and Rydgren (1974). The hatched regions in these histograms represent stars with strong blue veiling (no blue photospheric absorption features seen on our spectra). It appears that the spectral veiling just sufficient to hide the blue part of the photospheric spectrum corresponds to a particular Hα equivalent width. These data strongly suggest that the physical processes which account for the UV continuum and blue veiling are closely related to the origin of the observed line emission.

4. Many T Tauri stars show a discontinuous increase in their spectral energy distributions shortward of the

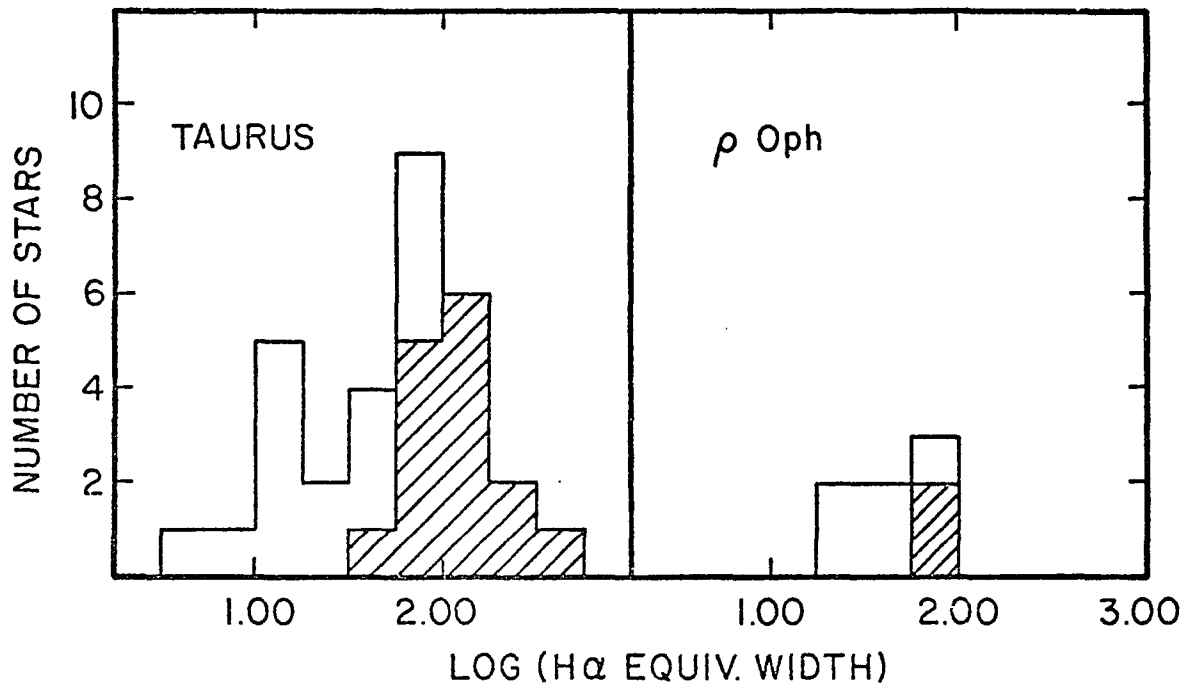

Fig. 3. Distributions of Hα Equivalent Widths.

In these histograms showing the number of stars as a function of Hα equivalent width, the stars with strong veiling of the blue photospheric features are indicated by hatching.

Balmer limit near 3650 Å. This is apparent in Kuhi's (1974) spectrum scanner observations and more dramatically in our spectra of stars such as GG Tau (Figure 1) and DE Tau. In these stars, it is certain that the UV continuum emission arises from Balmer continuum radiation.

The evidence presented above indicates that the UV continuum results from Balmer continuum emission together with unresolved Balmer line emission near the series limit, and that the blue veiling is due to a related continuous emission process with a spectral distribution somewhat bluer than a late-type photosphere. It is extremely tempting to identify the blue veiling with Paschen continuum emission. The B-V color of optically thin Paschen continuum radiation from a hot gas is on the order of $+0^{m}.5$; such a color is fully compatible with the observed properties of the blue veiling. It seems highly unlikely that H^{-} continuous emission (Dyck and Milkey 1972; Milkey and Dyck 1973) can account for the observed veiling, since the dominant free-bound component is too red. The following working hypothesis is therefore proposed: T Tauri stars are surrounded by hot ionized gaseous envelopes, which produce the observed line emission through discrete transitions and the veiling emission through free-bound and free-free hydrogen continuous emission.

The plausibility of this hypothesis has recently been explored in some detail by Kuan (1975). He has computed a series of expanding envelope models which treat the non-LTE line transfer problem, in an attempt to reproduce the observed characteristics of the T Tauri emission processes. These calculations show that the Balmer decrement and time-averaged Balmer emission line profiles can be understood in the context of such expanding envelope models. He also points out that the relative constancy of the Balmer emission line widths in velocity units seems incompatible with their origin in a strong chromosphere. Kuan finds that the Balmer emission lines are optically thick and that the expected optically thin Paschen continuum emission can readily account for the blue spectral veiling. However, the relatively small observed Balmer jumps in T Tauri spectra imply that the Balmer continuum is optically thick; this can only be understood if the envelope material nearest the star has a clumpy distribution. Kuan also presents evidence for a kinetic temperature of at least 20,000° K in the expanding envelope. These results offer considerable encouragement for seeking further tests of our working hypothesis.

Variability

Irregular light variations are characteristic of the T Tauri class. It is noted by Joy (1945) and reemphasized by Herbig and Rao (1972) that as a given T Tauri star varies

in brightness, the emission lines are usually strongest relative to the continuum at maximum light. Moreover, stars with strong emission often vary by tenths of a magnitude on a time scale of hours (Wenzel 1966; Gahm et al. 1974) while stars with weaker emission do not normally exhibit variations on this short a time scale. Gahm et al. (1974) have suggested that the variability of T Tauri stars is due to varying optical depth in the CS dust shell, but it is not clear how such a model can explain the rapidity of some of the brightness variations and the observed correlation between stellar magnitude and emission line strength. However, these observations are entirely consistent with the brightness variations in these stars being due principally to changes in the strength of the combined line and continuum emission from the CS envelope.

A more detailed examination of the brightness variations of T Tauri stars provides a further test of our basic working hypothesis. It is shown below that a model in which the envelope emission varies while the photospheric emission remains relatively constant can explain several additional properties of T Tauri star variability.

Henize and Mendoza (1973) found a correlation between spectral veiling and variability among the emission-line stars in the Chamaeleon T-association, in the sense that stars with noticeable veiling were observed to be

variable while those with little or no veiling did not appear to be variable. Our UBV photometry of T Tauri stars in the Taurus cloud has been combined with the published photometry of Varsavsky (1959), Smak (1964), and Mendoza (1968) to further explore the relationship between veiling and variability. The stars with at least four observations are sorted into three groups according to their observed blue spectral veiling and into four groups according to their observed range in B magnitude. The results appear in Table 6. There is a clear trend for the amplitude of variation to increase with the strength of the blue spectral veiling, confirming the effect reported by Henize and Mendoza. The more fragmentary data from the Rho Oph cloud (especially SR 4, SR 9, and SR 13) also support this picture. Such a correlation between veiling and amplitude of variation is to be expected if the photospheric emission is relatively constant while the strength of the veiling emission varies, since the stronger the veiling emission is relative to the photospheric radiation, the larger the amplitude of variation can be.

For a given T Tauri star, the amplitude of variation usually decreases with longer wavelength, being largest in the near ultraviolet and smallest in the near infrared. This trend is well established by the photographic UBVRI photometry of Nandy and Pratt (1972), the photoelectric

TABLE 6

Observed Range in B Magnitude as a Function of Blue Veiling

Blue Veiling	$\Delta B < 0^m.50$	$0^m.50 \leq \Delta B < 1^m.00$	$1^m.00 \leq \Delta B < 1^m.50$	$\Delta B \geq 1^m.50$
weak	4	1	0	0
moderate	3	0	1	0
strong	1	4	2	4

UBVRI photometry of Mendoza (1968), and the extensive scanner observations of RU Lup by Gahm et al. (1974). The addition of Balmer and Paschen continuous emission from the envelope to a late-type photosphere results in a decreasing ratio of veiling emission to photospheric emission with increasing wavelength in this spectral region. Variations in the envelope contribution to the total emission will consequently produce smaller variations at longer wavelengths, as observed for T Tauri stars.

Most T Tauri stars are redder when they are fainter. This is well demonstrated by the T Tauri stars DF Tau, BP Tau, and SR 13. Figure 4 shows the dependence of B-V color on V magnitude for these three stars, based on our photometry combined with that of Varsavsky (1959), Smak (1964), and Mendoza (1968). This observed behavior is easily understood in terms of our model. Since the veiling emission is bluer than the photosphere, a decrease in the envelope emission naturally increases the observed B-V color. However, this effect will be significant only as long as the veiling and photospheric emission are comparable. If the veiling emission is much stronger than the photospheric emission, varying envelope emission would not be expected to significantly change the observed color. The dependence of B-V color on V magnitude for three of the strong-emission stars in the Taurus cloud (DG Tau, HN Tau,

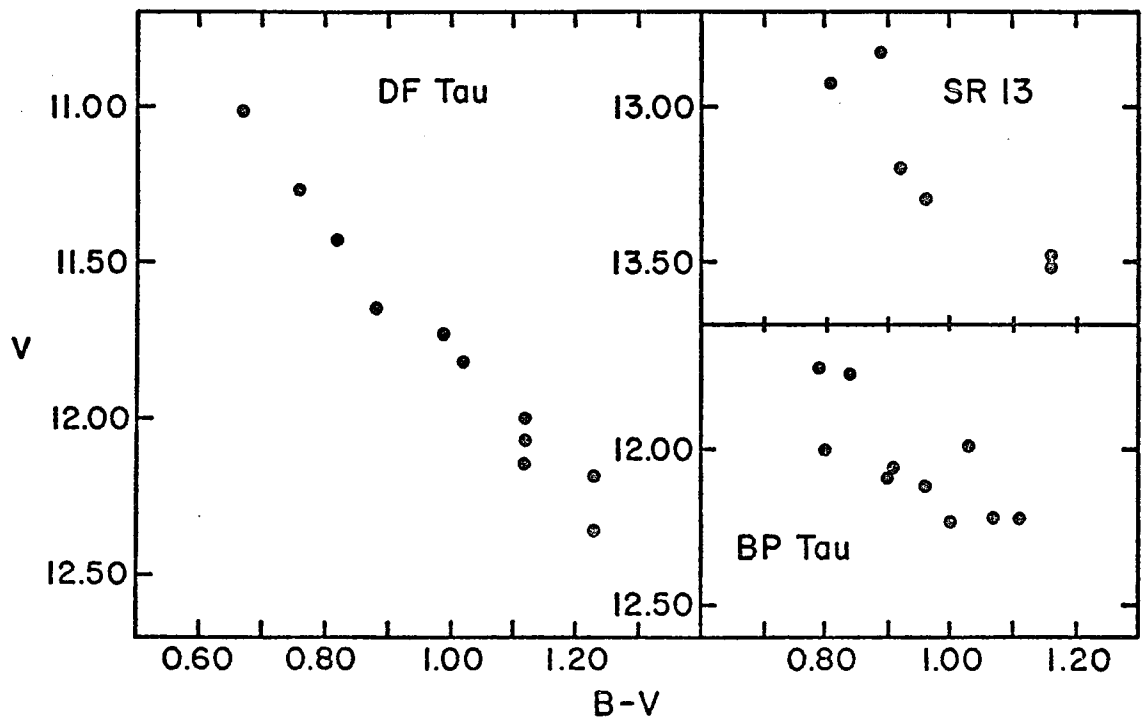

Fig. 4. Dependence of B-V Color on V Magnitude for DF Tau, BP Tau, and SR 13.

and CW Tau) is shown in Figure 5. As predicted, these stars show little or no change in B-V color as they vary in brightness. The photometric behavior of these strong-emission T Tauri stars provides further support for our assertion that the principal source of variability in T Tauri stars is the changing strength of the envelope emission.

The legitimate G- and early K-type T Tauri stars in the Taurus cloud (SU Aur, RY Tau, UX Tau A, and probably T Tau) normally exhibit slow brightness variations, often with unperiodic minima (Wenzel 1969). There is a question whether the amplitudes of variation of these stars can be explained by changes in their relatively weak envelope emission, and it is possible that a secondary mechanism is responsible for the variations of these T Tauri stars. These four stars have been excluded from the discussion of the correlation between veiling and amplitude of variation.

Our working hypothesis, which was advanced to account for the line emission and spectral veiling in T Tauri stars, also provides a natural explanation for many of the variability properties of these stars. This is additional evidence that our basic picture of T Tauri stars as surrounded by hot gaseous envelopes is correct.

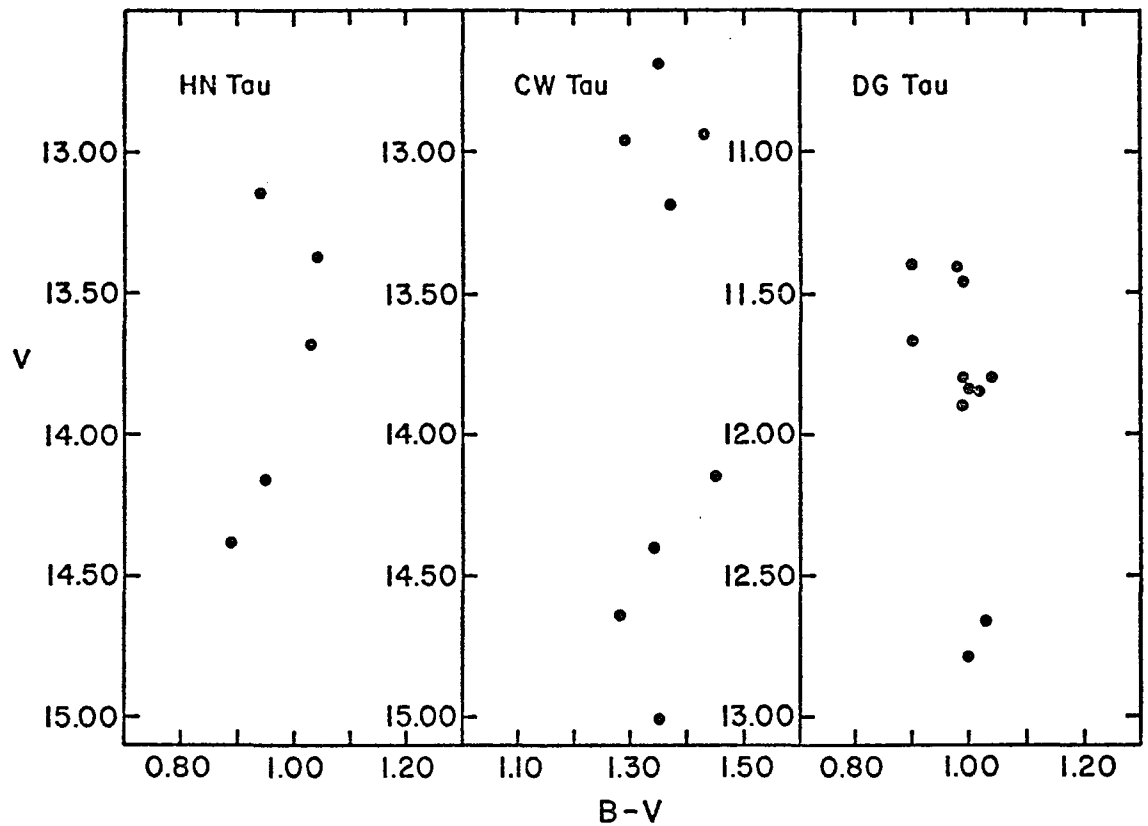

Fig. 5. Dependence of B-V Color on V Magnitude for the Strong-Emission Stars HN Tau, CW Tau, and DG Tau.

CHAPTER 4

THE INFRARED EXCESS

There seems to be a general acceptance in the literature that the IR excesses found in T Tauri stars result from optically thick CS dust shells surrounding the stars. As discussed in Chapter 1, there is substantial evidence that the class prototype, T Tau, has an optically thick dust shell, and it is not unreasonable to suppose that other members of the class are morphologically similar. The only dissenters to this view appear to be Herbig (1970), who wondered if chromospheric continuous emission might not be able to account for some or all of the observed excess, and Strom (1972), who points to the observed unit-slope relation between Hα flux and IR emission in T Tauri stars as evidence favoring a common gaseous origin for these two emission components.

A convincing test for the presence of optically thick CS dust shells around T Tauri stars is still wanting, for several reasons. First, the available observations are limited. Numerous IR observations have been made by Cohen (1973a, 1974), but he has no simultaneous optical photometry to complete the spectral energy distributions. Second, the

predictions of the CS dust shell model are hardly unique, since a judicious choice of assumptions and parameters can reproduce a broad range of IR properties. Third, it has not yet been demonstrated that we understand how to correct observations of T Tauri stars for interstellar and circumstellar extinction; this necessarily introduces uncertainty into the interpretation of the observed spectral energy distributions.

The extensive optical and IR observations made during the course of this investigation enable us to approach this problem anew. Our objective in this chapter is to obtain an understanding of T Tauri star spectral energy distributions which is as convincing and as quantitative as possible. One part of this involves extending into the IR the working hypothesis developed in the preceding chapter and seeing if emission from a hot gaseous envelope contributes significantly to the IR excess in T Tauri stars. The other principal question to be answered here is whether T Tauri stars really are surrounded by optically thick CS dust shells.

First, the predictions of both the optically thick CS dust shell model and the envelope emission model are compared on a qualitative level with the observed spectral energy distributions of T Tauri stars. This comparison suggests a direction for further investigation, which is

confirmed by quantitative fitting of the observations with theoretical models. In the course of this work, the problem of interstellar extinction and reddening for T Tauri stars is successfully handled, with somewhat surprising results. The understanding of T Tauri star spectral energy distributions which results is summarized at the end of the chapter.

Qualitative Evidence

This section begins with consideration of the expected IR behavior of photosphere-envelope and photosphere-dust shell models. The upper part of Figure 6 shows the spectral energy distribution of a K7 V star (Johnson 1966), along with two models in which an envelope emission contribution has been added to this photospheric distribution. The gaseous envelope has an electron temperature of 20,000^{o} K and is assumed optically thin at all wavelengths. In the two cases shown, the envelope contribution at the B filter is twice and five times the stellar B flux respectively. The major features apparent in the upper part of Figure 6 are:

1. The hydrogen continuous emission from the envelope can contribute significantly to the observed flux longward of 1 μ.

2. In the models, the minimum envelope contribution relative to the photosphere occurs near 1 μ. Thus, if changes in the envelope emission account for most of the

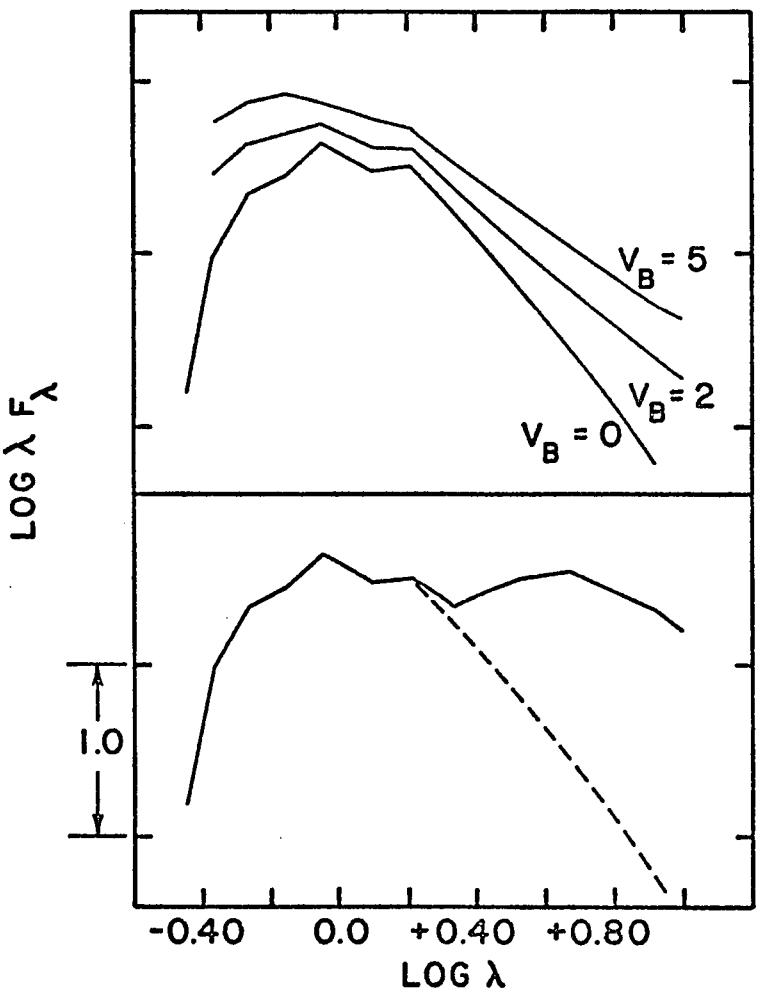

Fig. 6. Theoretical Spectral Energy Distributions of Photosphere-Envelope and Photosphere-Dust Shell Models.

(Top): K7 V star (v_B = 0) and two photosphere-envelope models (K7 V + 20,000° K envelope) with envelope flux at the B filter of twice and five times the stellar flux. (Bottom): K7 V star with a 750° K black body emission component.

observed light variations, there should be a minimum amplitude of variations near 1 μ.

3. As the strength of the envelope emission relative to the photosphere increases, the spectral energy distribution becomes flatter. Strong-emission T Tauri stars would therefore be expected to have substantial IR excesses.

4. The spectral energy distributions of the photosphere-envelope models decline monotonically longward of the flux maximum near 1 μ.

For the purpose of comparison, the lower part of Figure 6 shows the composite spectral energy distribution of a K7 dwarf and a 750° K black body source, the latter representing thermal emission from an optically thick CS dust shell. The characteristic double-peaked structure, which results from the superposition of two black bodies of significantly different temperature, is readily apparent.

The qualitative predictions of these two basic models may now be compared with observation. Figure 7 shows the observed spectral energy distributions of ten typical T Tauri stars. The data plotted represent the mean magnitudes derived from our photometry, with the R and I magnitudes estimated in a few cases from the colors measured by Mendoza (1968). In comparing these observations with the models in Figure 6, it should be remembered that there may be substantial interstellar and possibly circumstellar

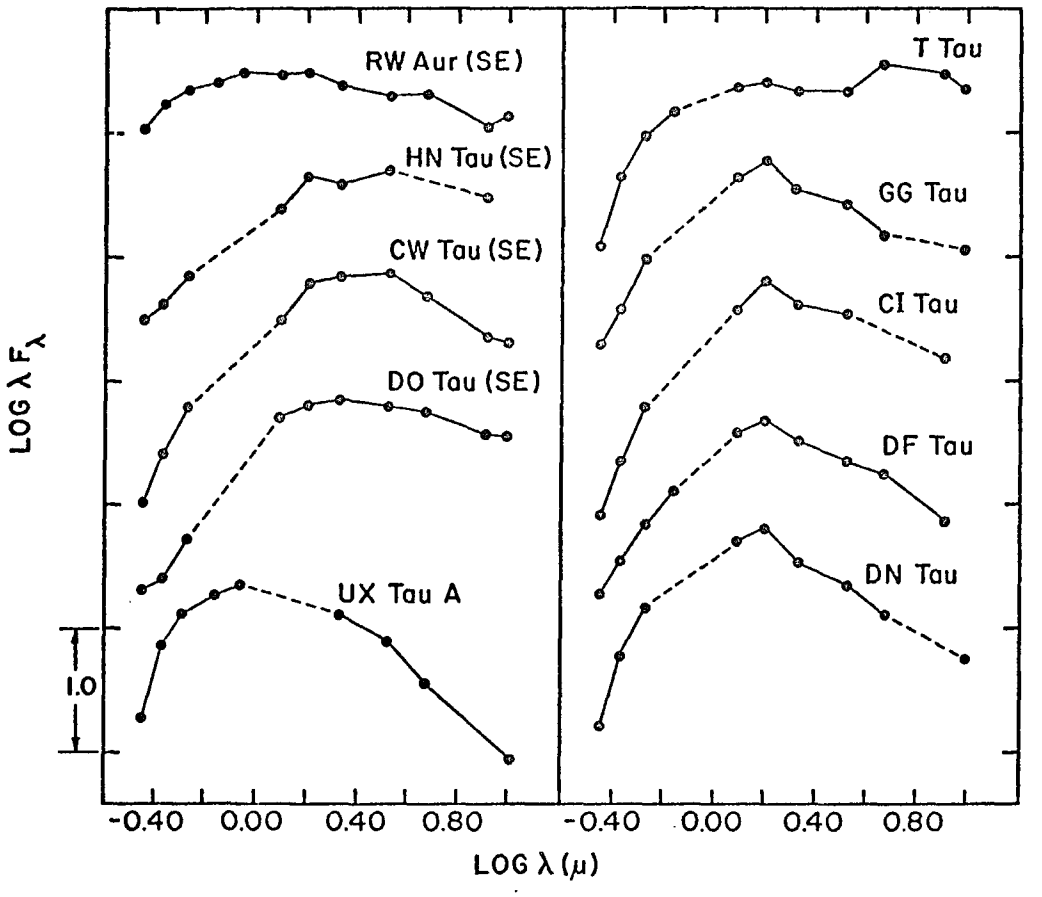

Fig. 7. Observed Spectral Energy Distributions from 0.36 to 10 μ of Selected T Tauri Stars.

Strong-emission stars are identified by "SE."

extinction at the shorter wavelengths in the real stars shown in Figure 7.

Most of the T Tauri stars in the Taurus and Rho Oph clouds have observed spectral energy distributions similar to those of GG Tau, CI Tau, DF Tau, and DN Tau (right side of Figure 7). These four stars all have spectral types of K5 or later and exhibit moderate veiling and line emission. The observed flux maximum occurs near the H filter at 1.6 μ, with the flux declining monotonically toward longer wavelength. The peak at the H filter is quite sharp relative to the adjacent filters.

The observed spectral energy distributions of four strong-emission stars (RW Aur, HN Tau, CW Tau, and DO Tau) are shown on the left side of Figure 7. These stars tend to have flatter IR spectral energy distributions, which is what one would expect for reddened stars with dominant envelope emission.

UX Tau A is a dG5 star with very weak line emission and veiling; the observed spectral energy distribution could well be that of a reddened G5 star without significant excess emission in the IR.

The observed spectral energy distribution of T Tau shows a double-peaked structure which may represent cool black body emission superimposed on the early K-type photosphere. However, this is the only star on our

observing program in either cloud which plainly shows such structure.

The IR photometry of Lee (1970) and of Catchpole and Glass (1974) shows that the sharp peak at the H filter is a characteristic of late K- and M-type stars and results from an opacity minimum near 1.6 μ in these cool stellar atmospheres. The presence of this peak in most of our T Tauri stars is evidence that the stellar photosphere is the dominant source of radiation in the 1 to 2 μ region of these objects. A similar conclusion was also reached by Grasdalen et al. (1975) from their observations of Orion population stars in the Chamaeleon T-association.

Additional information regarding the relation between the IR and optical emission is provided by the wavelength-dependence of T Tauri star brightness variations. The best illustration of this is the T Tauri star SR 13 in the Rho Oph cloud. Between 1973 and 1974, SR 13 became both fainter and redder at visual wavelengths. Our spectra show that both the Balmer emission line strength and the spectral veiling decreased during this time. The IR flux at the H filter decreased only slightly, but the flux longward of the H filter decreased even more. This observed behavior of SR 13 is fully consistent with the photosphere-envelope model, with the envelope emission simply decreasing between

1973 and 1974 while the photospheric emission remained relatively constant.

The evidence presented above favors the photosphere-envelope model for T Tauri stars and is difficult to reconcile with the CS dust shell model on several grounds:

1. The observed spectral energy distributions are qualitatively similar to those predicted by the photosphere-envelope model and, with the exception of T Tau, do not resemble the spectral energy distributions expected for stars surrounded by CS dust shells.

2. There is evidence that the stars with the strongest optical veiling and line emission also have the strongest IR excess. The simplest explanation of these observations seems provided by a model in which all of the observed continua are produced in the same region — a hot gaseous envelope surrounding the star. It is difficult to understand how a dust shell model can explain this behavior.

3. The correlated optical and IR variations of SR 13, together with the minimum amplitude of variation at 1.6 μ, are consistent with the photosphere-envelope model but appear to be incompatible with a CS dust shell model. Optical depth changes in a CS dust shell should result in anti-correlated optical and IR variations, while a star of variable photospheric luminosity inside a CS dust shell of

constant optical depth would not predict an amplitude minimum at 1.6 μ.

Quantitative Fitting

As shown in the preceding section, the qualitative evidence on the spectral energy distributions of T Tauri stars seems more consistent with the photosphere-envelope model than with the CS dust shell model. It is therefore reasonable to ask if T Tauri star spectral energy distributions can be understood quantitatively in terms of the photosphere-envelope model alone, without any CS dust. That is, do the observed spectral energy distributions, after correction for the effects of interstellar extinction, agree well with the predicted spectral energy distributions of the appropriate photosphere-envelope model? An affirmative answer to this question would be strong support for the pure photosphere-envelope model of T Tauri stars, while a negative answer would indicate that reality is more complex, probably involving CS dust shells.

The correction of the observed T Tauri star spectral energy distributions for interstellar extinction is an inherently difficult task, for several reasons. First, the presence of line and veiling emission results in unusual and uncertain intrinsic colors (Smak 1964; Aveni 1966), so that the standard method of estimating E(B-V) from observed minus intrinsic colors will likely give misleading results.

Moreover, the non-uniform distribution of obscuring material in the Taurus and Ophiuchus clouds means that an extinction estimate must be made for each star individually. Second, recent work by Carrasco, Strom, and Strom (1973) and by Grasdalen (1974a) demonstrates that the interstellar extinction law in dense young dark clouds deviates significantly from the "normal" interstellar law, in that the value of R, the ratio of total to selective extinction, is anomalously large in the dark cloud regions. The intimate association of T Tauri stars with young dark clouds strongly suggests that a dark cloud reddening law will be applicable, thus creating an additional parameter. Third, there is the possibility of absorption by CS dust in addition to extinction by interstellar dust (the distinction between these is that CS absorption only redistributes the flux in wavelength, while interstellar extinction removes energy from the beam). Because the absorbing properties of CS dust are poorly known, it is not clear how one would separate these two effects.

Two basic methods have been developed for estimating the B-V color excess of the T Tauri stars in the Taurus and Rho Oph clouds. In both cases, it is necessary to adopt a reddening law and to tacitly assume that there is no CS dust absorbing visual light and reemitting it in the IR. The assumption of the absence of CS dust is implicit in the pure

photosphere-envelope model for T Tauri stars, so that the validity of this assumption is tested simultaneously with that of the model.

The first method for estimating E(B-V) is based on visual minus IR colors, such as V-K and B-[4.8]. The observed color is taken from the averaged photometry, while the corresponding intrinsic color is estimated from a photosphere-envelope model of the appropriate spectral type and blue veiling parameter. Assumption of a specific reddening law enables one to obtain a value of E(B-V) from the resulting visual minus IR color excess. This technique provides considerable leverage, since the conversion of the visual minus IR color excess to E(B-V) is accomplished by dividing by a number in the range 3 to 5. Thus an uncertainty in the original color excess of $\pm 0^{m}.5$ can, in favorable cases, translate into an uncertainty in E(B-V) of only $\pm 0^{m}.1$.

The second method of estimating E(B-V) is based on the position of the star in the J-H, H-K two-color diagram. Because K- and M-type photospheres are characterized by a peak at the H filter relative to the J and K filters, they tend to have large J-H colors and small H-K colors (Lee 1970; Catchpole and Glass 1974). On the other hand, optically thin emission from a hot gaseous envelope has an H-K color which is larger than the J-H color. The result is

that the displacement of a late-type star in this diagram due to the addition of a hot envelope emission component (smaller J-H with increasing H-K) is roughly orthogonal to the displacement due to interstellar extinction with a dark cloud reddening law (larger J-H with increasing H-K). Therefore this diagram separates the effects of envelope emission and interstellar extinction in T Tauri stars and provides an estimate of E(B-V) which is independent of the visual minus infrared colors.

The J-H, H-K diagrams for the T Tauri stars in the Taurus and Rho Oph clouds are shown in Figures 8 and 9 respectively. The locus of unreddened K and M dwarfs is indicated by the solid line near the left side of each figure. The broken line is the expected locus of a K7 star with a 20,000° K envelope emission source, ranging from a pure photosphere at the upper left to a pure envelope emission source at lower right. In each figure, the arrow represents the reddening vector for the Ophiuchus dark cloud reddening law (Vrba et al. 1975); it is noted that other dark cloud reddening laws, such as that of NGC 2024 (Grasdalen 1974a), have slopes in this diagram which are closer to unity. The symbols in Figure 8 refer to strong-emission stars (filled triangles), G- and early K-type T Tauri stars (filled squares), and other T Tauri stars

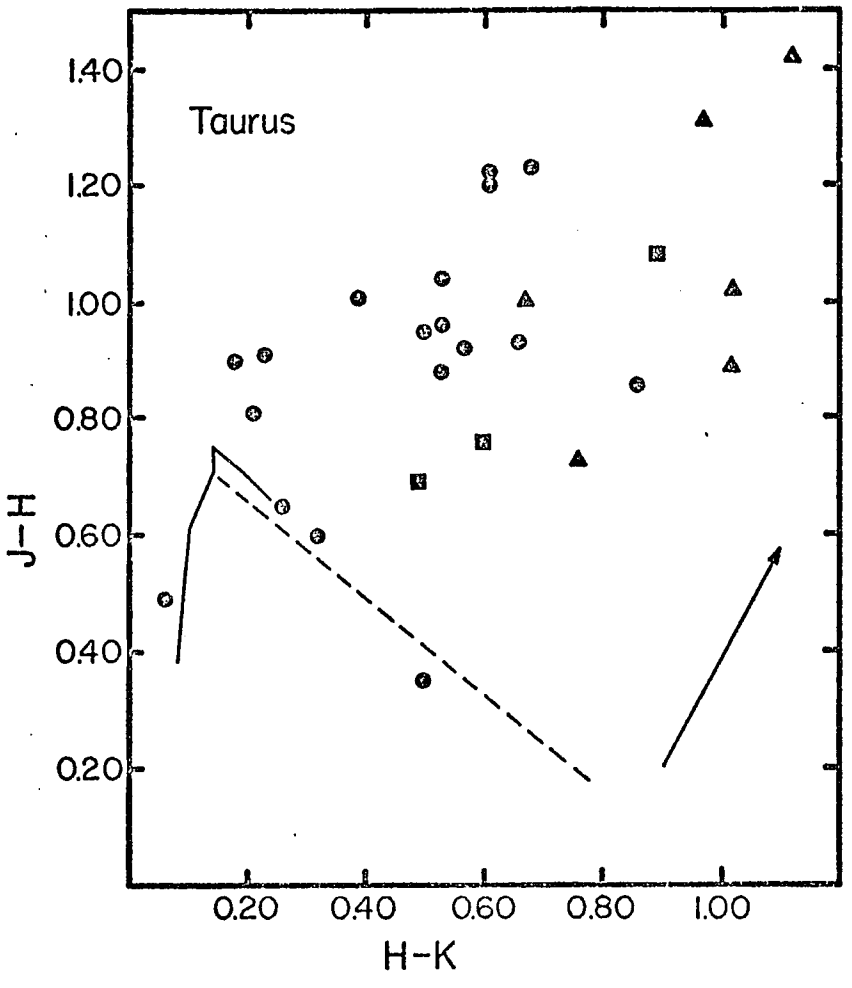

Fig. 8. J-H, H-K Diagram for T Tauri Stars in the Taurus Cloud.

Triangles are strong-emission stars, squares are G- and early K-type T Tauri stars, and circles are other T Tauri stars. Solid line at left is the locus of unreddened K and M dwarfs; broken line is the locus of all photosphere-envelope models with a K7 V star and 20,000° K envelope; arrow represents Rho Oph reddening vector.

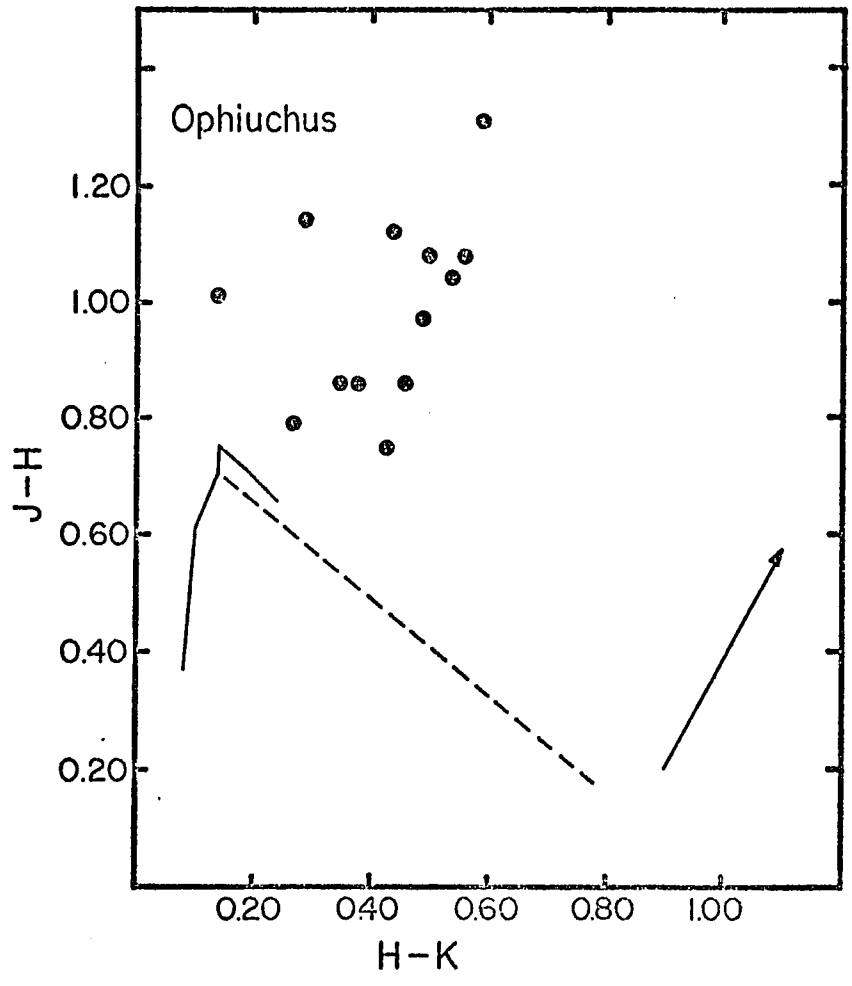

Fig. 9. J-H, H-K Diagram for T Tauri Stars in the Rho Oph Cloud.

Analogous to Figure 8.

(filled circles). In both J-H and H-K, the observational error is typically $\pm 0^{m}.1$ to $\pm 0^{m}.2$.

Several features in Figures 8 and 9 are worthy of note. First, within the observational errors, the region of the diagram occupied by the T Tauri stars is identical with the expected domain of reddened late-type stars with envelope emission. Second, the strong-emission stars are concentrated on the right side of Figure 8, exactly where the T Tauri stars with dominant envelope emission should be. Third, there is a striking absence of T Tauri stars on the right side of Figure 9, indicating a lack of true strong-emission stars in the Rho Oph cloud. This is further evidence of a significant difference in the T Tauri populations of the Taurus and Ophiuchus clouds.

E(B-V) values of T Tauri stars may be estimated from the position of the star in the J-H, H-K diagram in the following way. The point representing the star is projected down the adopted reddening vector until it intersects the line corresponding to the locus of all photosphere-envelope models of the appropriate spectral type (analogous to the broken line in Figures 8 and 9). This intersection gives the intrinsic J-H color of the star, so the J-H color excess may be found. E(B-V) is then obtained from E(J-H) through the form of the adopted reddening law. For late K and early M dwarfs, this technique is relatively insensitive to

spectral type, and it is not strongly dependent on envelope temperature in the range 10,000 to 30,000° K. With good IR colors and a known reddening law, this method should be capable of giving E(B-V) with an accuracy of about $\pm 0^{m}.1$.

For the T Tauri stars in the Rho Oph cloud, the extinction law derived by Vrba et al. (1975) is adopted. This extinction law is characterized by an R value of 4.45 and is based on photometric observations of several early-type stars embedded in the Rho Oph cloud. Since no determination of the extinction law in the Taurus complex is available, this same Ophiuchus reddening law is also adopted for the T Tauri stars in Taurus. However, it is apparent that a more extreme reddening law, with an even larger value of R, is required for at least a few of the Taurus cloud stars. In such cases, the extinction law with R = 5.5 derived by Grasdalen (1974a) for the NGC 2024 region is used.

The photosphere-envelope models used for estimating the intrinsic spectral energy distributions are constructed as follows. Photospheric spectral energy distributions over the range 0.36 to 3.5 μ for luminosity class V stars are taken from the compilation of Johnson (1966), supplemented with H-K colors from Veeder (1974). A black body with the effective temperature given by Johnson (1966) is fitted at L and used to estimate the stellar flux at 4.8, 8.4, and 10 μ.

A temperature of 20,000° K is adopted for the hot gaseous envelope because the presence of helium emission lines in T Tauri spectra indicates that the "standard" temperature of 10,000° K is too cool; independent support for this higher temperature is provided by the expanding envelope models of Kuan (1975). The flux from an optically thin free-bound and free-free hydrogen continuous emission source at this temperature is calculated at each of the standard filter wavelengths. The ratio of the envelope flux in the B filter to the stellar flux at B is defined to be the blue veiling parameter, v_B. For each spectral type and value of v_B, the envelope emission is scaled appropriately and the composite flux is calculated at each standard wavelength. The final grid of models includes all spectral types listed by Johnson (1966) from G5 V to M4 V, with v_B values of 0.0, 0.5, 1.0, 2.0, and 5.0, as well as a pure envelope emission source.

For each T Tauri star, the spectral type and blue veiling parameter are estimated from the spectra. A mean value of E(B-V) is obtained by the methods described above. This E(B-V) value and the adopted dark cloud reddening law are used to correct the observed fluxes for interstellar extinction. The resulting unreddened spectral energy distributions may then be compared with the appropriate photosphere-envelope model.

Figure 10 shows as filled circles the corrected spectral energy distributions of a number of T Tauri stars. An appropriate photosphere-envelope model, adjusted vertically for best fit, is also shown in each case as a solid line. With the exception of T Tau, the corrected observations shortward of 10 μ in Figure 10 are quite well described by the models. The major excess longward of 2 μ in T Tau probably represents black body emission from optically thick CS dust.

This agreement between model and observation shown in Figure 10 has been obtained despite a number of potential difficulties. First, the stars are variable in brightness, and our visual and IR photometry are usually not simultaneous, but rather an average of a small number of observations over several observing seasons. Second, photometric errors are not insignificant, especially for the faintest stars. Third, the proper reddening law has probably not been used in all cases. Fourth, the models are computed at discrete intervals in spectral type and blue veiling parameter, so that the adopted model is only approximately correct. And fifth, a constant envelope temperature has been assumed and the contribution of line emission in the filter bandpasses has been ignored.

The corrected spectral energy distributions of most of the other T Tauri stars which were observed in the Taurus

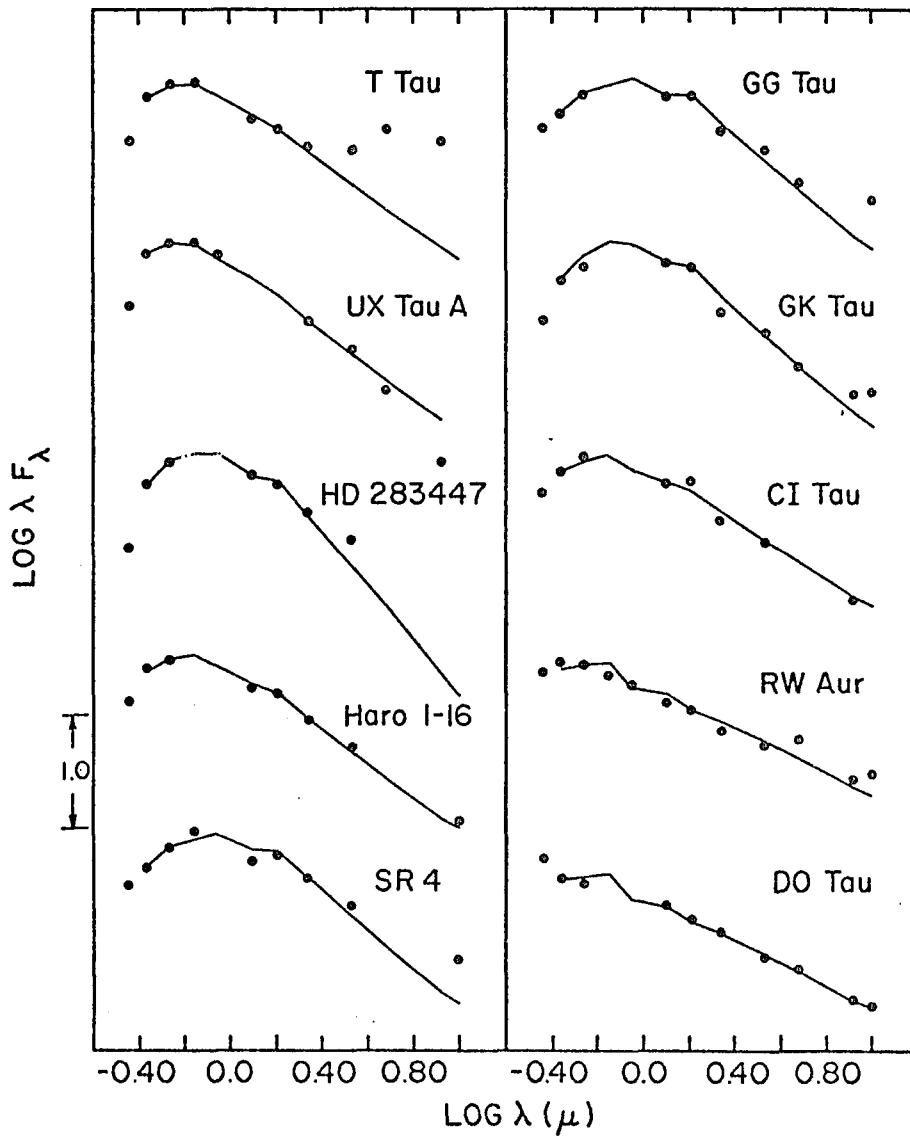

Fig. 10. Observations Corrected for Interstellar Extinction Compared with Models.

The filled circles show the observed spectral energy distributions of ten T Tauri stars corrected for interstellar extinction, while the solid lines are the appropriate photosphere-envelope models.

and Rho Oph clouds are also reasonably well approximated by the photosphere-envelope models. In those cases where some problem is encountered, it is usually of a sufficiently minor nature as to be attributable to the difficulties enumerated above. Aside from T Tau, only the G-type T Tauri stars SU Aur and RY Tau are seriously at variance with the photosphere-envelope models. It is possible that these two stars also have optically thick CS dust shells, although some evidence to the contrary is presented in the next section. This general agreement of the corrected spectral energy distributions with the photosphere-envelope models leads us to the conclusion that, shortward of 10 μ, the spectral energy distributions of most T Tauri stars are best understood in terms of a normal late-type photosphere together with the hydrogen continuous emission from a hot gaseous envelope. No support is found for the claim that optically thick CS dust shells are characteristic of the T Tauri class.

The mass of a typical gaseous envelope around a T Tauri star may be crudely estimated in the following way. Assume that the photospheric radiation can be represented by a black body of temperature T_* and radius R_*, and that the envelope emission is due to a volume of fully ionized gas with a temperature of $20{,}000^{\circ}$ K and a number density of N cm^{-3}. Then the mass of the envelope (in units of the

solar mass) is given by the expression

$$M_{env} = 5\times10^{-11} v_B (R_*/R_\odot)^2 \gamma (N_{10})^{-1}$$

where v_B is the blue veiling parameter, γ is the ratio of the stellar Planck function to a standard 4000° K Planck function at the B filter, and N_{10} is the number density in units of 10^{10} cm^{-3}. For typical values of $v_B = 2$, $R_*/R_\odot = 3$, and $\gamma = 1$, the expression reduces to $M_{env} = 10^{-9}(N_{10})^{-1}$. Kuan (1975) finds that in his uniform-flow expanding envelope models, a mass loss rate of 10^{-8} $M_\odot$ yr^{-1} corresponds to a density of about $N_{10} = 1$ at the base of the envelope. This gives an envelope mass of roughly 10^{-9} $M_\odot$. However, if the continuum-emitting part of the envelope is clumpy, as Kuan's models indicate, then the envelope mass would be smaller by several orders of magnitude. Thus the mass of a typical T Tauri star envelope is probably more like 10^{-11} $M_\odot$. Since the mass-loss rates of T Tauri stars are believed to be in the range 10^{-7} to 10^{-9} $M_\odot$ yr^{-1}, the replacement times for the envelopes should be on the order of days.

Silicate Features

Broad spectral features centered near 10 and 20 μ are observed in emission in some luminous late-type stars (e.g., Woolf and Ney 1969; Humphreys 1974) and in absorption against strong IR continuum sources such as the Galactic

Center (Hackwell, Gehrz, and Woolf 1970) and the Becklin-Neugebauer object in Orion (Gillett and Forrest 1973). These spectral features are usually attributed to the presence of finely divided silicate particles. Even though it has been shown in the preceding section that optically thick CS dust shells are not characteristic of the T Tauri class, this does not rule out the possibility of optically thin silicate emission features. Indeed, the expected presence of protoplanetary and other remnant material near T Tauri stars renders this not unlikely. In the minority of cases in which there is evidence for an optically thick CS dust shell (e.g., T Tau), silicate features might be seen either in emission or in absorption, depending upon the run of temperature with distance from the star in the CS dust shell. Finally, should a T Tauri star suffer a sufficiently large visual extinction, it is possible that a silicate interstellar absorption feature would be observable.

In a search for possible silicate features in T Tauri stars, some of the brighter stars on the observing program were observed through narrow-band filters centered at 8.4, 10.3, 11.1, and 12.6 μ, as well as through a broad-band filter centered at 20 μ. The observed spectral energy distributions of these stars in the 5 to 20 μ region are shown in Figure 11. Several points may be noted from these observations:

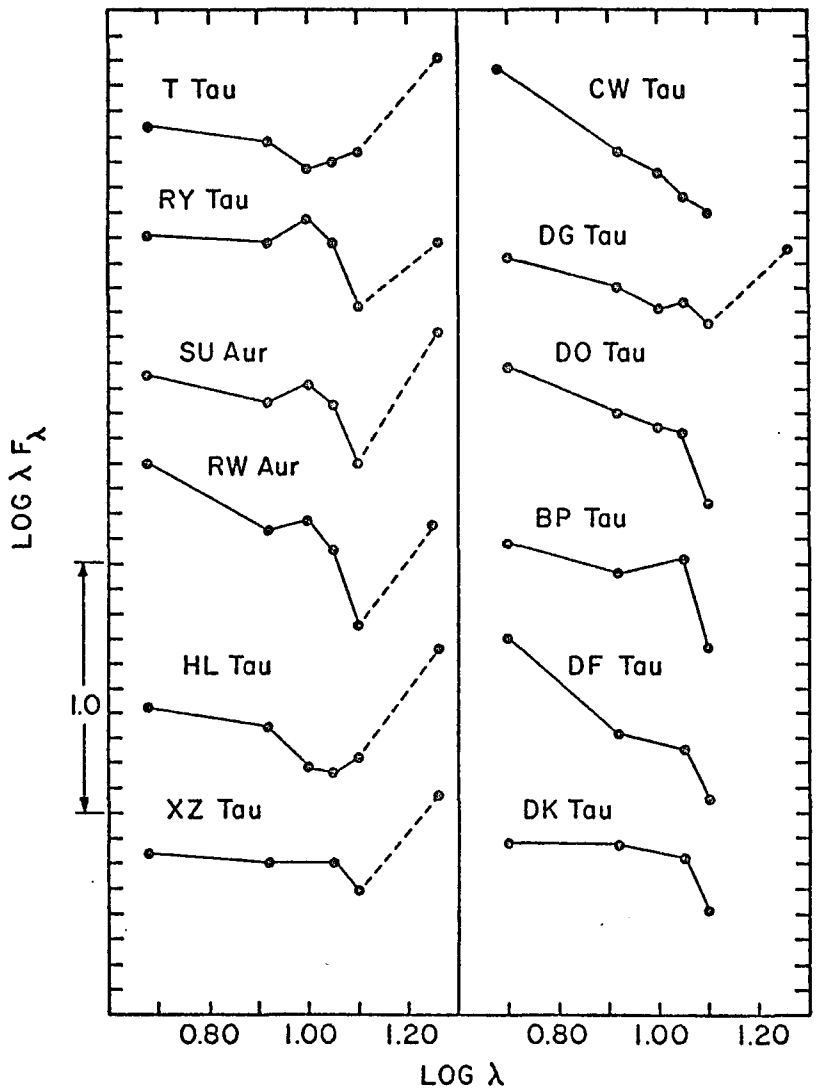

Fig. 11. Observed Spectral Energy Distributions of Brighter T Tauri Stars from 5 to 20 μ.

1. Some T Tauri stars plainly show emission features at 10 μ.

2. In all cases observed, the flux at 20 μ (in λF_λ units) is greater than or approximately equal to the flux at 10 μ.

3. Only one of the five strong-emission stars (RW Aur) shows a substantial 10 μ emission feature.

4. Two T Tauri stars (T Tau and HL Tau) have apparent absorption features at 10 μ.

The presence of 10 μ emission features in some T Tauri stars, together with the evidence against optically thick CS dust shells in these stars, is most simply interpreted as the result of optically thin clouds of small silicate particles around these stars. The observed 20 μ fluxes in these stars most likely also result from emission by the same silicate grains. The recent observations of the 4 to 8 μ region of the supergiant μ Cep by Russell, Soifer, and Forrest (1975) demonstrate that silicate emission can be present without any evidence of dust shortward of the 10 μ silicate feature. Using the ratio of 10 μ to 20 μ fluxes and the bandpass-averaged mass absorption coefficients computed by Gilman (1974), a characteristic temperature of 200 to 250° K is found for this material. This derived temperature implies that the distance of the silicate particles from the central star is on the order of

a few astronomical units. The masses of these clouds of silicate particles may be estimated from this temperature, Gilman's mass absorption coefficients, and the observed 20 μ fluxes. For seven luminous T Tauri stars in the Taurus cloud, the total masses of silicate particles are found to be in the range 10^{-7} to 10^{-8} $M_\odot$. The combined flux in the 10 μ and 20 μ emission features typically accounts for about five percent of the total observed luminosity of the star.

The inferred masses of small silicate particles around these stars correspond to approximately 10^3 years of mass loss (at 10^{-8} $M_\odot$ yr^{-1}) with complete silicate formation. Since the timescale for material leaving the stellar surface with escape velocity to reach a distance of 10 au is on the order of 10^1 years, it seems unlikely that the observed silicate particles represent a condensation in the mass outflow. Instead, it is suggested that the silicate particles are either interstellar grains from the remnant material near the star or else the result of condensation in a protoplanetary disk. Remnant material in a rotating system would tend to conserve angular momentum and accumulate in the equatorial plane of rotation, so that in either case one would expect a disk-like spatial distribution.

The relative weakness of the 10 μ emission features in the strong-emission stars is most easily explained as being due to the substantial envelope contribution at this

wavelength. The 10 μ absorption feature in T Tau is probably the result of an optical depth effect in the optically thick CS dust shell surrounding this star. Because of the greater opacity at 10 and 20 μ, the silicate features would be "formed" in a larger, cooler part of the dust shell than that responsible for the adjacent continuum dust emission; at 10 μ the larger area apparently does not make up for the smaller source function, so a silicate absorption feature is seen in this star. The observed presence of 10 μ emission features in SU Aur and RY Tau suggests that these two stars may not have optically thick CS dust shells, despite the inability in the preceding section to understand the spectral energy distributions of these stars in terms of the photosphere-envelope models. In the following section it is shown that the 10 μ absorption feature in HL Tau is very likely the result of interstellar extinction.

Further Evidence for Large Values of R

A key to understanding the spectral energy distributions of T Tauri stars is the adoption of a dark cloud reddening law with an anomalously large value of R. In the Rho Oph cloud, this approach is strongly supported by the observations of Carrasco, Strom, and Strom (1973) and of Vrba et al. (1975). In the Taurus cloud, however, there is no direct observational evidence for a large value of R.

Fortunately, an independent estimate of R in the Taurus complex can be made from the photometry of the strong-emission stars. For stars with strong envelope emission, the intrinsic B-[4.8] color is not strongly dependent on the assumed envelope temperature or on the underlying spectral type. Thus the color excess E(B-[4.8]) is readily obtained from the observed B-[4.8] color. From the definition of color excess,

$$A(V) = E(B-[4.8]) - E(B-V) + A(4.8)$$

where A(V) is the total visual extinction and A(4.8) is the extinction at 4.8 μ. For a 20,000°K envelope, the continuum B-V color is $0^m.50$. After allowing $-0^m.15$ for the contribution of line emission to the B-V color (Aveni 1966), the intrinsic B-V color is estimated to be $0^m.35$. The color excess E(B-V) can then be obtained from the observed B-V color. Through the adoption of the NGC 2024 reddening law, A(4.8) can be estimated from E(B-V) and thus a crude value of A(V) can be found. The ratio of A(V) to E(B-V) yields an approximate value of R. In this way, estimates of A(V) and R have been obtained for six reddened strong-emission stars in Taurus (HN Tau, HL Tau, CW Tau, DG Tau, DL Tau, and DO Tau). These resulting values of R range from 5 to 8. It should be noted that if the derived R value is greater than

5.5, then the adoption of the NGC 2024 reddening law provides only lower limits to both A(V) and R.

This procedure is admittedly crude, but the results do clearly support anomalously large values of R for the Taurus cloud. The only way to substantially reduce these estimates of R would be to adopt an intrinsic B-V color much smaller than $0^m.35$, so that E(B-V) becomes larger.

Observations of HL Tau provide a further check on the large values of A(V) and R derived above. This object appears to be the most heavily reddened T Tauri star observed in the course of this work, with the observed flux (in λF_λ units) peaking between 5 and 8 μ. The 10 μ region of HL Tau (see Figure 11) exhibits a silicate absorption feature with a depth estimated to be 0.12 dex. Observations of the Becklin-Neugebauer object (Gillett and Forrest 1973) and NGC 2024 #2 (Grasdalen 1974a) show that the 10 μ interstellar silicate absorption feature is usually accompanied by an ice absorption feature of about the same depth at 3.05 μ. An attempt was therefore made to observe this ice band in HL Tau with an InSb filterwheel spectrometer at the KPNO 1.3-m telescope. The observations are shown in Figure 12. The ice absorption feature is clearly present, and the depth of the feature is estimated to be 0.15 dex.

The reality of the ice absorption feature in HL Tau has been verified in two ways. First, it was independently

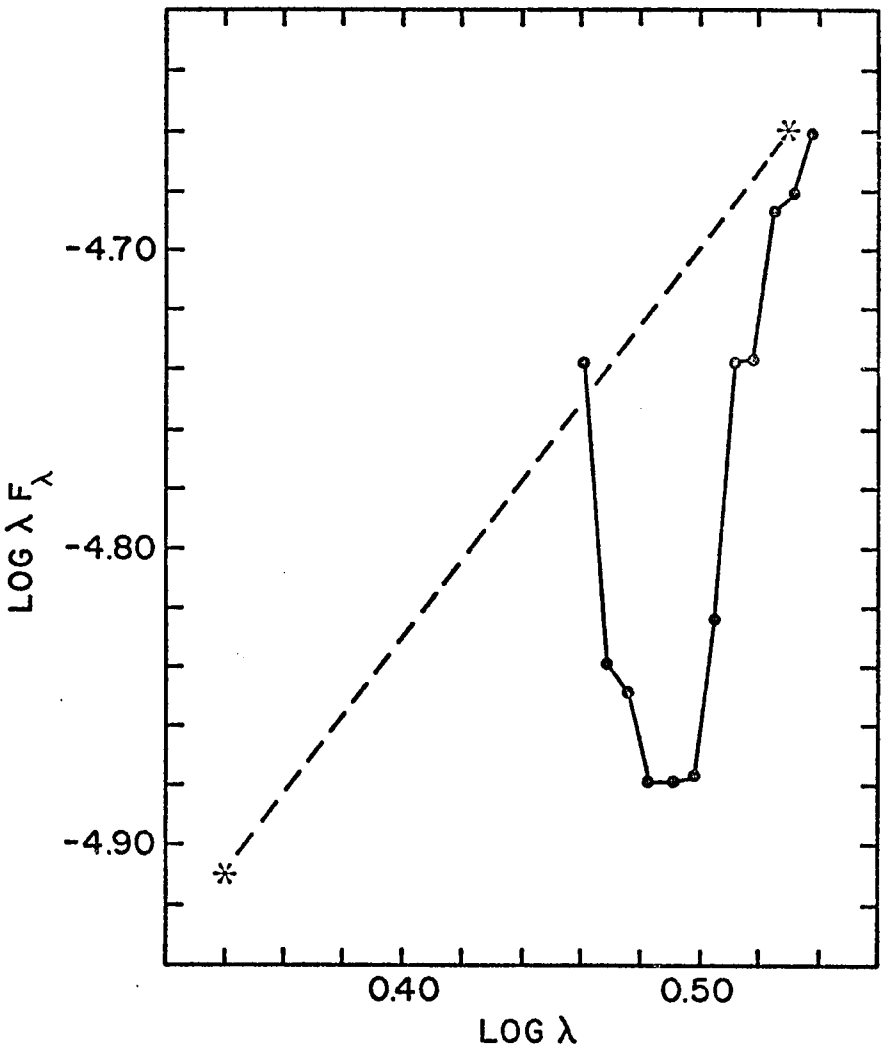

Fig. 12. Ice Absorption Feature at 3.05 μ in HL Tau.

The asterisks represent broadband K and L observations.

discovered by Cohen (1975) during a search for possible molecular features in T Tauri stars. Second, four T Tauri stars (HL Tau, XZ Tau, DG Tau, and DO Tau) were observed through IR filters centered at 2.2, 3.0, 3.5, and 3.8 μ on 1975 February 18 by S. E. Strom. These observations plainly show the ice band in absorption in HL Tau with essentially the same depth as determined from the spectrometer measurements. However, in the other three stars, there is no evidence of any ice band absorption to a limit of several hundredths of a dex.

The resulting ratio of ice to silicate absorption depths in HL Tau agrees well with the value of 1.13 given by Grasdalen (1974a). This agreement is evidence that the 10 μ absorption feature in HL Tau is interstellar in origin and that, like most other strong-emission stars, HL Tau does not have a major silicate emission feature at 10 μ. Grasdalen's (1974a) relation between A(V) and silicate absorption depth yields $A(V) = 11^m \pm 3^m$ for HL Tau. The method based on the B-[4.8] colors of strong-emission stars gives $A(V) = 7^m$ and $R = 7.4$ for HL Tau. Since this R value is greater than 5.5, the estimates of both A(V) and R from this method represent only lower limits. Therefore the agreement of these two independent estimates of A(V) may be regarded as satisfactory. This is strong support for the view that the large

values of A(V) and R derived for the six strong-emission stars are real.

A direct measurement of the extinction law in the Taurus complex would be of considerable interest, especially to check on the surprisingly large values of R (at least as large as 8) which have been derived by the crude technique described above. It should be remembered that recently-formed stars are not unbiased probes of the dark cloud extinction law, since the line of sight to such stars probably passes through some of the densest, most anomalous parts of the cloud.

Summary of Envelope Phenomena

In Chapter 3, the working hypothesis of a late-type star surrounded by a hot expanding gaseous envelope was advanced to qualitatively account for the line emission, the spectral veiling, and much of the variability observed in T Tauri stars. However, on the basis of the optical data considered, the validity of this model could not be conclusively established. Then in Chapter 4, a quantitative investigation of T Tauri star spectral energy distributions led to a remarkable discovery: when a dark cloud reddening law is used in correcting for interstellar extinction, the resulting intrinsic spectral energy distributions of most T Tauri stars are well approximated by the appropriate photosphere-envelope model.

It is emphasized that a dark cloud reddening law, with a large value of R, is crucial to this conclusion. The applicability of such a reddening law to T Tauri stars is not surprising, in view of the recent evidence for anomalous extinction in dense dark clouds (Carrasco, Strom, and Strom 1973; Grasdalen 1974a; Vrba et al. 1975) and the intimate association of T Tauri stars with such clouds. The erroneous use of a normal reddening law in place of a dark cloud reddening law leads to insufficient extinction corrections, especially in the visible, and thus to an overestimate of the true IR excess when a photosphere is fitted in the visual. It was the inability to understand the observed spectral energy distributions of T Tauri stars in terms of a normal reddening law which led Mendoza (1968) to propose the CS dust shell hypothesis.

There is now substantial evidence favoring the photosphere-envelope model for T Tauri stars. Kuan (1975) has demonstrated that the mean observed Balmer line profiles and Balmer decrements in T Tauri stars are compatible with an expanding envelope. Moreover he shows that the Balmer and Paschen continuous emission from the envelope can account for the observed UV and blue veiling. Willson (1974) emphasizes that the Fe I fluorescence phenomenon can best be understood in the context of an expanding envelope, where the velocity field plays a dominant role in exciting

the Fe I lines. Finally, it is shown in this investigation that the intrinsic spectral energy distributions shortward of 10 μ of most T Tauri stars are well described by the photosphere-envelope model of the appropriate spectral type and blue veiling parameter. Thus it is concluded that the photosphere plus hot gaseous envelope model is the correct theoretical description of the T Tauri stars.

No observational evidence is found to support the commonly-held beliefs that T Tauri stars as a class are surrounded by optically thick CS dust shells and that the line and veiling emission originate in a strong chromosphere. However, the class prototype, T Tau, is atypical in that it does appear to have an optically thick CS dust shell. Also, silicate emission features are observed in at least some T Tauri stars, indicating the presence of optically thin clouds of finely divided silicate particles near these stars.

This photosphere-envelope model directly accounts for five of the seven unusual observational properties of T Tauri stars listed in Chapter 1, thus providing a major step towards a unified physical understanding of the T Tauri phenomenon. The observed line emission is the natural result of discrete transitions in the gaseous envelope; a temperature gradient in the envelope seems required to explain such unlikely combinations as the high-excitation

He I λ 5876 emission line adjacent to the low-excitation Na I D emission lines. The spectral veiling in T Tauri stars is most simply explained as Balmer and Paschen continuous emission from the envelope. Thus the observed correlations between the emission line fluxes and the strength of the spectral veiling are the direct consequence of the common origin of these two emission components in the gaseous envelope. This is not necessarily evidence for a strong chromosphere, as Kuhi (1974) has asserted, since both the strong emission lines and the Balmer continuum are optically thick in the photosphere-envelope model. The true IR excess shortward of 10 μ in most T Tauri stars is readily accounted for by the IR extension of the same envelope continuous emission which gives rise to the spectral veiling. Since this true IR excess and the line emission both originate in the gaseous envelope, Strom's (1972) loose unit-slope correlation between Hα and IR fluxes in T Tauri stars is in accord with the photosphere-envelope model. The observed variability of T Tauri stars, which can be both rapid and of large amplitude, seems mostly due to temporal variations in the strength of the envelope emission. This provides a natural explanation for the correlation between the degree of veiling and amplitude of variations in T Tauri stars. Finally, the blue-displaced absorption components seen in the emission lines of many T Tauri stars are

probably the result of envelope material expanding away from the star along the line of sight, as suggested by Kuhi (1964).

As for the other two unusual observational properties listed in Chapter 1, the high lithium abundances found in T Tauri stars are now believed to represent the standard initial value, with the lower abundances in older late-type stars being the result of lithium depletion by convective mixing into the stellar interior (Reeves 1974). Thus the high lithium abundance in T Tauri stars is understood to be a natural consequence of their youth and is independent of the specific model adopted for the T Tauri phenomenon. The significance of the broad photospheric absorption lines in T Tauri stars, which suggest unusually large rotational velocities, will be considered in the next chapter.

The following physical picture of a T Tauri star thus emerges. The star has a relatively normal late-type (G, K, or M) photosphere and is surrounded by a hot expanding gaseous envelope. The spectral energy distributions of the strong-emission stars and the expanding envelope models of Kuan (1975) both support a kinetic temperature of at least $20{,}000^{\circ}$ K for the inner part of the envelope. Kuan also finds that the envelope material close to the star has a clumpy spatial distribution, suggesting a non-uniform heating mechanism. The Balmer lines and the

Balmer continuum are normally optically thick, while longward of the Balmer discontinuity, the hydrogen emission continua are optically thin. Emission-line widths and the blue-displaced absorption components indicate velocities of up to several hundred km sec^{-1} in the envelope. The presence of silicate emission features in some T Tauri stars shows that there are dust clouds near some members of the class, but at sufficient distance from the star so as to be optically thin and unable to emit significant flux shortward of 10 μ.

CHAPTER 5

THE EVOLUTIONARY STATE

The understanding of T Tauri star spectral energy distributions gained in Chapters 3 and 4 overcomes the serious uncertainties involving CS absorption and interstellar extinction and permits for the first time reliable estimates of the bolometric luminosities of a large number of T Tauri stars. These luminosities, together with effective temperatures derived from photospheric spectral types, represent the key to finding the evolutionary state of these stars.

The objectives of this chapter are (1) to determine the likely evolutionary state of the T Tauri stars in the Taurus and Rho Oph clouds, including age and mass ranges, and (2) to understand the unusual properties of T Tauri stars in terms of their evolutionary state. After the method of estimating bolometric luminosities has been detailed, the relative luminosities of pairs of T Tauri stars and the locus of the T Tauri stars in the H-R diagram are used to find the most likely evolutionary state of the stars. Some evidence regarding evolution during the T Tauri phase is then presented. Finally, the question of the energy source for the envelope emission is considered and a

possible link between the envelope phenomenon and the evolutionary state of the stars is suggested.

The following possibilities for the evolutionary state of the T Tauri stars are considered:

1. The T Tauri stars are low-mass stars evolving toward the ZAMS along Hayashi-Henyey QSET's. It is noted that Larson's models follow these conventional tracks subsequent to the mass infall phase.

2. The T Tauri stars are low-mass stars in a hydrodynamic phase of evolution, still accreting optically-thick shells of remnant gas and dust. Thus they correspond to the phase of mass infall in Larson's (1969, 1972) models.

3. The T Tauri stars are high-mass stars in a hydrodynamic phase of evolution preceding their arrival on the appropriate ERT. This possibility is based on Grasdalen's (1973) interpretation of V1057 Cyg and FU Ori.

4. It is also conceivable that the T Tauri stars represent a transition between the first and second cases — still surrounded by remnant CS gas and dust, but with insufficient mass infall to influence the evolution of the star.

If the first alternative is correct, the T Tauri stars should be located in a band in the H-R diagram above the ZAMS and parallel to the predicted QSET isochrones. In the second case, there should be evidence of optically thick CS dust shells and infalling material, and the stars would

not necessarily exhibit a correlation between bolometric luminosity and effective temperature. T Tauri stars identified with the third possible evolutionary state should show characteristics similar to those of the second possibility, but in a sufficiently large sample one would also expect to find some high-mass stars already on their ERT's. In the fourth case, the T Tauri stars would mimic the first alternative, but with some evidence for CS dust shells.

Bolometric Luminosities

The bolometric luminosities of the T Tauri stars in our sample are obtained in the following way. First, the interstellar extinction is estimated according to the method outlined in Chapter 4. The mean observed fluxes are then corrected for this interstellar extinction and an attempt is made to fit these corrected observations with an appropriate photosphere-envelope model. If the resulting fit is not good (many residuals exceding 0.1 dex), small changes in E(B-V) or other permissable photosphere-envelope models are tried. The Rho Oph cloud extinction law is adopted, except that the NGC 2024 law is used in a few cases where a larger value of R seems required. In the great majority of cases, either the initial attempt or the second or third iteration provides a satisfactory fit with the theoretical model. The photosphere plus envelope model is then used to estimate the flux at the standard filters for which observations are

lacking; this includes in almost all cases the important R and I filters, which should be observed in any future investigations. Finally, λF_λ is integrated over log(λ) by the trapezoidal rule from 0.36 to 10 μ to give the bolometric luminosity. Distances of 150 pc for the Taurus cloud and 170 pc for the Rho Oph cloud are assumed in converting the luminosity to solar units. In order to avoid possible bias in the resulting luminosities, no further attempts were made to improve the fit of the observations to the model once the luminosity had been calculated. The determination of the bolometric luminosity of a typical T Tauri star, GG Tau, is shown in detail in Appendix I.

The luminosities which result from this procedure are lower limits to the true luminosity, since flux emitted shortward of 0.36 μ and longward of 10 μ is not considered. After correction for interstellar extinction, the flux maximum is usually near 1 μ and the fraction of the total flux likely to be emitted longward of 10 μ is seen to be insignificant. On the other hand, neglect of the flux emitted shortward of 0.36 μ in stars with strong envelope emission probably leads to a significant underestimate of the total luminosity. However, this seems preferable to the uncertainties involved in trying to estimate corrections for envelope emission in the Balmer and Lyman continua.

For HL Tau, XZ Tau, and DG Tau, the attempts at fitting photosphere-envelope models indicate that the interstellar extinction is characterized by $R > 5.5$. In these three cases, the interstellar extinction at 4.8 μ is estimated using the NGC 2024 reddening law and an appropriate photosphere-envelope model is forced to pass through the corrected 4.8 μ flux. Integration over the spectral energy distribution of the model from 0.36 to 10 μ provides a crude estimate of the bolometric luminosity of these three stars. These values are likely to be lower limits to the true luminosity of the star.

In the case of T Tau, it is assumed that the apparent CS absorption is independent of wavelength and that all of the observed reddening is interstellar; this is supported by the good fit with the model shortward of 2 μ. However, if the CS absorption is not gray, then the derived luminosity of T Tau will probably be overcorrected for interstellar extinction and hence slightly too large. The E(B-V) value for RY Tau is crudely estimated from the observed B-V value, and the resulting luminosity is rather uncertain. The observed B-V color of SU Aur is very close to that expected for a G2 III star, so no correction for interstellar extinction is made. If SU Aur is slightly reddened, then the true luminosity will be a little larger than the value obtained above.

A number of different effects contribute to the uncertainty of the bolometric luminosity values:

1. The adopted spectral type and blue veiling parameter may not be correct. Experiments on GG Tau (K7, $v_B = 2$ adopted) show that a difference of two to three spectral subclasses changes the luminosity by as much as 0.1 dex, while varying v_B in the range 1 to 5 at spectral type K7 affects the luminosity by only about 0.02 dex. The smallness of this latter effect is partly due to the visual minus IR colors being insensitive to veiling in late K stars and thus leading to similar estimates of E(B-V).

2. The adopted reddening law may differ from the actual law. For example, use of the NGC 2024 law in place of the Rho Oph law for GG Tau increases the luminosity by 0.07 dex.

3. There may be photometric errors, especially in the 1 to 3 μ region. If the magnitudes near the flux maximum were systematically in error by $0^m.1$, the derived luminosity could be affected by as much as 0.04 dex.

4. Variability of these stars may contribute to the uncertainty in the bolometric luminosity. This will be particularly true in cases where the star exhibits large amplitude variations and we have only a small number of non-concurrent optical and IR observations.

5. The neglect of the Lyman and Balmer continuum emission will systematically underestimate the total luminosities of the stars with strong envelope emission.

6. The adopted mean distances to the two dark clouds may be in error. It is noted in Chapter 2 that the distance to the Taurus complex is still somewhat uncertain.

7. The true distances of individual T Tauri stars may deviate from the mean distance to the dark cloud complex. A probable spread in distances to the Taurus cloud stars, inferred from the projected size of the complex, leads to an additional uncertainty in the luminosity of about ±0.1 dex. This differential distance problem should be less severe in the more compact Rho Oph cloud.

Considering only the first four sources of uncertainty, it is estimated that the internal mean error in the derived luminosities ranges from about ±0.1 dex in the better cases (good spectral type and reliable UBV and JHKL photometry) to perhaps ±0.2 dex in the less favorable cases. The crude luminosity estimates for HL Tau, XZ Tau, and DG Tau may be even more uncertain.

The experiments with GG Tau also demonstrate that the fitting procedure is not a substitute for a priori knowledge of parameters such as the spectral type and reddening law. When the best estimates of E(B-V) appropriate to the specific models are used, the corrected

TABLE 7

Reddening Corrections and Bolometric Luminosities

Star	Sp	Log($L/L_\odot$)	E(B-V)	Ext. Law	Model sp	Model v_B	Fit	Notes
T Tau	K1	1.38	0.58	a	K0	1	CS dust shell	
RY Tau	G5	1.21	0.46:	a	G5	0.5	very poor	
SU Aur	G2 III	0.87:	0	-			poor	
UX Tau A	G5	0.68	0.44	a	G5	0.5	good	
HD 283447	K2	0.97	0.49	a	K3	0.5	model low at L	
RW Aur	?	0.88	0.34	b	env		model low at 4.8 μ	
GG Tau	K7	0.59	0.57	a	K7	2	good	
DM Tau	M3:	-0.52	0.19:	a	M3	5	luminosity uncertain	
LkHα 266 A	K7	0.36	0.75	a	K7	2	J and H bad?	
HN Tau	?	0.53	0.75	b	env		fair	
HL Tau	?	1.53:		c	env		luminosity uncertain	4
XZ Tau	M2	1.01:		c	M2	1	luminosity uncertain	4
CW Tau	K5:	0.91	0.88	b	env		fair	3
CX Tau	M2	-0.37	0.11	a	M2	0.5	model high at B	1
FP Tau	M2.5	-0.42	0.10	a	M3	0	good	1
DH Tau	M0	?					IR photometry inconsistent	1
DI Tau	M1	-0.15	0.26	a	M0	0.5	good	1
GI Tau	K7	0.41	0.65	a	K7	2	model low at 4.8 μ	
GK Tau	K5	0.71	0.64	a	K5	1	good	
CZ Tau	M2	-0.30	0.59	a	M2	0.5		1
DD Tau	M1	0.31	0.80	a	M2	5	model low at B, L	1
AA Tau	M1	0.23	0.47	a	M0	5	fair	1
BP Tau	K7:	0.29	0.37	a	K7	2	fair	3
DE Tau	M1	0.32	0.54	a	M1	5	L is questionable	1
DF Tau	M1	?					can fit with K7, but not M1	1

TABLE 7, Continued

Star	Sp	Log($L/L_\odot$)	E(B-V)	Ext. Law	Model sp	Model v_B	Fit	Notes
DK Tau	K7	0.77	0.71	a	K7	5	model low at 8.4 μ	
DN Tau	M0	0.17	0.30	a	M0	0.5	model low at 4.8 μ	
FN Tau	M2	0.04	0.70	a	M2	1		
DG Tau	?	1.50:		c	env		luminosity uncertain	4
DO Tau	M1	0.91	0.90	b	env		good	2
DL Tau	K7	0.55	0.63	b	K7	5	need more envelope	2
CI Tau	K5	0.66	0.79	b	K5	5	good	2
Haro 1-1	?	0.10:	0.50	a	M0	5	model high at K	
Haro 1-4	K7	0.65	0.77	a	K7	0.5	good	
Haro 1-8	K5:	0.20	0.70	a	K5	1	fair	
SR 4	K7	0.61	0.66	a	K7	2	good	
SR 9	K5	0.82	0.50	a	K3.5	1	fair	
SR 10	?	0.04	0.47	a	M2	5	good	
SR 12	M1	-0.02	0.15	a	M2.5	0	good	
SR 13	M2	0.14	0.22	a	M4	1	M2 doesn't fit well	
Haro 1-16	K2	0.82	0.80	a	K2	1	good	
Do-Ar 51	K7-M0	0.48	0.68	a	K7	0.5	fair	

Extinction Laws: a = Rho Oph
b = NGC 2024
c = R > 5.5

Notes: 1. Sp from Joy and Abt (1974).
2. Sp from Herbig (1974).
3. Sp from Joy (1949)
4. crude luminosity; see text.

observations of GG Tau are fit equally well by both the K7, $v_B = 2$ and the K5, $v_B = 2$ models. In addition, the Rho Oph and NGC 2024 reddening laws lead to equally good fits of GG Tau to the K7, $v_B = 2$ model. These results show how difficult it is to separate the effects of spectral type and reddening solely on the basis of broad-band photometry. Furthermore, a reasonable fit of the corrected observations to the model does not ensure that the proper model and correct reddening law have been chosen.

The derived luminosities of the T Tauri stars in our sample are given in Table 7. This table also includes the assumed photosphere-envelope model, the adopted E(B-V) value and reddening law, and comments regarding the fit of the corrected observations to the assumed model.

A Test for Hydrodynamic Evolution

The possibility that the T Tauri stars represent a hydrodynamic rather than a quasi-static equilibrium phase of PMS evolution can be tested in the following manner. In a sample of coeval PMS stars evolving along QSET's in the H-R diagram, the bolometric luminosity should be largest for stars having earlier spectral type. However, for stars in a hydrodynamic phase of evolution, the path in the H-R diagram may be more complex and a star of later spectral type could well be more luminous than a coeval companion of earlier spectral type (Larson 1969, 1972).

The Taurus and Rho Oph clouds contain a number of pairs of T Tauri stars with angular separations generally less than 30", which corresponds to a minimum linear separation of about 4000 au. It is argued that most if not all of these pairs represent physically-associated coeval stars. These pairs of T Tauri stars are now examined for cases in which the component of later spectral type is also the more luminous. If such a pair were indeed coeval, it would be evidence for a hydrodynamic phase of evolution.

RW Aur A and B. The spectral type of RW Aur A is unknown, while that of RW Aur B has been estimated as K3 (Herbig 1962). The separation of the stars (1".2) is too small for individual photometry.

HL Tau and XZ Tau. The spectral type of XZ Tau is near M2, while that of HL Tau is unknown due to strong spectral veiling. HL Tau almost certainly has the greater bolometric luminosity.

LkHα 266 A and B. The spectral type of LkHα 266 A is near K7, while that of the fainter B component is near M2. Individual IR photometry is not available.

UX Tau A and B. UX Tau A has a spectral type of G5. A spectrum of UX Tau B was not obtained during this work, but Joy and Abt (1974) give the spectral type as dM2.5e. UX Tau A has the greater bolometric luminosity.

CW Tau, FM Tau, and HD 283447. The spectral type of HD 283447 is near K2, but the spectral types of CW Tau and FM Tau are unknown because of strong veiling.

CX Tau and FP Tau. CX Tau is about one spectral subclass earlier than FP Tau and is slightly brighter in the visual. CX Tau has the greater bolometric luminosity.

DH Tau and DI Tau. The spectral type of DI Tau is approximately M0. The spectrum of DH Tau is well veiled, but there are weak TiO bands in the red similar to the bands in DI Tau. The bolometric luminosities are about the same.

GI Tau and GK Tau. A careful examination of our spectra shows that the spectral type of GK Tau is about K5, while that of GI Tau is definitely a little later, about K7. GK Tau has the greater bolometric luminosity.

CZ Tau and DD Tau. The fainter component CZ Tau has a spectral type of M2. Our spectrum of the brighter component DD Tau shows strong veiling, but in the red there are TiO bands slightly less advanced than those of CZ Tau. Joy and Abt (1974) classify DD Tau as dM1e, in good agreement with our spectrum. DD Tau has the greater bolometric luminosity.

UZ Tau p and f. Neither of these stars was observed during the course of this investigation.

SR 24 N and S. Because of the faintness of these stars, our spectra are not adequate for classification.

Haro 1-14 and companion. The companion is definitely brighter in the visual and its K3 spectral type is earlier than the K5-K7 spectral type of Haro 1-14. Individual IR photometry of these stars is not available.

Do-Ar 51 and Do-Ar 52. The spectral type of Do-Ar 51 is approximately K7 or M0, while that of Do-Ar 52 is less certain but seems to be near M1. The bolometric luminosity of Do-Ar 51 is greater than that of Do-Ar 52.

Of the 13 pairs of T Tauri stars considered above, there are five cases in which the component of earlier spectral type has the greater bolometric luminosity and two cases in which individual IR photometry is lacking, but the component of earlier spectral type is brighter in the visual. For one pair, the spectral types and luminosities are similar, while the remaining five pairs are indeterminate because individual photometry or spectral types are not available. No cases are found in which the component of later spectral type has the greater bolometric luminosity.

The five cases in which the component of earlier spectral type has the greater bolometric luminosity are not biased by interstellar extinction effects. In two cases (CX Tau and FP Tau; GI Tau and GK Tau), essentially identical values of E(B-V) are derived for both stars. The reddening of DD Tau appears to be slightly larger than that of CZ Tau, but this difference does not affect the relative

luminosities. Values of E(B-V) were not obtained for UX Tau B and Do-Ar 52 due to a lack of UBV photometry, but these stars are fainter than their companions at both visual and IR wavelengths. Since extinction effects are small in the IR, it is highly unlikely that these components of later spectral type can have the greater bolometric luminosity.

These observations are fully consistent with the T Tauri stars in the Taurus and Rho Oph clouds being relatively low-mass stars approaching the ZAMS along QSET's. There is no evidence here for evolution on a hydrodynamic timescale, although this small test is incapable of completely eliminating such a possibility.

More than 50 T Tauri and related late-type stars in the Taurus complex are included in the Herbig-Rao catalog, while not a single massive young star is known to be associated with this cloud. The early-type emission-line star AB Aur is located on the edge of the Taurus complex, but its spectral type of B9 and luminosity near the ZAMS (Strom et al. 1972) indicate a mass of probably no more than 3 $M_{\odot}$. This conspicuous absence of stars similar to the post-outburst phases of FU Ori and V1057 Cyg casts serious doubt on the possibility that the T Tauri stars in the Taurus cloud are high-mass stars in a hydrodynamic phase of evolution. However, this does not conflict with the rather compelling evidence from V1057 Cyg (Grasdalen 1973) that in

one case a star of approximately 8 $M_\odot$ once had the appearance of a T Tauri star. Instead, it simply suggests that the T Tauri phenomenon may be associated with a considerable range in stellar mass.

The Locus in the H-R Diagram

The observed locus of the T Tauri stars in the log L, log T_{eff} plane provides further evidence on their evolutionary state. It has already been shown above that the T Tauri stars in the Taurus and Rho Oph clouds are unlikely to be high-mass stars in a hydrodynamic phase of evolution, so the remaining viable descriptions of the T Tauri stars are Larson's picture of protostars accreting remnant material and the conventional QSET models for isolated contracting protostars, both referring to stars of lower mass. Moreover, the observed absence of optically thick CS dust shells around most of the T Tauri stars in our sample restricts any identification with Larson's models to the phase when the shell of remnant material is clearing. Larson's (1972) models for low-mass PMS stars predict that such stars should not be observed substantially above the conventional QSET isochrone for 1×10^6 years and that the most luminous stars at a given spectral type should show evidence of CS dust shells and infalling material.

The positions of the T Tauri stars in the theoretical H-R diagram are based on the bolometric luminosities

obtained by integration over the corrected spectral energy distributions and on effective temperatures derived from photospheric spectral types. The adopted spectral types are primarily from the spectra obtained during this investigation, but since the format of our spectra is not convenient for accurate spectral classification, several additional sources were also utilized. The spectral types adopted for T Tau, RY Tau, and SU Aur are those given by Herbig and Rao (1972); these types are entirely consistent with our spectra and are based on better observational material. Likewise, the homogeneous revised spectral types of Joy and Abt (1974) for some of the M-type T Tauri stars are adopted in preference to the closely similar types estimated from our spectra. In addition, spectral types for three strong-emission stars were kindly communicated by Herbig (1974). Finally, spectral types for CW Tau and BP Tau are taken from Joy (1949), but with some reservations; our spectra of these stars are too strongly veiled to yield photospheric spectral types, but the veiling may have been weaker when Joy obtained his spectra. The adopted spectral types are listed in Table 7, along with the bolometric luminosities and related information.

The effective temperature calibration given by Johnson (1966) for luminosity class V is used to obtain effective temperatures from the spectral types (exception:

SU Aur, G2 III). Because the T Tauri stars are believed to lie above the ZAMS in the H-R diagram, one would expect their surface gravities to be less than those of corresponding luminosity class V stars. However, since luminosity class IV is not defined for the later K and M stars and the spectroscopists (Joy 1945, 1949; Herbig 1962, 1974; Joy and Abt 1974) insist that T Tauri stars look more like dwarfs than giants, the luminosity class V calibration is adopted. In the event that a luminosity class intermediate between III and V is more appropriate for the T Tauri stars, then the values of log T_{eff} should be reduced systematically by perhaps 0.02 dex; this will not seriously influence the results which follow.

The log L, log T_{eff} diagrams for the T Tauri stars in the Taurus and Rho Oph clouds are shown in Figures 13 and 14. In each figure, the main sequence is indicated by a solid line and isochrones for ages of 10^5 and 10^6 years (Iben and Talbot 1966) are sketched as broken lines. Stars for which a bolometric luminosity can be estimated but which lack photospheric spectral types are indicated by arrows at the appropriate level on the right side of each figure.

As shown in Figures 13 and 14, the T Tauri stars in the Taurus and Rho Oph clouds are concentrated in a band in the H-R diagram, approximately parallel to the predicted isochrones. The lower boundary of the main band is some

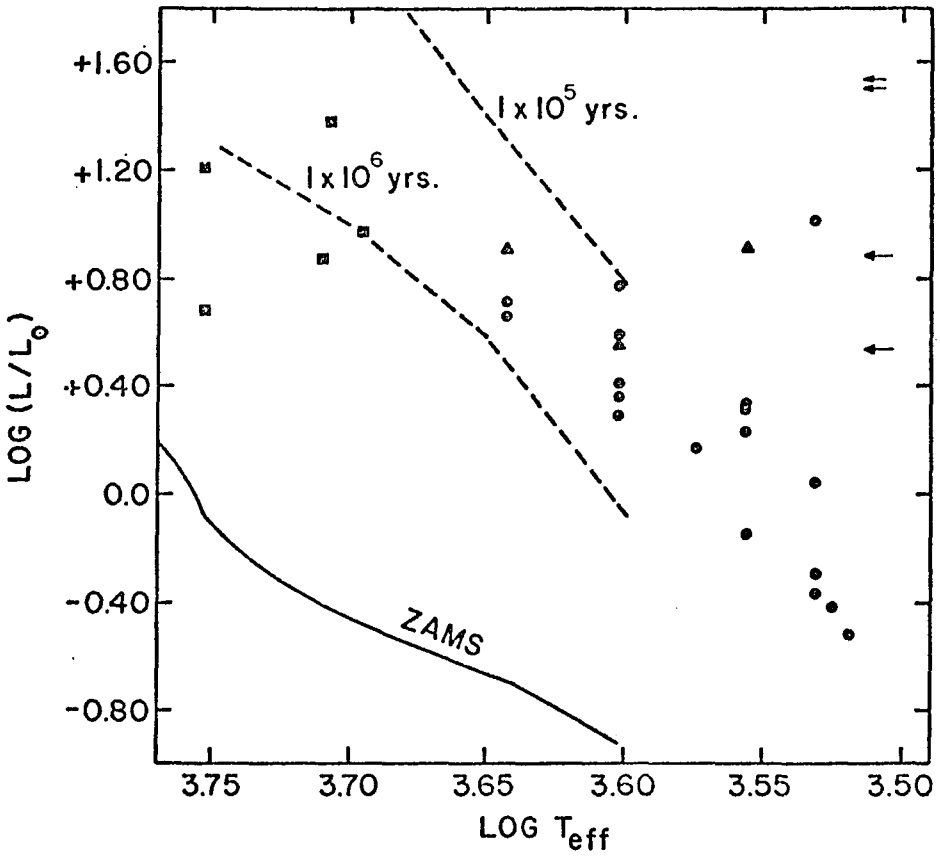

Fig. 13. H-R Diagram for T Tauri Stars in the Taurus Cloud.

The ZAMS is indicated by a solid line and two isochrones are shown as broken lines. Triangles are strong-emission stars, squares are G- or early K-type T Tauri stars, and circles are other T Tauri stars. Stars with unknown photospheric spectral types are indicated by arrows at the appropriate luminosity.

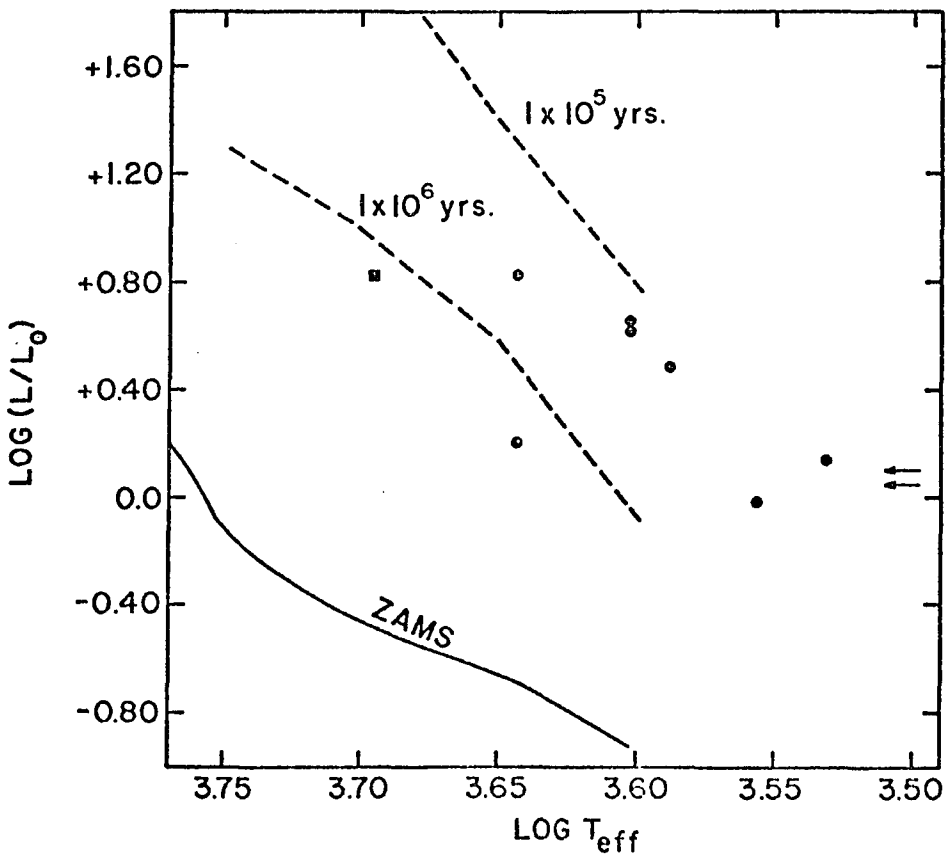

Fig. 14. H-R Diagram for T Tauri Stars in the Rho Oph Cloud.

Analogous to Figure 13.

three magnitudes above the ZAMS and corresponds roughly to the 10^6 year isochrone.

There are now several observational results for the T Tauri stars which are in disagreement with the picture outlined by Larson. First, the T Tauri stars are found generally above the isochrone for 10^6 years in the H-R diagram, with several stars (DO Tau, XZ Tau) lying substantially above this isochrone; Larson's models predict that the observed locus should be below the isochrone for 10^6 years. Second, it has been shown that optically thick CS dust shells are not common among the T Tauri stars investigated here. Third, inverse P Cygni profiles, which could be evidence for mass infall, are plainly observed in only one T Tauri star in our sample. This star is DM Tau, which happens to be the lowest luminosity T Tauri star observed in either cloud. Thus it is concluded that there is no observational basis for identifying the T Tauri stars in the Taurus and Rho Oph clouds with either the accretion or shell-clearing phases of Larson's models.

This disagreement between the details of Larson's models and the observed T Tauri stars is not evidence against his basic premises that the collapse of a protostellar cloud must be non-homologous and that the protostar will initially be surrounded by a dense cloud of remnant material. As shown by Strom, Grasdalen, and Strom (1974) in

their study of Herbig-Haro objects and related stars, mass loss rather than mass infall characterizes even the youngest observable PMS stars. This mass outflow, beginning at an early age while the star is still embedded in its natal cloud, probably disperses the remnant protostellar material, thus precluding the final accretion phase envisioned by Larson. Once the mass infall ceases, Larson's model protostars join the QSET appropriate for their mass and follow this to the ZAMS.

The fact that the locus of the T Tauri stars in the H-R diagram is parallel to the predicted isochrones, together with the absence of a viable alternative interpretation, strongly suggests that the conventional quasi-static equilibrium theory is the correct theoretical description of the T Tauri stars in the Taurus and Rho Oph clouds. Through comparison of the observed positions of these stars in the H-R diagram with theoretical QSET models, the ranges in mass and age can be estimated. It is noted, however, that the deduced ranges are sensitive to the PMS model details, especially to the treatment of the opacity in the outer part of the star. From a comparison with the isochrones of Iben and Talbot (1966), it is found that the T Tauri stars in the Taurus and Rho Oph clouds (see Figures 13 and 14) have ages generally less than 10^6 years, with most apparently older than 10^5 years. DO Tau and XZ Tau are likely candidates for

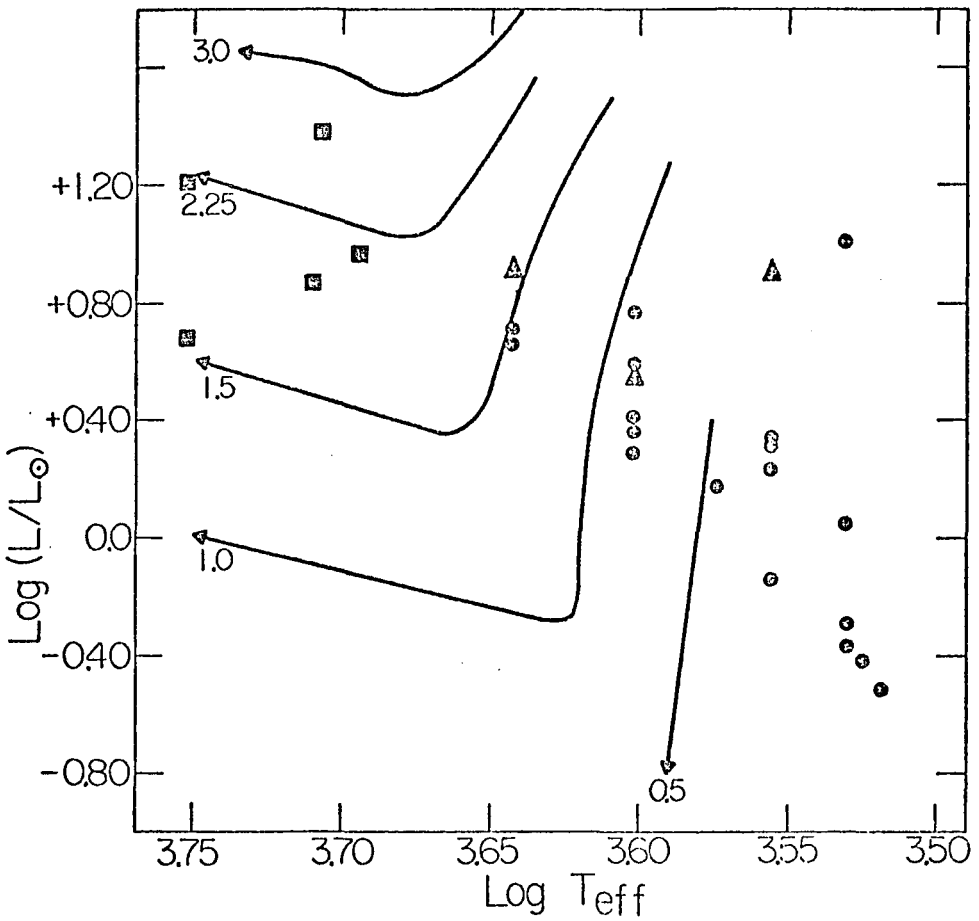

Fig. 15. Taurus Cloud Stars Compared with Theoretical Evolutionary Tracks in the H-R Diagram.

Iben's evolutionary tracks for stars of 0.5, 1.0, 1.5, 2.25, and 3.0 $M_{\odot}$ are shown as solid lines.

very young T Tauri stars, based on their position well above the main band of T Tauri stars. Figure 15 shows the evolutionary tracks of Iben (1965) superimposed on the log L, log T_{eff} diagram for the T Tauri stars in the Taurus cloud. From this it appears that the masses of the Taurus cloud T Tauri stars are less than 3 $M_{\odot}$, with most being less than about 1 $M_{\odot}$. A similar mass range is found for the T Tauri stars in the Rho Oph cloud. With the exception of the G and early K stars, the T Tauri stars in these two clouds appear to be still in the vertical or Hayashi phase of evolution. The evolutionary tracks of Ezer and Cameron (1967a, 1967b), which claim an improved treatment of the opacity over Iben's models, suggest slightly smaller masses and younger ages for the T Tauri stars in our sample.

Evolution During the T Tauri Phase

A scenario for PMS evolution has been suggested recently by Strom, Grasdalen, and Strom (1974). In their view, protostars collapse and form in dense regions of dark interstellar clouds. A newly-formed star has a small peculiar velocity (typically 1-2 km sec^{-1}) relative to the cloud and begins its slow journey toward the cloud boundary, still surrounded by remnant material. During this early phase (age less than about 10^5 years), the star is believed to have a high rate of mass loss and strong envelope emission; this conclusion is based on observations of

reflection nebulae associated with Herbig-Haro stars. As the stellar wind dissipates the remnant material surrounding the star and the star drifts toward the surface of the cloud, the visual extinction diminishes. Meanwhile, the evolution of the star causes the bolometric luminosity, the mass-loss rate, and the strength of the envelope emission to decrease with time. When the star has dispersed its remnant material and is sufficiently close to the dark cloud boundary, it becomes readily observable at visual wavelengths. Strom, Grasdalen, and Strom identify the T Tauri objects with stars in this stage of evolution. The mass-loss rate and the strength of the envelope emission continue to decrease with time as the star evolves toward the ZAMS and the star soon ceases to exhibit the characteristics of the T Tauri class.

It is clear that the strength of the envelope phenomena, as measured by the mass-loss rate and the envelope emission, decreases between the T Tauri phase and the ZAMS (e.g., Skumanich 1972). Thus it is reasonable to suppose that this same trend occurs within the T Tauri phase, as suggested in the scenario. The strong-emission stars have been picked out spectroscopically as the subset of the T Tauri class with the strongest envelope emission. Moreover, Kuhi (1964, 1966) has shown that the strong-emission stars have the highest mass-loss rates among the

T Tauri stars; this point is further supported by the measurement of the emission-line widths on our spectra. Thus the strong-emission stars are established as the members of the T Tauri class with the strongest envelope phenomena. If the basic scenario is correct, these stars should also be among the youngest T Tauri stars. This would be evidenced both as unusually large bolometric luminosities, indicating stars higher up on their evolutionary tracks, and greater visual extinctions resulting from the stars being more deeply embedded in their natal clouds.

The relatively large sample of T Tauri stars in the Taurus cloud permits a test of this hypothesis. Figure 16 shows histograms in which the number of T Tauri stars is presented as a function of both bolometric luminosity and visual extinction; strong-emission stars are indicated by hatching. As a group, the strong-emission stars are seen to be more luminous than the average T Tauri star and to have greater visual extinctions. Both of these results support the identification of the strong-emission stars as being a young subset of the T Tauri class. This is also additional evidence for the validity of the scenario outlined by Strom, Grasdalen, and Strom.

A crude estimate of the timescale for the strong-emission phase can be obtained from the fraction of the Taurus cloud T Tauri stars which appear to be strong

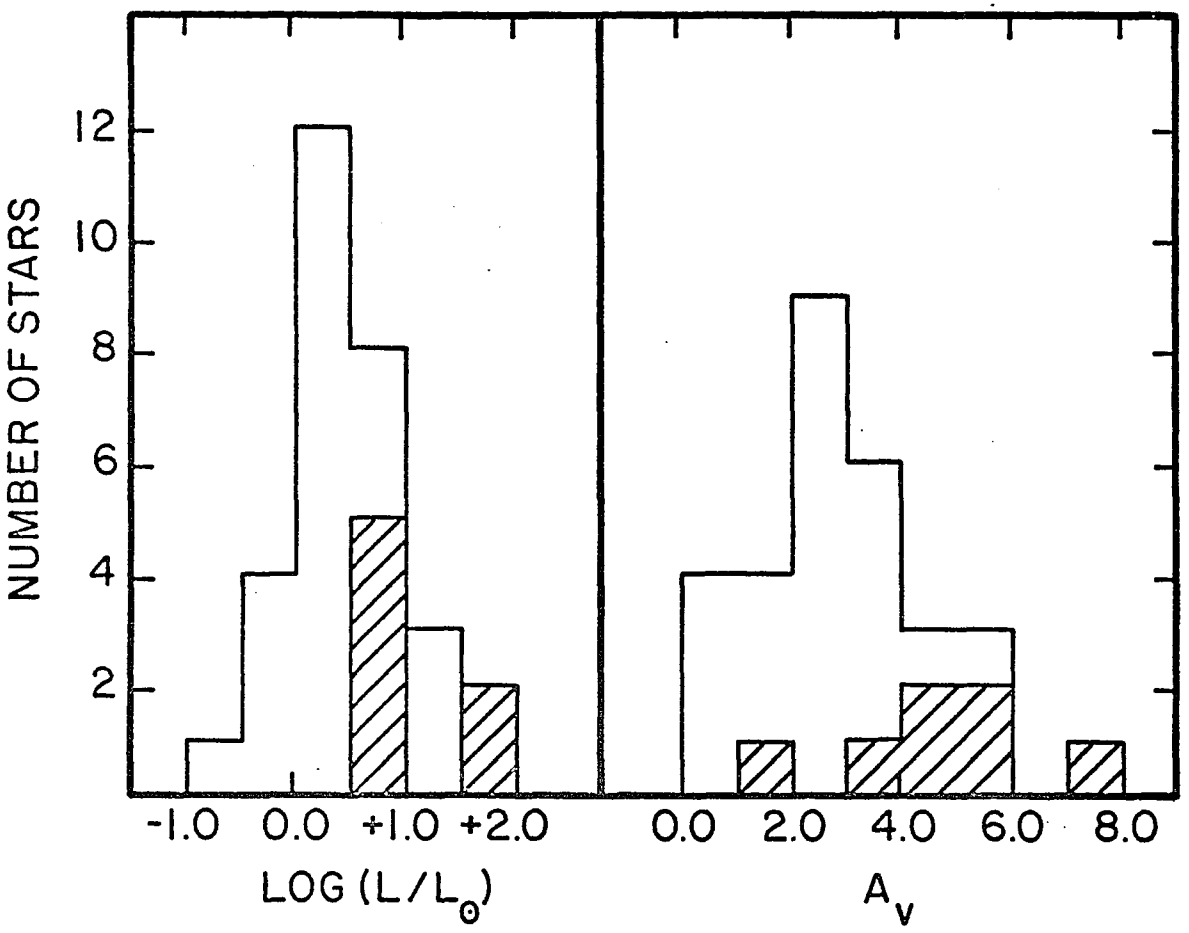

Fig. 16. Histograms Showing the Number of Taurus Cloud T Tauri Stars as a Function of Bolometric Luminosity and Total Visual Extinction.

Strong-emission stars are indicated by hatching.

emission stars. Seven of the 34 T Tauri stars observed spectroscopically in Taurus are classified as strong-emission stars. However, our observing program is biased towards the inclusion of strong-emission stars (the G:e stars), so this sample should not be used for statistical purposes. Examination of the Herbig-Rao catalog indicates that all of the likely strong-emission stars in the Taurus complex are included in our sample. Thus the fraction of strong-emission stars in Taurus is estimated to be 7/56, based on the 56 T Tauri stars listed in the Herbig-Rao catalog. If it is assumed that (a) all of the strong-emission stars have been identified, (b) the T Tauri phase lasts 10^6 years, (c) all T Tauri stars pass through a strong-emission phase, and (d) the rate of star formation in Taurus has been constant for the last 10^6 years, then a timescale for the strong-emission phase of $1\text{-}2\times10^5$ years is obtained.

There are seven known strong-emission stars in the Taurus cloud, while only one of the T Tauri stars in the Rho Oph cloud, SR 10, exhibits the characteristics of a strong-emission star. However, the spectroscopic appearance of SR 10 differs somewhat from that of the typical strong-emission star in the Taurus cloud, in that the Balmer emission lines are both narrower and weaker and the forbidden emission spectrum is far less developed. The spectral

energy distribution of SR 10 can be fitted by a well-veiled early M star model and the resulting luminosity is significantly smaller than the values found for the strong-emission stars in Taurus. Thus it appears that SR 10 is not really comparable to the luminous strong-emission stars observed in the Taurus cloud.

The apparent absence of luminous strong-emission T Tauri stars, Herbig Ae-Be stars, and Herbig-Haro objects in the Rho Oph cloud is strongly suggestive of a significant difference between the populations of the Taurus and Rho Oph clouds. Thus it appears that the Taurus complex has a PMS population with a range in age, including some very young objects, while the Rho Oph cloud has only an older PMS population. The simplest interpretation is that star formation is continuing in the Taurus complex but that no stars have been formed recently in the Rho Oph cloud.

However, there is another possible explanation for the apparent absence of strong-emission T Tauri stars and other very young objects in the Ophiuchus region. The dense opaque knots in the Taurus complex generally have radii on the order of a few tenths of a parsec, based on their size on the Palomar Sky Survey prints and a distance of 150 pc, while the opaque part of the Rho Oph cloud has a radius of about a parsec. Herbig (1962) summarizes the evidence from radial velocities and proper motions which indicates that

the peculiar velocities of the T Tauri stars in the Taurus complex are on the order of 1 to 2 km sec^{-1}; the preliminary results from Herbig's (1975) recent spectroscopic work also support this value. Thus the time required for a typical Taurus cloud star to drift to the surface of its natal cloud should be no more than several times 10^5 years. If the same peculiar velocities apply to the stars in the Rho Oph cloud, then the corresponding drift times for stars in this cloud are at least 5×10^5 years. Using the timescale of $1\text{-}2\times10^5$ years for the strong-emission phase, it is seen that T Tauri stars in the Taurus complex should be near the edge of their natal clouds at the completion of the strong-emission phase, while T Tauri stars in the Rho Oph cloud should still be deeply embedded in the dark cloud material. Thus on the basis of cloud sizes and drift times, there is a plausible alternative explanation for the apparent absence of luminous strong-emission T Tauri stars in the Rho Oph cloud. This same argument would also apply to the Herbig Ae-Be stars and Herbig-Haro objects, since the characteristic ages of these are believed to be similar to the timescale of the strong-emission phase (Strom, Strom, and Grasdalen 1975).

The evidence presented above indicates that the strength of the envelope phenomena decreases with age during the T Tauri phase and that the strong-emission stars represent a young subset of the T Tauri class. Moreover, a

comparison of visual extinctions demonstrates that the strong-emission T Tauri stars in the Taurus complex are still partially embedded in their natal clouds, while the other T Tauri stars have generally wandered away from the most obscured regions. Thus the duration of the strong-emission phase should be similar to the drift times in the Taurus complex. The independently-determined estimates of these two timescales are in fact comparable; this agreement supports the validity of both this basic picture and the crude timescales involved.

The Envelope Energy Source

Up to this point, the emphasis has been on seeking an understanding of *what* a T Tauri star is. It has been shown that the T Tauri stars studied in the two clouds are relatively low-mass PMS stars with ages generally less than 10^6 years, and that most of the unusual properties characterizing the T Tauri class are the manifestation of the hot gaseous envelope surrounding the star. However, this does not answer the fundamental question of *why* these young stars have such large and luminous CS envelopes. It seems likely that the key to this problem is the identification of the energy source which powers the envelope.

Previous work on the energy source for T Tauri star emission has focused on an extension of the solar case, with acoustic waves generated in the strong convection zones

steepening into shocks as they move upward and thus heating the region above the photosphere (Dumont et al. 1973; Schwartz 1974). However, the separation of the observed spectral energy distributions into photosphere and envelope components via the adopted models casts doubt on this hypothesis. A good example is CI Tau, which almost belongs in the strong-emission subset. The total luminosity between 0.36 and 10 μ is found to be 4.6 $L_\odot$, while the appropriate K5, $v_B = 5$ model attributes 2/3 of this emission (3.1 $L_\odot$) to the envelope. For the true strong-emission stars, the envelope emission certainly accounts for more than half of the total observed luminosity (not including the unobserved Lyman and Balmer continua) and amounts to at least several $L_\odot$. Assuming a duration of 10^5 years for the strong-emission phase with an average envelope luminosity of 4 $L_\odot$, one obtains a conservative estimate of 5×10^{46} ergs emitted by the envelope during this phase alone. There are still some difficulties in understanding how the relatively weak solar chromosphere and corona can be heated by mechanical energy from the convection zones (Stein and Leibacher 1974), so it is not clear that this mechanism can explain cases in which more than half of the total luminosity is apparently passed through the photosphere in a non-radiative form.

The locus of the T Tauri stars in the H-R diagram (Figures 13 and 14) is between the regions occupied by the

dwarfs and giants of the corresponding spectral types. Since most of the T Tauri stars are K or M stars still on their Hayashi tracks, they should be in convective equilibrium and intermediate in structure between the K and M dwarfs and the K and M giants. But neither the dwarfs nor the giants of spectral type K and M exhibit anything approaching the envelope activity of the T Tauri stars, so it seems unlikely that the envelopes around T Tauri stars can derive their energy simply from the stellar convection zones.

A third bit of evidence regarding the envelope energy source is provided by the pairs of T Tauri stars CX Tau and FP Tau, CZ Tau and DD Tau, and DH Tau and DI Tau. These presumably-coeval pairs contain stars of closely similar spectral type (indicating almost identical masses) but of noticeably different envelope emission strength. This suggests that the strength of the envelope emission depends not only upon the mass and age of the T Tauri star, but also on one or more additional parameters.

The one basic physical characteristic which seems to distinguish the T Tauri stars from the normal dwarfs and giants of spectral type K and M is the apparently much larger rotational velocities of the T Tauri stars relative to the normal late-type stars (Herbig 1957). It is therefore suggested that the additional parameter is the stellar

angular momentum, and that the presence of hot gaseous envelopes around T Tauri stars is intimately related to the rapid axial rotation of these stars.

It is currently believed that stars of all masses are formed with substantial angular momentum, and that the present low rotational velocities of the G, K, and M dwarfs are the result of a spindown process, probably involving braking due to magnetic fields and stellar mass loss (e.g., Kraft 1970). The rotational velocity break near spectral type F5 corresponds to the onset of a strong outer convection zone in main sequence stars and indicates that the spindown process depends upon the presence of a convective envelope in the star. Apparently this convection zone generates and twists the stellar magnetic field, leading to heating of the region above the photosphere and resulting in the loss of both mass and angular momentum from the star.

The T Tauri stars combine rapid axial rotation with strongly convective structure, substantial mass loss, and possibly large primordial magnetic fields. One would therefore expect these stars to be experiencing a significant loss of angular momentum. This leads us to suggest that the T Tauri stars be identified with low-mass convective protostars undergoing a rapid initial spindown, and that this rapid spindown is responsible for the envelope phenomena in these stars.

The actual rotational velocities of T Tauri stars are poorly known, because spectroscopic estimates of Vsin(i) require high-dispersion spectra and most T Tauri stars are simply too faint to be observed with a coudé spectrograph. The range in projected rotational velocity of 20 to 65 km sec^{-1} given by Herbig (1957) refers to four bright G- and early K-type T Tauri stars, all of which show rather weak envelope emission relative to the photosphere. Unfortunately there are no determinations of the rotational velocities of the youngest members of the T Tauri class, the strong-emission stars. Let us suppose, however, that these stars initially have an equatorial rotational velocity of several hundred km sec^{-1}, which is a large fraction of the break-up velocity for stars with radii of 2 to 3 $R_\odot$.

The e-folding time (t, in years) for loss of angular momentum due to a radial mass outflow uncoupling from the star at the Alfven radius (R_A) is given by the expression:

$$t = (5.05(R_A/R_*)^2(\dot{M}/M))^{-1}$$

where R_* is the stellar radius, $\dot{M}$ is the mass-loss rate in solar masses per year, and M is the stellar mass in units of the solar mass. For a typical strong-emission T Tauri star, it is estimated that $R_A = 5R_*$ (evidence for a number on this order is given by Willson 1975), $\dot{M} = 10^{-7}$ (Kuhi 1966), and $M = 1$. These values lead to an e-folding time for angular

momentum loss of about 10^5 years, which is similar to the timescale of the strong-emission phase estimated previously. This result is especially sensitive to the ratio R_A/R_*, for which we have only a crude estimate. Nevertheless this demonstrates that the timescale of the initial spindown could be comparable to that of the strong-emission phase.

The rotational kinetic energy of a star goes as the square of the angular velocity, so that most of the energy should be lost during the early part of the spindown process. Consider a fully-convective star of unit solar mass with a radius of 3 $R_\odot$ and an initial rotational velocity of 200 km sec^{-1}. If the radius were reduced to 2 $R_\odot$ by evolutionary contraction and the rotational velocity decreased to 40 km sec^{-1} through angular momentum loss, the star would have to lose between 5×10^{46} and 1×10^{47} ergs of excess rotational energy. Thus the excess rotational kinetic energy of a T Tauri star spinning down from near break-up velocity is comparable to the conservative estimate of the energy radiated by the envelope during the strong-emission phase. However, this remarkable agreement depends upon the rotational velocities of the strong-emission stars being significantly larger than those of Herbig's G- and early K-type T Tauri stars, and there is as yet no direct observational evidence for this.

This similarity of energies suggests a picture in which the rotational kinetic energy of the star is dumped above the photosphere and provides the energy radiated by the envelope. This energy transfer probably involves the star's magnetic field, perhaps analogous to solar flaring, and results in the heating of some of the gas near the star to quite high temperature ($> 20{,}000^{\circ}$ K). A simple calculation shows that most of the energy deposited in the envelope is radiated away and no more than several percent goes into kinetic energy of mass outflow. Coupling of the rotational energy to the envelope by time-variable magnetic fields provides a mechanism for changing the rate at which energy is dumped in the envelope, thus possibly accounting for the variability of the T Tauri stars. Moreover, magnetic fields twisting and reconnecting would tend to concentrate the released energy in localized regions, which could explain Kuan's (1975) result that the hot gas near the star has a clumpy spatial distribution.

One consequence of this suggestion for the envelope energy source is that it may not be correct to include the envelope emission when comparing the observed luminosity with theoretical tracks in the H-R diagram, since the envelope would be independent of the energy which flows up through the star and out the photosphere. The points corresponding to the stars with the strongest envelope

emission would be moved downward in the H-R diagram by as much as 0.5 dex but the estimated maximum age of the T Tauri stars would not be significantly affected, as this is based on stars with weak envelope emission.

Some support for this basic picture of T Tauri stars is provided by Willson's (1975) work on the Fe I fluorescent lines in RW Aur. She points out that the observed emission-line profiles show evidence of occultation by the star near zero velocity rather than on the red side of the line, indicating that stellar rotation is the dominant source of line broadening. Her estimate of the e-folding time for the loss of angular momentum in RW Aur is similar to the value derived above, and she speculates that the mass loss in RW Aur may be centrifugally driven, due to the star rotating near break-up velocity.

This tentative identification of the T Tauri phenomenon with an early PMS phase of rapid angular momentum loss provides at least a plausible model for these objects. Envelope mass loss enables the star to lose much of its initial angular momentum, while radiative energy losses from the envelope can serve as a sink for the star's excess rotational kinetic energy. This would provide a natural link between the evolutionary state of these stars and the presence of the CS envelopes. It is emphasized that this picture is only suggestive and that additional observational

and theoretical work will be required to determine the validity of this hypothesis, especially with regard to the rotational kinetic energy as a possible source of envelope energy.

Summary of Evolutionary State

Four possible evolutionary identifications of the T Tauri stars in the Taurus and Rho Oph clouds are considered, and three of these are rejected on observational grounds. The conspicuous absence of massive ($M > 3\ M_{\odot}$) young stars in the Taurus complex, together with the lack of evidence for hydrodynamic evolution among the pairs of T Tauri stars, rules out the possibility that these T Tauri stars are high-mass stars in a hydrodynamic phase of evolution. The discovery that most T Tauri stars are not surrounded by optically thick CS dust shells and the spectroscopic evidence indicating mass outflow rather than mass infall strongly argue against an identification of these T Tauri stars with either the thick-shell phase or the clearing dust-shell phase of Larson's models. It is suggested that young PMS stars develop a strong stellar wind which terminates the mass infall and disperses the remnant material at a much earlier epoch than Larson's models predict.

In the absence of any alternative identification, the observed locus of the T Tauri stars in the H-R diagram

parallel to the predicted QSET isochrones is taken as proof that these are young PMS stars of low mass evolving toward the ZAMS along conventional Hayashi-Henyey quasi-static equilibrium tracks. A comparison with theoretical evolutionary tracks indicates ages generally less than 10^6 years and masses less than 3 $M_\odot$. Since the T Tauri phase is completed while the star is still well above the ZAMS, there must be a substantial post-T Tauri phase of PMS evolution during which the star has a relatively normal spectroscopic appearance.

This identification of the T Tauri stars in the Taurus and Rho Oph clouds as PMS stars of low mass does not argue against Grasdalen's (1973) conclusion that V1057 Cyg was once an 8 $M_\odot$ T Tauri star. Rather, this suggests that the T Tauri class may include a few stars of high mass along with the more numerous low-mass stars.

The high bolometric luminosities and large visual extinctions of the strong-emission stars relative to the other T Tauri stars in the Taurus cloud are evidence that the strong-emission stars represent a young subset of the T Tauri class. This supports the view that the mass-loss rate and envelope emission strength decrease with time not only between the T Tauri phase and the ZAMS, but also during the T Tauri phase. The fraction of strong-emission stars in the Taurus complex and the estimated times for these stars

to drift out of their natal clouds suggest a timescale of only $1\text{-}2\times10^5$ years for the strong-emission phase. If this is correct, the presence of luminous strong-emission T Tauri stars may be considered another signpost of recent star formation (Strom, Strom, and Grasdalen 1975).

The results presented in this chapter do not clearly identify the source of the envelope energy in T Tauri stars and thus do not establish with certainty the desired fundamental link between the evolutionary state of the stars and the observed envelope properties. However, the large relative envelope luminosities in some T Tauri stars and the lack of envelope activity around normal stars of similar structure argue against acoustic waves from the stellar convection zones being the source of the envelope energy. Instead, it is suggested that rapid axial rotation is the parameter which distinguishes the T Tauri stars from the other late-type stars and that the T Tauri phenomenon is the manifestation of convective PMS stars undergoing a phase of rapid angular momentum loss. The similarity between the stellar rotational kinetic energy lost during a spindown from near break-up velocity and the thermal energy radiated away by the envelope during the T Tauri phase is suggestive, but it remains to be shown that some T Tauri stars really do rotate near break-up velocity and that the excess rotational kinetic energy is actually deposited in the envelope. If

this basic picture of T Tauri stars is indeed correct, the one remaining observational property listed in Chapter 1 (broad photospheric absorption lines) will be neatly accounted for and the reason for the existence of T Tauri stars will be at least qualitatively understood.

APPENDIX I

BOLOMETRIC LUMINOSITY OF GG TAU

In this appendix, the method of correcting observations of T Tauri stars for interstellar extinction and thus determining the bolometric luminosity is illustrated in greater detail. The T Tauri star GG Tau is taken as a typical example and is used to show exactly how these calculations are performed.

The available photometry of GG Tau consists of five sets of UBV measurements, one set of JHKL observations, and bolometer measurements at 2.2, 3.5, 4.8, and 10 μ; the mean observed magnitudes are listed in the "Mag" column in Table 8. By means of the absolute calibration of the photometry, these magnitudes are transformed into values of log λF_λ on a system with a convenient zeropoint:

$$\log \lambda F_\lambda = -m(\lambda)/2.5 + \log C(\lambda)$$

The values of log λF_λ are given in the third column of Table 8 and the calibration constants are listed in the "log $C(\lambda)$" column in Table 9.

Our spectrum of GG Tau indicates a spectral type of approximately dK7 and a blue veiling parameter $v_B \approx 2$. The appropriate K7, $v_B = 2$ model is given in Table 9 both in

TABLE 8

GG Tau: Magnitudes and Fluxes

Filter	Mag	log λF_λ	$(\log \lambda F_\lambda)_o$	λF_λ	$\lambda F_\lambda \times \delta\lambda$
U	$13^m.58$	-0.24	1.19	15.49	0.62
B	13.65	+0.04	1.30	19.95	1.80
V	12.24	+0.44	1.47	29.51	3.10
R			(1.55)	35.48	3.73
I			(1.60)	39.81	4.98
J	8.61	+1.09	1.43	26.92	3.50
H	7.60	+1.23	1.44	27.54	3.31
K	7.35	+0.99	1.13	13.49	2.16
L	6.43	+0.87	0.97	9.33	1.59
4.8	5.96	+0.62	0.69	4.90	0.96
8.4			(0.22)	1.66	0.27
10	4.01	+0.51	0.54	3.47	0.14

TABLE 9

Model, Conversion Factors, and Reddening Law

Filter	Model Mag	log λF_λ	log C(λ)	A(λ)/E(B-V)
U			5.19	6.16
B	$10^m.10$	1.46	5.50	5.45
V	9.28	1.63	5.34	4.45
R	8.48	1.70	5.09	3.65
I	7.80	1.75	4.87	2.58
J	7.30	1.61	4.53	1.47
H	6.68	1.60	4.27	0.90
K	6.43	1.36	3.93	0.60
L	6.03	1.03	3.44	0.42
4.8	5.58	0.77	3.00	0.31
8.4	4.85	0.37	2.31	0.20
10	4.60	0.27	2.11	0.14

terms of magnitudes and log λF_λ. The photospheric part of this model is constructed from Johnson's (1966) colors for K7 V, with the H magnitude from Veeder's (1974) mean H-K colors and the 4.8, 8.4, and 10 μ fluxes from a black body source fitted at the L filter. For the envelope part of the model, the relative fluxes at the standard filter wavelengths are obtained from the equations for optically thin free-bound and free-free hydrogen continuous emission (Kaplan and Pikelner 1970) at a temperature of 20,000° K. These are scaled so that the envelope flux is twice the photospheric flux at the B filter and the two fluxes at each wavelength are then combined to give the values listed in Table 9. Because the U filter straddles the Balmer jump and the Balmer continuum may be optically thick, no attempt is made to evaluate the model flux at U.

The correction of the observed fluxes for interstellar extinction procedes as follows. First, three independent estimates of E(B-V) are obtained, assuming the Rho Oph reddening law (last column, Table 9).

1. V-K method. The observed V-K color of GG Tau is $4^m.89$, while the intrinsic color from the model is $2^m.85$. According to the Rho Oph reddening law,

$$E(B-V) = E(V-K)/3.85 = (4.89-2.85)/3.85 = 0^m.53$$

2. B-[4.8] method. The observed B-[4.8] color of GG Tau is $7^m.69$, while the intrinsic color from the model is $4^m.52$. According to the Rho Oph reddening law,

$$E(B-V) = E(B-[4.8])/5.14 = (7.69-4.52)/5.14 = 0^m.62$$

3. J-H, H-K method. The observed colors of GG Tau are J-H = $1^m.01$, H-K = $0^m.39$. Projection of this point down the reddening vector in the J-H, H-K diagram to the K7 locus yields $(J-H)_o = 0^m.67$. According to the Rho Oph reddening law,

$$E(B-V) = 1.75E(J-H) = 1.75(1.01-0.67) = 0^m.59$$

These three values of E(B-V) are averaged to give $0^m.58$ as the best estimate of E(B-V) for GG Tau. The observed fluxes of GG Tau in Table 8 are now corrected for interstellar extinction by means of this value of E(B-V) and the ratios $A(\lambda)/E(B-V)$ for the Rho Oph reddening law given in Table 9; the results are shown in the "$(\log \lambda F_\lambda)_o$" column in Table 8 (note: $A(\lambda)$ is in magnitudes, so one must divide by 2.5 to get the extinction in dex).

The corrected observations of GG Tau are also shown in the second column of Table 10, where they are compared with the K7, $v_B = 2$ model fitted at the H filter. The residuals "δ" in the logarithmic fluxes are given in the next column of Table 10, while the last column shows these

TABLE 10

GG Tau: Comparison with Model

Filter	$(\log \lambda F_\lambda)_o$	K7, $v_B = 2$	δ	δ+0.01
B	1.30	1.30	0.00	+0.01
V	1.47	1.47	0.00	+0.01
J	1.43	1.45	+0.02	+0.03
H	1.44	1.44	0.00	+0.01
K	1.13	1.20	+0.07	+0.08
L	0.97	0.87	-0.10	-0.09
4.8	0.69	0.61	-0.08	-0.07

residuals adjusted to bring their sum as close to zero as possible. The fit longward of 2 μ is not as good as the fit at shorter wavelengths, but this could well be due to photometric errors. However, none of the adjusted residuals exceed 0.10 dex and the fit is considered to be satisfactory. GG Tau was not observed in the R and I filters or at 8.4 μ, so the adjusted K7, $v_B = 2$ model is used to provide estimates of the fluxes at these three standard wavelengths; these are shown in parentheses in the "$(\log \lambda F_\lambda)_o$" column in Table 8.

The corrected logarithmic fluxes in Table 8 are now converted to values of λF_λ, which are shown in the fifth column of Table 8. Finally, these are integrated over $\log(\lambda)$ from the U filter to 10 μ by the simple trapezoidal approximation. The terms for this integral sum are given in the last column of Table 8. The summation of these terms yields a 0.36 to 10 μ luminosity for GG Tau of 26.16 units. A standard unreddened G2 V star at the distance of the Taurus complex (150 pc) has a luminosity of 6.58 units on this system, so the bolometric luminosity of GG Tau is 4.0 $L_\odot$ or $\log(L/L_\odot) = +0.60$.

When the luminosity of GG Tau was determined for this investigation, the author obtained estimates of E(B-V) using both the K7, $v_B = 1$ and K7, $v_B = 2$ models. The respective values of E(B-V) are $0^m.56$ and $0^m.58$, and the mean

value of $E(B-V) = 0^{m}.57$ was actually employed. This slightly smaller reddening leads to $\log(L/L_{\odot}) = 0.59$ rather than the value of 0.60 derived above. However, for the sake of simplicity and clarity, the calculations in this appendix have been carried through on the basis of the K7, $v_B = 2$ model only.

REFERENCES

Ambartsumian, V. A. 1947, Stellar Evolution and Astrophysics (Erevan: Acad. Sci. Armenian S. S. R.).

Anderson, L., and Kuhi, L. V. 1969, in Non-Periodic Phenomena in Variable Stars, ed. L. Detre (Dordrecht: D. Reidel), p. 93.

Aveni, A. F. 1966, Ap.J. 144, 666.

Bertiau, F. C. 1958, Ap.J. 128, 533.

Bonsack, W. K. 1961, Ap.J. 133, 340.

Bonsack, W. K., and Greenstein, J. L. 1960, Ap.J. 131, 83.

Carrasco, L., Strom, S. E., and Strom, K. M. 1973, Ap.J. 182, 95.

Carswell, R. F., Hilliard, R. L., Strittmatter, P. A., Taylor, D. J., and Weymann, R. J. 1975, Ap.J. 196, 351.

Catchpole, R. M., and Glass, I. S. 1974, M.N.R.A.S. 169, 69p.

Cohen, M. 1973a, M.N.R.A.S. 161, 97.

———. 1973b, M.N.R.A.S. 164, 395.

———. 1974, M.N.R.A.S. 169, 257.

———. 1975, paper presented at the Ensenada Meeting of the A.S.P.; to be published in Pub. A.S.P.

Dolidze, M. V., and Arakelyan, M. A. 1959, Sov. A.J. 3, 434.

Dumont, S., Heidmann, N., Kuhi, L. V., and Thomas, R. N. 1973, Astr. and Ap. 29, 199.

Dyck, H. M., and Milkey, R. W. 1972, Pub. A.S.P. 84, 597.

Ezer, D., and Cameron, A. G. W. 1967a, Canadian J. Phys. 45, 3429.

Ezer, D., and Cameron, A. G. W. 1967b, Canadian J. Phys. 45, 3461.

Gahm, G. F. 1970, Ap.J. 160, 1117.

Gahm, G. F., Nordh, H. L., Olofsson, S. G., and Carlborg, N. C. 1974, Astr. and Ap. 33, 399.

Garrison, R. F. 1967, Ap.J. 147, 1003.

Gillett, F. C., and Forrest, W. J. 1973, Ap.J. 179, 483.

Gilman, R. C. 1974, Ap.J. 188, 87.

Grasdalen, G. L. 1973, Ap.J. 182, 781.

———. 1974a, Ap.J. 193, 373.

———. 1974b, unpublished data, Kitt Peak National Observatory, Tucson, Arizona.

Grasdalen, G., Joyce, R., Knacke, R., Strom, S. E., and Strom, K. M. 1975, A.J. 80, 117.

Grasdalen, G. L., Strom, K. M., and Strom, S. E. 1973, Ap.J. 184, L53.

Hackwell, J. A., Gehrz, R. D., and Woolf, N. J. 1970, Nature 227, 822.

Haro, G. 1949, A.J. 54, 188.

Hayashi, C., Hoshi, R., and Sugimoto, D. 1962, Progr. Theoret. Phys. Suppl. 22, 1.

Henize, K. G., and Mendoza V., E. E. 1973, Ap.J. 180, 115.

Herbig, G. H. 1945, Pub. A.S.P. 57, 166.

———. 1952, J.R.A.S.Can. 46, 222.

———. 1957, Ap.J. 125, 612.

———. 1958, Ap.J. 128, 259.

———. 1960, Ap.J. Suppl. 4, 337.

———. 1961, Ap.J. 133, 337.

———. 1962, Advances in Astr. and Ap. 1, 47.

Herbig, G. H. 1970, Mem. Soc. Roy. Sci. Liège 19, 13.

———. 1974, personal letter to author, dated 2 Dec 1974.

———. 1975, paper presented at the Ensenada Meeting of the A.S.P.; to be published in Pub. A.S.P.

Herbig, G. H., and Rao, N. K. 1972, Ap.J. 174, 401.

Humphreys, R. M. 1974, Ap.J. 188, 75.

Iben, I. 1965, Ap.J. 141, 993.

Iben, I., and Talbot, R. J. 1966, Ap.J. 144, 968.

Imhoff, C. L., and Mendoza V., E. E. 1974, Revista Mexicana de Astronomía y Astrofísica 1, 25.

Johnson, H. L. 1964, Bol. Obs. Tonantzintla y Tacubaya 3, 305.

———. 1966, Ann. Rev. Astr. and Ap. 4, 193.

Joy, A. H. 1945, Ap.J. 102, 168.

———. 1949, Ap.J. 110, 424.

Joy, A. H., and Abt, H. A. 1974, Ap.J. Suppl. 28, 1.

Kaplan, S. A., and Pikelner, S. B. 1970, The Interstellar Medium (Cambridge: Harvard University Press).

Knacke, R. F., Strom, K. M., Strom, S. E., Young, E., and Kunkel, W. 1973, Ap.J. 179, 847.

Kraft, R. P. 1970, in Spectroscopic Astrophysics, ed. G. H. Herbig (Berkeley: Univ. of Calif. Press), p. 385.

Kuan, P. 1975, Ap.J. 202, in press.

Kuhi, L. V. 1964, Ap.J. 140, 1409.

———. 1966, Ap.J. 143, 991.

———. 1970, Mem. Soc. Roy. Sci. Liège 19, 295.

———. 1974, Astr. and Ap. Suppl. 15, 47.

Larson, R. B. 1969, M.N.R.A.S. 145, 271.

Larson, R. B. 1972, M.N.R.A.S. 157, 121.

Lee, T. A. 1970, Ap.J. 162, 217.

Low, F. J., Johnson, H. L., Kleinmann, D. E., Latham, A. S., and Geisel, S. L. 1970, Ap.J. 160, 531.

Mendoza V., E. E. 1966, Ap.J. 143, 1010.

———. 1968, Ap.J. 151, 977.

Milkey, R. W., and Dyck, H. M. 1973, Ap.J. 181, 833.

Nandy, K., and Pratt, N. 1972, Astrophys. and Space Sci. 19, 219.

Reeves, H. 1974, Ann. Rev. Astr. and Ap. 12, 437.

Russell, R. W., Soifer, B. T., and Forrest, W. J. 1975, Ap.J. 198, L41.

Rydgren, A. E. 1974, unpublished data, The University of Arizona, Tucson, Arizona.

Schwartz, R. D. 1974, Ap.J. 191, 419.

———. 1975, Ap.J. 195, 631.

Skumanich, A. 1972, Ap.J. 171, 565.

Smak, J. 1964, Ap.J. 139, 1095.

Stein, R. F., and Leibacher, J. 1974, Ann. Rev. Astr. and Ap. 12, 407.

Strom, S. E. 1972, Pub. A.S.P. 84, 745.

Strom, S. E., Grasdalen, G. L., and Strom, K. M. 1974, Ap.J. 191, 111.

Strom, S. E., Strom, K. M., and Grasdalen, G. L. 1975, Ann. Rev. Astr. and Ap. 13, in press.

Strom, S. E., Strom, K. M., Yost, J., Carrasco, L., and Grasdalen, G. 1972, Ap.J. 173, 353.

Struve, O., and Rudkjøbing, M. 1949, Ap.J. 109, 92.

Varsavsky, C. M. 1959, Ap.J. 132, 354.

Veeder, G. J. 1974, A.J. 79, 1056.

Vrba, F. J., Strom, K. M., Strom, S. E., and Grasdalen, G. L. 1975, Ap.J. 197, 77.

Walker, M. F. 1956, Ap.J. Suppl. 2, 365.

———. 1972, Ap.J. 175, 89.

Wenzel, W. 1966, Mitt. veränderl. Sterne 4, No. 4.

———. 1969, in Non-Periodic Phenomena in Variable Stars, ed. L. Detre (Dordrecht: D. Reidel), p. 61.

Willson, L. A. 1974, Ap.J. 191, 143.

———. 1975, Ap.J. 197, 365.

Woolf, N. J., and Ney, E. P. 1969, Ap.J. 155, L181.